INFORMATION TO USERS

This manuscript has been reproduced from the microfilm master. UMI films the text directly from the original or copy submitted. Thus, some thesis and dissertation copies are in typewriter face, while others may be from any type of computer printer.

The quality of this reproduction is dependent upon the quality of the copy submitted. Broken or indistinct print, colored or poor quality illustrations and photographs, print bleedthrough, substandard margins, and improper alignment can adversely affect reproduction.

In the unlikely event that the author did not send UMI a complete manuscript and there are missing pages, these will be noted. Also, if unauthorized copyright material had to be removed, a note will indicate the deletion.

Oversize materials (e.g., maps, drawings, charts) are reproduced by sectioning the original, beginning at the upper left-hand corner and continuing from left to right in equal sections with small overlaps. Each original is also photographed in one exposure and is included in reduced form at the back of the book.

Photographs included in the original manuscript have been reproduced xerographically in this copy. Higher quality 6" x 9" black and white photographic prints are available for any photographs or illustrations appearing in this copy for an additional charge. Contact UMI directly to order.

UMI

A Bell & Howell Information Company
300 North Zeeb Road, Ann Arbor MI 48106-1346 USA
313/761-4700 800/521-0600

UNIVERSITY OF OKLAHOMA

GRADUATE COLLEGE

A STUDY OF THE USE OF KELEX 100 FOR REMOVAL OF CADMIUM USING LIGAND-MODIFIED MICELLAR-ENHANCED ULTRAFILTRATION

A Dissertation

SUBMITTED TO THE GRADUATE FACULTY

in partial fulfillment of the requirements for the

degree of

Doctor of Philosophy

By

Kay Kuhlemeier Bjornen

Norman, OK

1999

A STUDY OF THE USE OF KELEX 100 FOR REMOVAL OF CADMIUM USING LIGAND-MODIFIED MICELLAR-ENHANCED ULTRAFILTRATION

A Dissertation APPROVED FOR THE DEPARTMENT OF CHEMISTRY AND BIOCHEMISTRY

BY

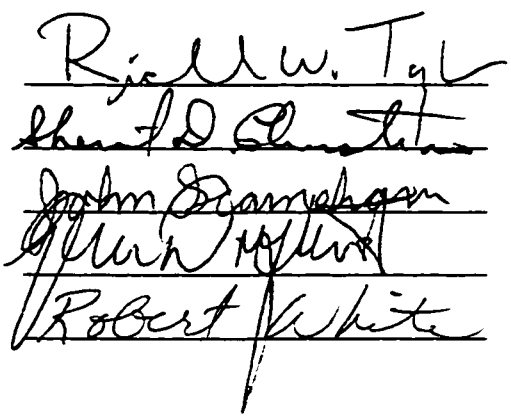

Acknowledgements

I am grateful to Dr. Richard Taylor for his guidance and endless patience. I would also like to thank the members of my advisory committee, Dr. Sherril Christian, Dr. Glenn Dryhurst, Dr. Robert White and Dr. John Scamehorn for their help and advice over the course of my time at OU.

Thanks to my father and mother, Charles and Wilma Kuhlemeier, for believing in me so strongly that I had to believe in myself and for providing the extra pairs of hands I needed to get this done. Thanks also to my husband, Kevin, and my sons, Paul and Joel, for the countless vacations, weekends and holidays sacrificed. I am also grateful to the many, many friends who provided advice, support and occasional sick child babysitting service. Somehow this whole experience was tremendously enriched by knowing so many marvelous people. I am particularly grateful to those who've shared bench space and expertise with me: Laura Haley, Olga Ivanova, Neeraj Khanna, Carlos Rodriguez and Don Simmons. A special thanks also to Steve Weber and Patronalia Hanley at the OGS who came through with the mercury analyzer and occasional last resort help with the AA.

Finally, I would like to gratefully acknowledge the financial support of the University of Oklahoma Department of Chemistry and Biochemistry, U.S. Department of Education and National Science Foundation.

TABLE OF CONTENTS

List of Tables.....vi

List of Figures.....x

Abstract.....xvii

CHAPTER

I. Introduction.....1

II. Experimental.....40

III. Results..... 67

IV. Discussion.....174

Bibliography.....200

LIST OF TABLES

TABLE		PAGE
I-1	Loss of mercury to the environment by source	4
I-2	EPA criteria for safe levels of mercury and cadmium	7
I-3	1998 standards for discharge of wastewaters containing cadmium	9
I-4	Structure and CMC of surfactants	14
I-5	Equilibria and cumulative formation constants for cadmium in water	28
I-6	Equilibria and cumulative formation constants for mercury in water	29
I-7	Relevant equilibria and equilibrium constants for 8-hydroxyquinoline	33
I-8	Solubility equilibria and log Ksp's for metal-8HQ complexes	34
I-9	Equilibria and cumulative formation constants for mercury and cadmium complexes of thiourea	35
I-10	Species distribution diagram for Hg^{2+} and thiourea	37
I-11	Species distribution diagram for Cd^{2+} and Kelex	38
II-1	Analytical wavelengths, typical detection limits and optimum working range for metals determined by AA	58
II-2	Volumes of reagents for CVAA sample digestion using 300 and 60 mL BOD flasks	63

III-1	Summary of protonation constants for Kelex 100 in surfactant solution and Kelex 100 and 8HQ in 80% (w/w) methanol:water	88
III-2	Summary of Kelex 100 metal ion titrations	112
III-3	SED results for solution blanks comparing membrane treatments	116-7
III-4	Cd^{2+} retained by the membrane for different membrane treatments	118
III-5	SED results for D.D. water blanks with treated membranes	118
III-6	SED results for Cd^{2+} in 5 mM $C_{12}(EO)_6$ surfactant solution without ligand for different membrane treatments	120
III-7	SED results for Cd^{2+} in 0.05 M $CPNO_3$ surfactant solution without ligand for different membrane treatments	121
III-8	SED results for Cd^{2+} in 5 mM $C_{12}(EO)_6$ solution at pH 6.0 with different membrane treatment techniques.	123
III-9	SED results for Cd^{2+} in 5 mM $C_{12}(EO)_6$ solution at pH 7.0 with different membrane treatment techniques	124

III-10	SED results for Cd^{2+} in 5 mM $C_{12}(EO)_6$ solution at pH 9.0 with different membrane treatment techniques	125
III-11	SED results for Cd^{2+} in 0.05 M $CPNO_3$ solution at pH 7.0 with different membrane treatment techniques	126
III-12	Comparison of SED results with and without Kelex 100 in 0.05 M $CPNO_3$ solution at pH 9.0 with different membrane treatment techniques	127
III-13	SED results for 0.5 mM Kelex 100 in 5 mM $C_{12}(EO)_6$ with pretreated membranes and no Cd^{2+}	129
III-14	SED results for 0.5 mM Kelex 100 in 0.05 M $CPNO_3$ with pretreated membranes and no Cd^{2+}.	130
III-15	Comparison of $[Cd^{2+}]_{Tot}$ and $\%R_{Cd}$ for SED results at pH 9.0 in $CPNO_3$ with 0.50 mM Kelex 100	133
III-16	Comparison of $[Cd^{2+}]_{Tot}$ and $\%R_{Cd}$ for SED results at pH 9.0 in $C_{12}(EO)_6$ with 0.50 mM Kelex 100	134
III-17	SED results for varying concentrations of Cd^{2+} with Kelex 100 in $C_{12}(EO)_6$ at pH 9.0	136
III-18	SED results for varying concentrations of Cd^{2+} in 0.05 M $CPNO_3$ with 0.5 mM Kelex 100 at pH 9.0	138

III-19	SED results for study of rejection of Cd^{2+} in $C_{12}(EO)_6$ as a function of pH	141
III-20	Effect of pH on SED results for Cd^{2+}-Kelex system in $CPNO_3$	143
III-21	SED results for study of rejection of Cd^{2+} by 0.5 mM Kelex 100 in 5 mM $C_{12}(EO)_6$ as a function of [NaCl] at pH 9.0	148
III-22	SED results for study of rejection of Cd^{2+} and Zn^{2+} by 0.5 mM Kelex 100 in 5 mM $C_{12}(EO)_6$ as a function of pH	149
III-23	SED results for study of rejection of Cd^{2+} and Ca^{2+} by 0.5 mM Kelex 100 in 5 mM $C_{12}(EO)_6$ at pH 9.0	150
III-24	Comparison of %R for UF experiments without Kelex 100	158
III-25	Comparison of calculated % rejection for SED and UF separations of Cd^{2+}	158
III-26	Comparison of hot and cold digestions	169
IV-1	Protonation constants for old and new Kelex	177
IV-2	Corrected values of $\%R_{Cd}$ for 0.50 mM Kelex SED experiments in $C_{12}(EO)_6$ surfactant solution with different membrane treatment techniques at pH 7.0	185
IV-3	Corrected values of $\%R_{Cd}$ for 0.50 mM Kelex SED experiments in $CPNO_3$ surfactant solution with different membrane treatment techniques at pH 7.0	186

LIST OF FIGURES

FIGURE		PAGE
I-1	Schematic diagram of the environmental cycle of mercury	3
I-2	Simplified structure of a surfactant monomer	12
I-3	Regions of micellar polarity	15
I-4	Monomer-micelle equilibrium	17
I-5	Stirred cell ultrafiltration apparatus	19
I-6	Diagram of the LM-MEUF process	23
I-7	Diagram of an SED cell	26
I-8	Structure of 7-(4-Ethyl-1-methyloctyl)-8 -hydroxyquinoline	32
I-9	Structure of 1-decyl-2-thiourea	34
II-1	Diagram of thin layer chromatography plates	47
II-2	^{1}H-NMR spectrum of purified Kelex 100	48
II-3	Structure and ^{1}H-NMR peak assignments for purified Kelex 100	49
II-4	UV-visible spectrum of 0.5 mM Kelex 100 in 5 mM $C_{12}(EO)_6$ solution titrated with $CuCl_2$ solution	51
II-5	Plot of absorbance versus mmoles of copper titrant for standardization of Kelex 100 stock solution	52
II-6	Cold vapor apparatus for atomic absorbtion analysis of mercury	61

II-7	Calibration curve for CVAA analysis of mercury using 60 mL BOD flasks	64
II-8	Calibration curve for CVAA analysis of mercury using 300 mL BOD flasks	65
III-1	Protonation equilibria of alkylated 8-hydroxyquinoline	68
III-2	Schematic diagram of ligand equilibria	69
III-3	UV-visible spectra pH titration of 0.05 M $CPNO_3$ solution from pH 2.0 to pH 13.0	73
III-4	Plot of absorbance versus pH at 388 nm for titration of 0.05 M $CPNO_3$ solution blank	74
III-5	UV-visible spectra of pH titration 0.5 mM Kelex 100 in 0.05 M $CPNO_3$ solution from pH 2.0 to 7.0	75
III-6	UV-visible spectra of 0.5 mM Kelex 100 in 0.05 M $CPNO_3$ solution from pH 7.5 to 12.5	76
III-7	Plot of pH versus absorbance at 388 nm for 0.5 mM Kelex 100 in 0.05 M $CPNO_3$ solution from pH 2 to pH 12.5	77
III-8	Plot of pH versus absorbance at 388 nm with fitted curve for titration of 0.5 mM Kelex in 0.05 M $CPNO_3$ solution	78.
III-9	UV-visible spectra of pH titration of 0.1 M SDS solution blank pH 2.5 to pH 13.0	79
III-10	Plot of pH versus absorbance at 356 nm for pH titration of 0.1 M SDS solution blank from pH 2.5 to 11.0	80

III-11	UV-visible spectra of 0.5 mM Kelex 100 in 0.1 M SDS solution	81
III-12	Plot of pH versus absorbance at 356 nm for titration pH 2.4 and pH 12.4 of 0.5 mM Kelex in 0.1 M SDS solution	82
III-13	UV-visible spectra of pH titration of 0.5 mM Kelex 100 in 0.05 M $C_{12}(EO)_6$ solution from pH 2.0 to pH 10.5	83
III-14	UV-visible spectra of pH titration of 0.5 mM Kelex 100 in 0.05 M $C_{12}(EO)_6$ solution from pH 11.0 to pH 13.0	84
III-15	Plot of pH versus absorbance for spectrophotometric pH study of 0.5 mM Kelex 100 in 50 mM $C_{12}(EO)_6$	85
III-16	Plot of pH versus absorbance at 258 nm for spectrophotometric pH study of 0.125 mM Kelex 100 in 80% methanol:water	86
III-17	Plot of pH versus absorbance for spectrophotometric pH study of 0.125 mM 8-hydroxyquinoline in 80% (w/w) methanol:water	87
III-18	UV-visible spectra of Kelex 100 in 0.05 M $CPNO_3$ solution titrated with Cd^{2+}	92
III-19	Plot of absorbance versus ratio of moles Cd^{2+} to moles Kelex 100 for titration of Kelex 100 in 0.05 M $CPNO_3$ at pH 8.6	93
III-20	UV-visible spectra of Kelex 100 in 0.05 M DDAO solution titrated with Cd^{2+}	94

III-21	Plot of absorbance versus ratio of moles Cd^{2+} to moles Kelex 100 for titration of Kelex 100 in 0.05 M DDAO at pH 8.7	95
III-22	UV-visible spectra of Kelex 100 in 0.05 M $C_{12}(EO)_6$ solution titrated with Cd^{2+}	96
III-23	UV-visible spectrum of 0.170 mM Kelex 100 in 0.05 M $C_{12}(EO)_6$ solution with 5.0 mM CHES at pH 9.0 titrated with Cd^{2+}	97
III-24	Plot of absorbance at 406 nm versus ratio of moles Cd^{2+} to moles Kelex 100 for titration of 0.17 mM Kelex 100 in a solution of 0.05 M $C_{12}(EO)_6$ at pH 9.0	98
III-25	UV-visible spectra of 0.528 mM Kelex 100 in 0.05 M CO660 solution with 5.0 mM CHES at pH 9.3 titrated with Cd^{2+}	99
III-26	Plot of absorbance at 394 nm versus ratio of moles Cd^{2+} to moles Kelex 100 for titration of 0.5 mM Kelex 100 in a solution of 0.05 M CO660 at pH 9.3	100
III-27	UV-vis spectra of Hg^{2+} in D.D. H_2O at pH 1.5	101
III-28	UV-visible spectrum of 0.528 mM Kelex 100 in a solution of 0.05 M $CPNO_3$ at pH 8.4 titrated with Hg^{2+}	102

III-29	Plot of absorbance at 430 nm versus ratio of moles Hg^{2+} to moles Kelex 100 for titration of 0.50 mM Kelex 100 in 0.05 M $CPNO_3$ solution at pH 8.4	103
III-30	UV-visible spectra of 0.528 mM Kelex 100 in 0.05 M CO660 solution at pH 8.9 titrated with Hg^{2+}	104
III-31	Plot of absorbance at 460 nm versus ratio of moles Hg^{2+} to moles Kelex 100 for titration of 0.50 mM Kelex 100 in CO660 at pH 8.9	105
III-32	UV-visible spectra of 0.528 mM Kelex 100 in DDAO solution at pH 8.5 titrated Hg^{2+}	106
III-33	Plot of absorbance at 430 nm versus ratio of moles Hg^{2+} to moles Kelex 100 for titration of 0.50 mM Kelex 100 in DDAO at pH 8.5.	107
III-34	UV-visible spectra of 0.5 mM Kelex 100 in a solution of 0.05 M $CPNO_3$ solution at pH 7.5 titrated with Pb^{2+}	108
III-35	UV-visible spectra of 0.528 mM Kelex 100 in CO660 solution at pH 5.7 titrated with Pb^{2+}	109
III-36	UV-visible spectra of 0.528 mM Kelex 100 in CO660 solution at pH 7.7 titrated with Pb^{2+}	109
III-37	UV-visible spectra of 0.528 mM Kelex 100 in DDAO solution at pH 7.5 titrated with Pb^{2+}	110

III-38	Plot of %rejection of Cd^{2+} as a function of $[Cd^{2+}]_O$ for 0.5 mM Kelex 100 in 5 mM $C_{12}(EO)_6$ surfactant solution at pH 9.0	137
III-39	Plot of rejection of Cd^{2+}, % as a function of $[Cd^{2+}]_O$ in 0.05 M $CPNO_3$ with 0.5 mM Kelex 100 at pH 9.0	139
III-40	Plot of % rejection of Cd^{2+} as a function of pH in $C_{12}(EO)_6$ for 0.5 mM Kelex 100	142
III-41	Plot of SED results expressed as average %rejection Cd^{2+} and %expulsion Cd^{2+} as a function of pH in 0.05 M $CPNO_3$	144
III-42	Plot of UF results for Cd^{2+} at pH 6.0 in 0.05 M $CPNO_3$ solution without ligand and with 0.5 mM Kelex	153
III-43	Plot of UF results for Cd^{2+} at pH 6.0 in 0.05 M $C_{12}(EO)_6$ solution without ligand and with 0.5 mM Kelex	154
III-44	Plot of UF results for Cd^{2+} at pH 9.0 with and without ligand in 0.05 M $CPNO_3$ solution	155
III-45	Plot of UF results for Cd^{2+} at pH 9.0 with and without ligand in 5 mM $C_{12}(EO)_6$ solution	156
III-46	Plot of UF results for Cd^{2+} at pH 4.0 in 0.05 M $C_{12}(EO)_6$ solution with 0.5 mM Kelex	157
III-47	Structures of PAN and Dithizone	160
III-48	UV-vis spectra of formation of mercury (II) PAN complex with in 80% methanol:water	161

III-49	UV-vis spectra of 0.02 mM PAN-Hg^{2+} complex in $C_{12}(EO)_6$ surfactant solution titrated with 1-hexyl-2-thiourea	162
III-50	UV-vis spectra of the exchange reaction of 0.20 mM copper (II) dithizonate with mercury (II) at pH 1.0	164
III-51	Calibration line for dual wavelength determination of mercury by exchange with copper (II) dithizonate	165
III-51	CVAA calibration curve	167
III-52	Plot of average absorbance for CVAA calibration curves	171
IV-1	Structure of the active ingredient of the old formulation of Kelex 100	171
IV-2	Structure of the active ingredient of the new formulation of Kelex 100	176
IV-3	Plot of Cd^{2+} rejection (%) as a function of $[Cd^{2+}]_o$	189

Abstract

Ligand-modified micellar-enhanced ultrafiltration (LM-MEUF) is a membrane based separation method for removal of metal ions from aqueous solutions. An amphilic ligand which will selectively complex the target ion is solubilized in surfactant micelles and added to the waste stream. Semi-equilibrium dialysis (SED), ultrafiltration (UF) and spectrophotometric titration methods have been used to investigate the properties and effectiveness of a commercially available ligand, Kelex 100, for removal of toxic metals ions with LM-MEUF using several different surfactant solutions. The use of alkylated thiourea ligands for removal of mercury was also studied.

Kelex 100 was purified and the active ingredient, 7-(4-Ethyl-1-methyloctyl)-8-hydroxyquinoline, was isolated. Protonation equilibria in cationic ($CPNO_3$), anionic (SDS) and nonionic ($C_{12}(EO)_6$) surfactant solutions, as well as 80% (w/w) methanol-water solution, were studied. The protonation constants were found to be shifted in a predictable manner consistent with solvent polarity and micellar charge. Metal-ligand stoichiometry in cationic ($CPNO_3$) and neutral (DDAO, CO660 and/or $C_{12}(EO)_6$) were determined for Kelex 100 with cadmium and mercury. Ligand to metal stoichiometry was 2:1 in all cases for mercury. Cadmium was 2:1 in neutral surfactant but 3:1 at high ligand to metal ratio in cationic surfactant.

Kelex 100 is an effective ligand for targeting cadmium with LM-MEUF.. SED experiments at pH 9.0 in either neutral ($C_{12}(EO)_6$) or cationic ($CPNO_3$) surfactant showed >99% rejection of cadmium. The effects of varying ligand to

metal ratio and pH were examined in both $CPNO_3$ and $C_{12}(EO)_6$ solutions as well as the effects of added electrolyte, a weakly competing ion (Ca^{2+}) and a strongly competing ion (Zn^{2+}) in $C_{12}(EO)_6$ solution.

Ultrafiltration experiments were conducted to further investigate separation of cadmium and to determine whether lowering pH would be effective for breaking the ligand-metal complex. By stripping the complex, the unbound metal can be separated and the ligand regenerated and reused. UF results confirmed greater than 99% rejection in both surfactant solutions at pH 9.0. However, stripping was not as effective for UF as it was for SED. Experiments at pH 6.0 showed significant rejection of cadmium in UF studies while SED experiments showed almost zero rejection in $C_{12}(EO)_6$ and expulsion of cadmium into the permeate with $CPNO_3$ solution.

Chapter 1

Introduction

Cadmium and mercury in the environment

Discharge of industrial wastes is the major source of water pollution from the group 12 heavy metals cadmium and mercury. Both occur in natural, unpolluted waters at very low levels with cadmium typically below 10 ng/L (1,2) and mercury between 20 and 60 ng/L (3). Anthropogenic sources have increased levels of both metals significantly in many waterways raising concerns for human health. In the best known case of industrial mercury poisoning, methylmercury laden effluent was released untreated into the Minamata Bay in Japan. The subsequent elevation of mercury levels in the fish and shellfish that formed a staple of the local diet caused symptoms that became known as Minamata disease. Though symptoms were first identified in 1953, discharge continued to pollute the bay until at least 1960 (31), poisoning 121 people with 46 fatalities. The increased awareness of potential environmental disaster generated by the Minamata incident and others (5), have led to improved regulation, monitoring and treatment technologies for toxic industrial wastes.

The toxicity of mercury has been widely recognized for many years. The expression "mad as a hatter" was derived from the manifestations of mercury poisoning seen in hatters who used mercury for felting fur hats in the 19th century. Exposure in humans occurs through the skin, gastrointestinal tract and respiratory tract. Symptoms include weakness and exhaustion, tremors,

delirium and blindness with chronic exposure shown to be teratogenic and carcinogenic (2). The effects of mercury pollution of water are particularly far reaching due to the chemical properties of mercury. The metal is inert in water with low solubility; however, the presence of oxygen quickly oxidizes it to the hydrated, divalent cation. Microbes present in bottom sediments convert the cation to the methyl or dimethyl form, which is readily absorbed by living organisms. Once within the cell membrane, it reacts with sulfhydryl groups and continued diffusion into the cell creates a concentration gradient referred to as bioaccumulation. Once concentrated in the cells of lower organisms, the effects are telescoped up the food chain. A diagram of the mercury cycle is shown in Figure I.1.

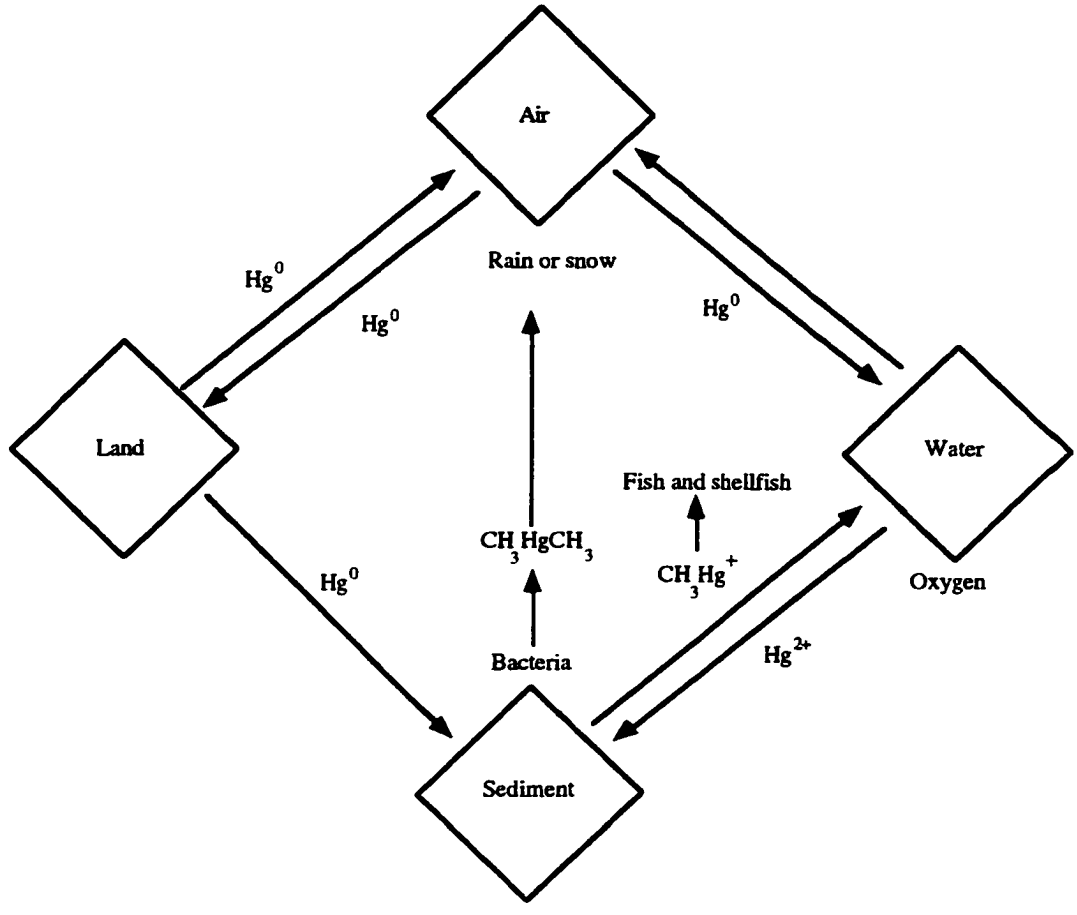

Figure I.1 Schematic diagram of the environmental cycle of mercury. (Adapted from ref. 2)

The largest single source of mercury pollution is emissions from coal-fired power plants and waste incinerators. A report on the status of mercury by the U.S. Environmental Protection Agency (U.S. EPA) in 1979 listed losses to air from coal utilities as 40.71 metric tons and 104.48 metric tons from burning of all fossil fuels (2). Mercury contained in coal and petroleum is readily vaporized and can be carried great distances in the atmosphere before being deposited by atmospheric precipitation as runoff or surface water. However,

industrial sources also accounted for 87.7 metric tons of mercury discharged directly into waterways. Significant industrial sources of mercury include chlor-alkali processing, in which mercury cathodes are used to produce chlorine gas and sodium hydroxide, and manufacture of electrical apparatus such as lamps and batteries. These two uses accounted for 55% of the projected 1985 U.S. mercury consumption (3). Table I.1 shows mercury losses for some representative industries.

Table I.1 Loss of mercury to the environment by source in metric tons/year[a]

Industrial source	**Air**	**Water**	**Land**
Copper smelting	40.77	2.26	45.29
Fuel oil consumption	16.94	0	0.02
Caustic manufacturing	0	7.61	1.9
Chloralkali manufacturing	14.84	2.93	226.83
Tube/switch manufacturing	0	10.23	8.7

(a) Ref. 2

Since environmental legislation was enacted beginning in the late 1970's, mercury pollution of water has decreased significantly.

Cadmium is a relatively rare element, found only in the presence of zinc ores and commonly produced as a byproduct of zinc or lead mining and smelting (7). The production of zinc and cadmium is highly enriched in zinc at ratios from 100:1 to 1000:1. Though found in the same group in the periodic table as mercury, the chemistry of cadmium varies in that it is always divalent in water and does not readily form carbon-metal bonds. Therefore, it is not found in the

readily absorbed alkyl form. Cadmium is highly toxic. The most common route for acute human exposure is through inhalation of cadmium oxide dust or fumes. Symptoms of cadmium poisoning from inhalation include emphysema, renal damage, anosmia, yellowing of teeth and minor liver damage (7). Human ingestion of 14.5-326 mg has been shown to cause severe abdominal pain, nausea, vomiting, diarrhea, headache and vertigo but is not lethal (9). Less well documented are the symptoms of chronic exposure to low levels of cadmium in food and water. A single well publicized case occurred in Japan between 1947 and 1955, when a number of cases of Itai-Itai (Ouch-ouch) disease were reported. It was named for the primary symptom which was painful bone deformities. The source of the problem was eventually traced to effluent from a zinc mine released into the Jintsu river. Studies determined that cadmium, like mercury, was concentrated into the tissues of fish which were a dietary staple of the local population. Further studies have revealed that risk for cadmium toxicity is increased by dietary factors such as calcium deficiency, as well as smoking and occupational exposure, and that cadmium, like mercury, bioaccumulates (10). Cadmium in soil and irrigation water contributes to dietary exposure, which is the most important route of exposure for the segment of the population not in high risk groups. Typical dietary uptake of cadmium in the U.S. is about 30 μg/day, mostly from fruits, vegetables and grains. The biological half-life in humans is estimated to be between 15 and 25 years (7).

Mercury and cadmium have no known physiological function so their presence in living organisms is the result of exposure to contaminants. The Clean Water Act of 1977 designated both as priority pollutants and directed the

EPA to publish criteria for the maximum amount of these and other pollutants which could safely be present in ground and surface water. Criteria for maximum safe levels of exposure in freshwater for both human health and aquatic life are shown in Table I.2. Criteria for cadmium are expressed as functions of the hardness level (as calcium carbonate) of the water because cadmium toxicity decreases with increasing hardness (9).

Table 1.2 - U.S. EPA criteria for safe levels of mercury and cadmium in freshwater to protect aquatic life.

	24 hour average (μg/L)	Maximum allowable (μg/L)
Mercury (b)	0.00057	0.0017
Cadmium(a,c)	$e^{(1.05[\ln(\text{hardness})-8.53]}$	$e^{(1.05[\ln(\text{hardness})-3.73]}$

(a) Cadmium concentration is expressed as a function of hardness (mg/L $CaCO_3$) (b) Ref 11 (c) Ref 9

Cadmium and mercury in industrial wastewater

The mercury cell method of manufacturing chlorine gas and caustic soda is a major source of direct mercury contamination of water. A mercury cell is made up of titanium or carbon anodes, a flowing mercury cathode and purified sodium chloride brine. The electrolysis of the brine forms chlorine gas and the reduced sodium is removed as an amalgam with the mercury. The amalgam is pumped to a second electrolytic cell known as a denuder where the sodium reacts with water to form sodium hydroxide. The stripped amalgam is recycled back to the first cell. This process produces two waste and disposal problems. The first results from the need to replenish the depleted brine. As additional salts are added to the brine it must be treated to remove impurities, particularly alkaline earth metals and sulfate ions. The presence of these impurities in the cell reduce operating efficiency and create scaling problems on the anode. Conventional treatment involves first adding barium or calcium to precipitate sulfate. The brine solution is then adjusted to about pH 11 and carbonate added to precipitate other metals as carbonates or hydroxides. The resulting sludge must be further

treated for disposal due to the presence of 150-1500 ppm mercury. The second waste stream results from water discharged from the denuder. Mercury levels in the wastewater range from 3-18 ppm (2). A common and effective treatment method for removal of mercury from wastewater is to precipitate it as mercuric sulfide through addition of sodium sulfide. An alternative method used for treatment of brine is addition of sodium borohydride to reduce mercury ions to metal which coalesce as droplets and amalgamate on the surface of the sodium borohydride.

The metal finishing industry is the largest consumer of cadmium in the U.S. and the largest producer of cadmium waste. Electroplating processes produce the most cadmium water pollution. An estimated 160 metric tons of cadmium were discharged in wastewater in 1977 (7). Potential sources of metal finishing waste include (13):

1. Production rinsewater
2. Electroplating baths - dumping as well as spills
3. Recharge of ion exchange units
4. Plant cleanup
5. Vent scrubber water
6. Sludges and filter cakes resulting from normal operations as well as waste treatment and cleanup

Typical concentrations range from low in rinsewater (15-50 mg/L) to very high in plating baths (23,000-43,000 mg/L) (13,14). A huge reduction in levels of cadmium is necessary to meet standards for discharge. Table I.3 shows current U.S. federal regulations and proposed European Commission standards. Both

are based on the best available technology (BAT) economically achievable standard. An analysis done by the U.S. EPA of permit violations shows that cadmium is one of the ten parameters most often out of compliance(6).

Table I.3 1998 standards for discharge of wastewaters containing cadmium and mercury .

Regulated source	Metal	One day maximum (mg/L)	30 Day Avg (mg/L)
Mine drainage (a)	Hg	0.002	0.001
Chloralkali mercury cells(a)	Hg	0.11	0.048
Metal finishing(a)	Cd	0.69	0.26
Metal finishing(b)	Cd	---	0.29
Metal finishing(b)	Hg	---	0.05

(a) U.S. EPA effluent limitations achievable with best available technology (BAT) economically achievable (ref 15) (b) European Commission (EC) standards (ref 16)

Detoxification, neutralization and dewatering (DND) is the conventional treatment method for electroplating waste (16, 6) used by about 75% of metal finishing operations. The detoxification step involves chemical oxidation of cyanide followed by precipitation of the cadmium and other metals as metal hydroxides at about pH 10. An ion exchange step may be necessary for preconcentration of the rinsewater. The resulting precipitate is filtered (dewatered) and the effluent neutralized prior to discharge. DND is comparatively inexpensive but requires disposal of large quantities of solid waste. Disposal of solid wastes containing toxic species is regulated under the Resource Conservation and Recovery Act (RCRA) resulting in additional disposal costs.

Many electroplating facilities are small shops for which the cost of such treatment is prohibitive. Reducing the quantity of solid waste generated reduces cost. Commercial electrochemical treatment units are available which are designed to concentrate and recover metals for recycling instead of disposing of them as a sludge. Cadmium has sufficient commercial value to make recycling a viable alternative to disposal. A study of the effectiveness of these units was done by the U.S. EPA. A new design which helped overcome reduced mass transfer rates at low concentrations was tested but effectiveness varied widely. These units were found to be most effective for shops where the composition of the treated water was relatively constant. The recovered metals were found to be of high purity and suitable for recycling. (17)

Solvent extraction was found to be a feasible alternative treatment for small shops in a study by McDonald (18). A high molecular weight amine, Alamine 336, was dissolved in xylene and used to extract metals, including cadmium, in the presence of chloride. Ninety eight percent of the 8-10 ppm cadmium present in wastewater samples could be extracted with a single extraction. However, the separation was only somewhat selective, since under most experimental conditions zinc and chromium were also extracted. Also, analysis of total organic carbon showed an increase of 50 ppm for each extraction cycle. No effort was made to treat the wastewater for removal of dissolved organic solvent.

Additional efforts to recover metals from metal finishing wastewater in order to recycle them have led to the use of techniques such as electrodialysis, ultrafiltration and reverse osmosis as pretreatments for precipitation or as

posttreatment if levels are still too high for discharge (19). These techniques have been limited by membrane fouling problems due to the presence of colloidal material or oil and grease.

Ligand-Modified Colloid-Enhanced Ultrafiltration (LM-CEUF) is a surfactant-based separation technique which was developed to selectively remove target ions from a wastewater stream. Surfactant-based techniques have a number of advantages over the conventional techniques described above. Surfactants are generally less expensive than either extraction or electrochemical methods due to the high costs of energy and organic solvents. The efficient separation of the target species also precludes the need for the additional treatment steps necessary for disposal of precipitated solids. Precipitation of metals from many wastewaters may produce very small quantities of toxic compounds coprecipitated with large quantities of relatively innocuous materials such as iron hydroxide or calcium carbonate. In addition, aqueous surfactant-based methods are environmentally benign and do not produce secondary pollutants which must be monitored, as is the case for the dissolved organics in solvent extraction.

As an introduction to the LM-CEUF technique, a brief description of surfactant chemistry and the background of surfactant-based separations follows.

Background of surfactants and surfactant based separations

A surfactant, or surface active agent, is a compound which derives its properties from a characteristic structure which usually consists of a long chain, hydrophobic tail group attached to a polar, hydrophilic head group as shown in Figure I.2. The tail group is generally 12-16 carbons long and may consist of a single chain, double chain, branched chain or substituted aromatic group. The head group may be charged, such as a quaternary amine or a carboxylate group, or neutral, such as polyoxyethylenes. Zwitterionic surfactants possess two groups, one cationic and one anionic, such that overall charge varies with pH. Surfactants are classified according to the structure of the head group: cationic, anionic, nonionic or zwitterionic.

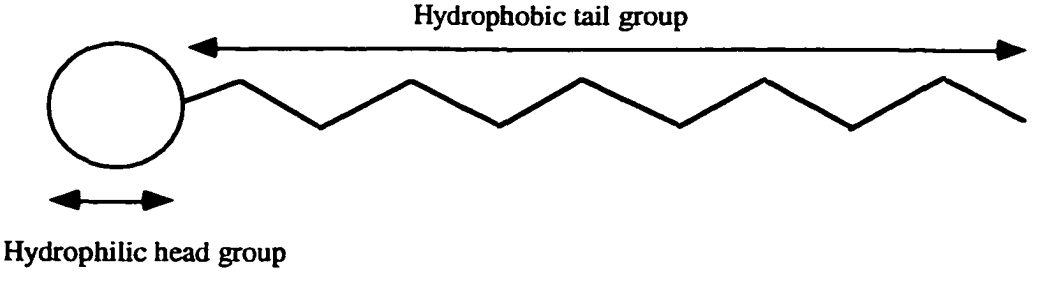

Figure I.2 Simplified structure of a surfactant monomer.

A representative of each class of surfactant was used for the LM-CEUF ligand studies presented here. The name and structure of each are shown in Table I.4. Cetylpyridinium nitrate ($CPNO_3$) was the cationic surfactant used in most cases. The nitrate counterion was substituted for the chloride present in the

commercial surfactant, cetylpyridinium chloride (CPC), in order to reduce side equilibria, resulting from formation of metal chloride complexes and to avoid precipitation of $PbCl_2$. Polyoxyethylene nonylphenyl ether ($NP(EO)_{10}$ or CO660) was the nonionic surfactant used in some of the preliminary studies; however, it was unsuitable for use in spectrophotometric studies due to the presence of a chromophore which absorbs in the same region as Kelex 100. In later studies, hexaoxyethylene *n*-dodecyl ether ($C_{12}(EO)_6$) was substituted because it lacks a chromophore and has a high degree of purity and monodispersity. Spectrophotometric titrations as a function of pH were also performed in solutions containing sodium dodecyl sulfate (SDS), a common anionic surfactant, and the zwitterionic surfactant *N,N*-dimethyl-(*n*-dodecyl)-amine-*N*-oxide (DDAO). Separation studies were not done in DDAO because at the high pH (7.0-9.0), where Kelex 100 complexed the target metals most effectively, DDAO has an overall neutral charge. Based on titration results, it appeared that little additional information could be obtained beyond studies done in the nonionic surfactants, $C_{12}(EO)_6$ and CO660. SDS was not used for separation studies, either, due to the tendency for the negatively charged micelles to nonselectively bind metal ions.

Table I.4 Structure and CMC of surfactants

Surfactant	Structure	CMC (M) [a]
Cetyl pyridinium nitrate ($CPNO_3$)	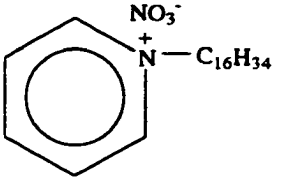	6.1×10^{-4} (b)
Cetyl pyridinium chloride (CPC)	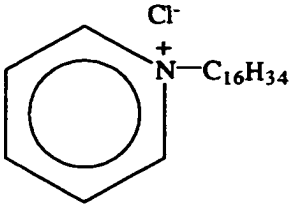	9.0×10^{-4} (c)
Polyoxyethylene nonylphenyl ether ($NP(EO)_{10}$ or CO660	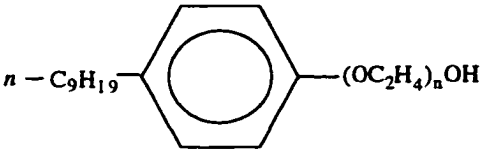	7.5×10^{-5} (d)
Hexaoxyethylene *n*-dodecyl ether ($C_{12}(EO)_6$)	$n-C_{12}H_{25}(OC_2H_4)_6OH$	8.7×10^{-5} (e)
Sodium dodecyl sulfate (SDS)	n-$C_{12}H_{25}SO_4^-$, Na^+	8.2×10^{-3}(f)
N,*N*-dimethyl-(*n*-dodecyl)-amine-*N*-oxide (DDAO)	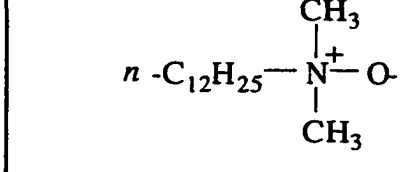	2.1×10^{-3}(g)

(a) at 25°C (b) Ref. 50 (c) Ref. 69 (d) Ref. 67 (e) Ref. 68 (f) Ref. 66 (g) Ref. 70

In aqueous solution, surfactant monomers are solubilized throughout the bulk solution and adsorbed at the air-water interface until a characteristic concentration known as the critical micelle concentration (CMC) is reached. At this point, the monomers begin to assemble into loose aggregates known as micelles. An important characteristic of the CMC is that there is an abrupt break in a number of solution properties, including surface tension and conductivity.

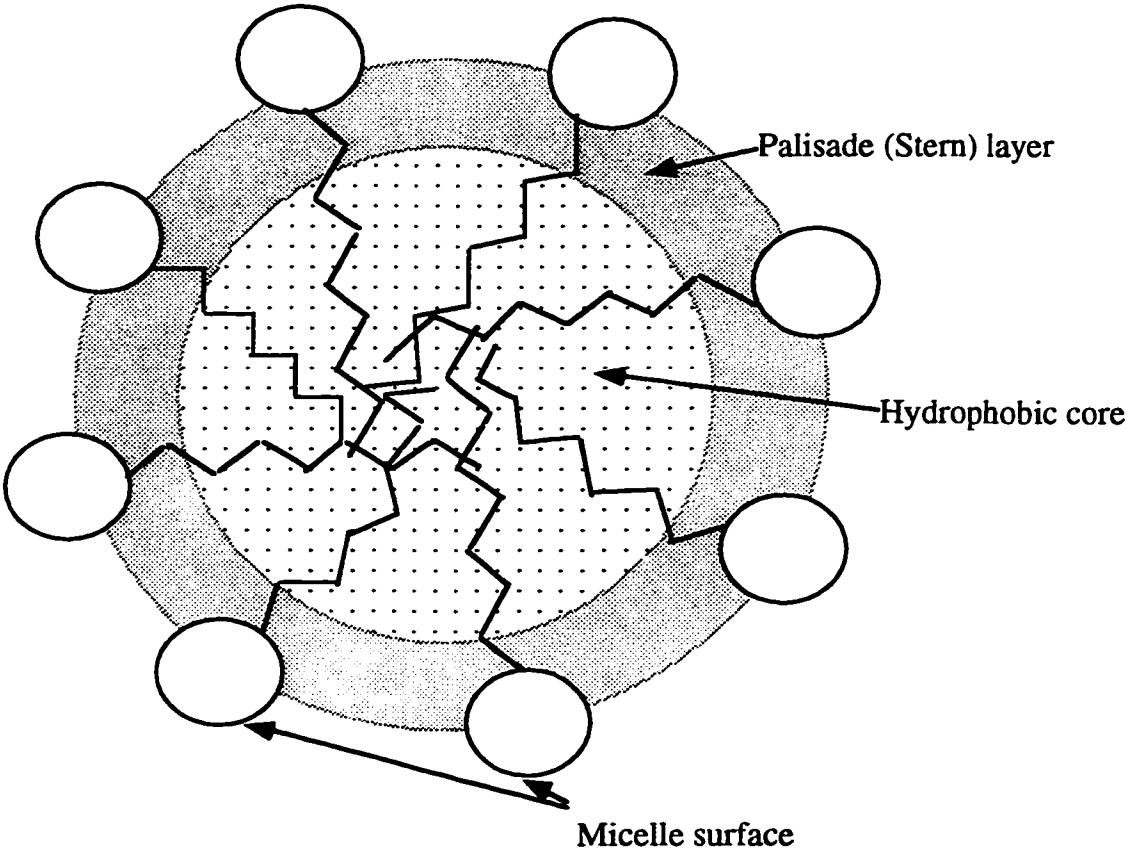

Figure I.3 Diagram of the regions of micellar polarity.

These changes are the basis for different experimental techniques for determining the CMC of a given surfactant (20). The driving force for the formation of micelles is the reduction in free energy achieved by concentrating the hydrophobic tails at the center of the micelle. This reduces the interaction of the tail groups with the polar, aqueous environment. The hydrophilic head groups form a polar "surface" and the polarity decreases moving inward. The different regions of the micelle are shown in Figure I.3. Monomers remain in dynamic equilibrium with the micelles such that there is a rapid exchange of monomer between the micelles and the bulk solution (Figure I.4). Added surfactant will generally increase the number of micelles but does not change the concentration of monomer in solution.

The number of monomers which make up a micelle is known as the aggregation number (n). Micellar shape and aggregation number are generally a function of the shape and polar nature of the head group and the length of the hydrophobic tail. Near the CMC, aggregation numbers are low, generally below 100, and micelles are roughly spherical in shape. At higher surfactant concentrations, aggregation numbers increase and micelles may be elongated and rod-like or flattened into a disk. Other factors which affect the shape and size of micelles include temperature and the concentration and type of other solutes present (20). Membrane separations may be adversely affected by changes in micelle shape.

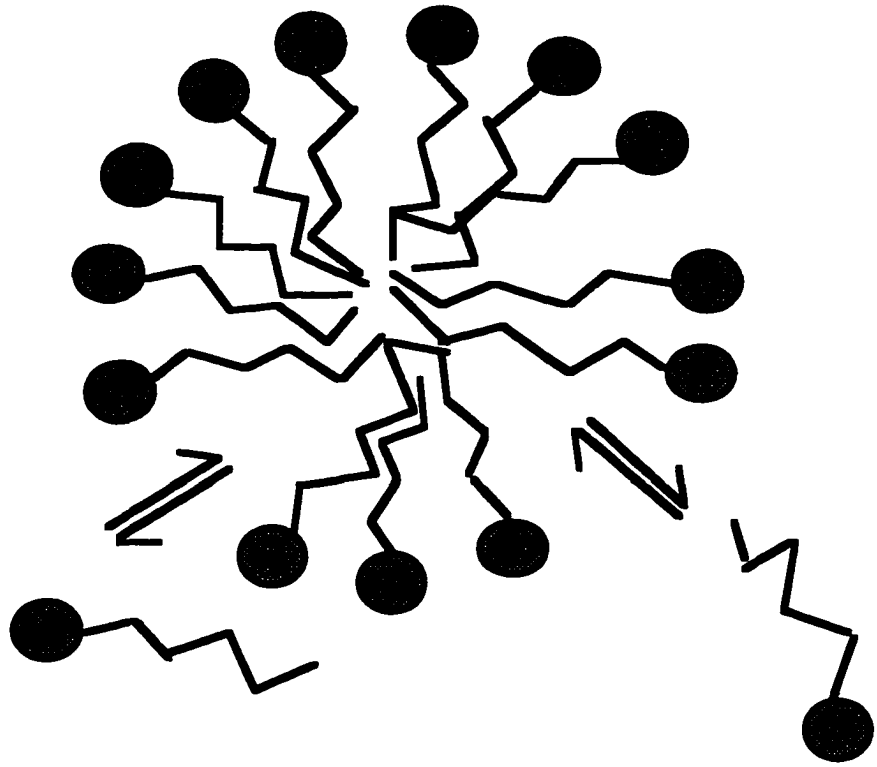

Figure I.4 Monomer-micelle equilibrium

Ionic surfactants have a charged headgroup, either cationic or anionic, and an associated counterion of opposite charge. Between the micellar head groups and extending into the first few carbons of the hydrocarbon tail is the region known as the palisade layer or Stern layer. This has been described as essentially a concentrated electrolyte solution in ionic surfactants, due to the presence of charged headgroups, bound counterions and water of hydration

(21). The innermost region is formed by the intertwined tail groups. It is the most hydrophobic and is essentially hydrocarbon-like in nature.

These variations in polarity in a micelle give surfactants their most useful property, the ability to solubilize a wide range of substrates. At the charged surface, ions of opposite charge are held through electrostatic attraction. Solutes that are polar but not ionic, such as alcohols and esters, can be solubilized in the palisade layer and fats and oils and other nonpolar materials are incorporated into the core. Amphiphiles such as long chain fatty acids are oriented such that the polar end is held towards the micelle surface with the tails extending into the core (22, 23).

The polar surface of nonionic surfactants is formed by hydrated ether oxygens. Since the headgroups are uncharged, the change in polarity from the exterior of the micelle to the interior is not as great as it is for ionic micelles. Polar solutes are bound through dipole-dipole interactions, ion-dipole interactions and hydrogen bonding at the micelle surface rather than electrostatic forces.

Micellar-Enhanced Ultrafiltration (MEUF)

Micellar-enhanced ultrafiltration (MEUF) is a separation technique in which surfactant is added to wastewater in order to solubilize organic or ionic solutes. A stirred cell MEUF apparatus is shown in Figure I.5. The waste stream is fed into an ultrafiltration cell with the surfactant. The surfactant

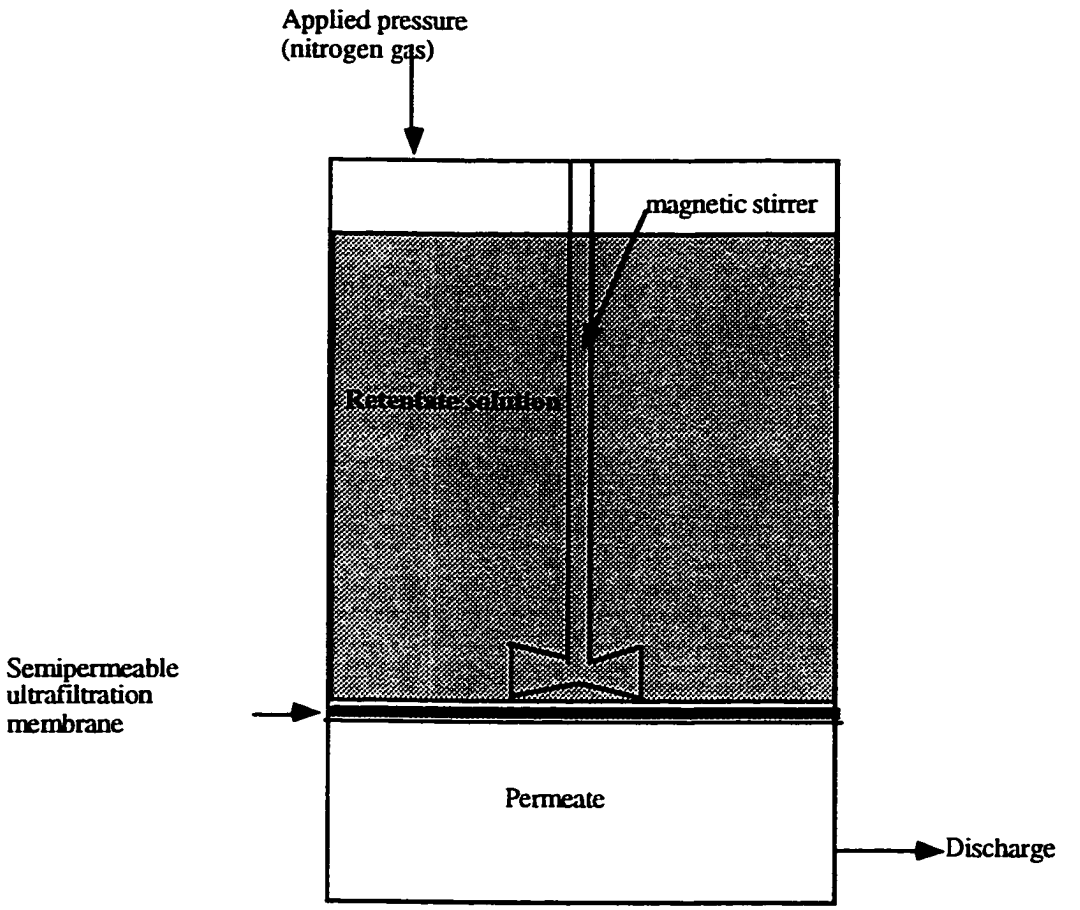

Figure I.5 Stirred cell ultrafiltration apparatus.

concentration is maintained well above the CMC, ensuring that most of the surfactant is present as micelles. Solutes are solubilized into the interior of the micelle or held at the surface of the micelle. Nitrogen pressure applied to the ultrafiltration cell causes the wastestream to be forced through an ultrafilter or semipermeable membrane with pore sizes such that micelles are retained while allowing the bulk solution to pass through. Membranes used in this study had a molecular weight cutoff (MWCO) of 5000. The resulting effluent, or permeate, is largely free of target solutes and is suitable for recycling or disposal. The retentate phase contains the concentrated target species. It is then stripped of the target species and the surfactant is recycled back into the MEUF cell. The effectiveness of the separation is expressed in terms of percent rejection (%R) of the target species, X, by the membrane as shown in Equation I.1, where $[X]_P$ and $[X]_R$ represent the concentration of the target species, X, in the permeate and retentate, respectively.

$$\%R = \left(1 - \frac{[X]_P}{[X]_R}\right) \times 100 \qquad \textbf{Equation I.1}$$

This technique has been shown to be quite effective for separation of low molecular weight organic solutes such as benzene, cyclohexane and hexane from water (32). Experiments with 4-tert-butylphenol in 1-hexadecylpyridinium chloride surfactant produced greater than 99% rejection of the organic solute (30). Substituting an anionic surfactant will allow metal ions to be removed

simultaneously. The negatively charged micelles will bind metal cations through electrostatic attractions (25). In experiments with mixtures of three metals, cadmium, zinc and copper, Scamehorn et al. showed that all three metals could be removed with at least 96% rejection using SDS (26). However, most waste streams will have high concentrations of electrolytes that are not of concern for disposal purposes. Since the binding mechanism for ions in MEUF is based solely on charge, the available binding sites will be quickly saturated by such multivalent cations as calcium and magnesium. Therefore, a method for selectively removing only those ions of concern, so called target ions, would have great advantage.

Ligand-Modified Colloid-Enhanced Ultrafiltration (LM-CEUF)

A technique which more selectively targets toxic ions is ligand-modified colloid-enhanced ultrafiltration (LM-CEUF). There are two types of LM-CEUF classified according to the type of colloid used to bind the target ions. The first type, known as ligand-modified polyelectrolyte-enhanced ultrafiltration (LM-PEUF) binds target ions with high molecular weight polymers which contain ionizable side groups. The side groups dissociate in solution and ions of opposite charge are bound by electrostatic attraction. Selectivity is introduced through the use of ligands which bind metal ions and create a multivalent anionic species. The negatively charged complexes are then bound to a cationic polyelectrolyte. The second type of LM-CEUF is ligand-modified micellar enhanced-ultrafiltration (LM-MEUF). An amphiphilic ligand with a chelating

head group is added to a waste stream where it preferentially complexes with the target species. It is then solubilized into the surfactant micelle where it is retained behind the membrane during ultrafiltration. A simple diagram of the LM-MEUF process is shown in Figure I.6. As with MEUF, the surfactant is added at concentration well in excess of the CMC.

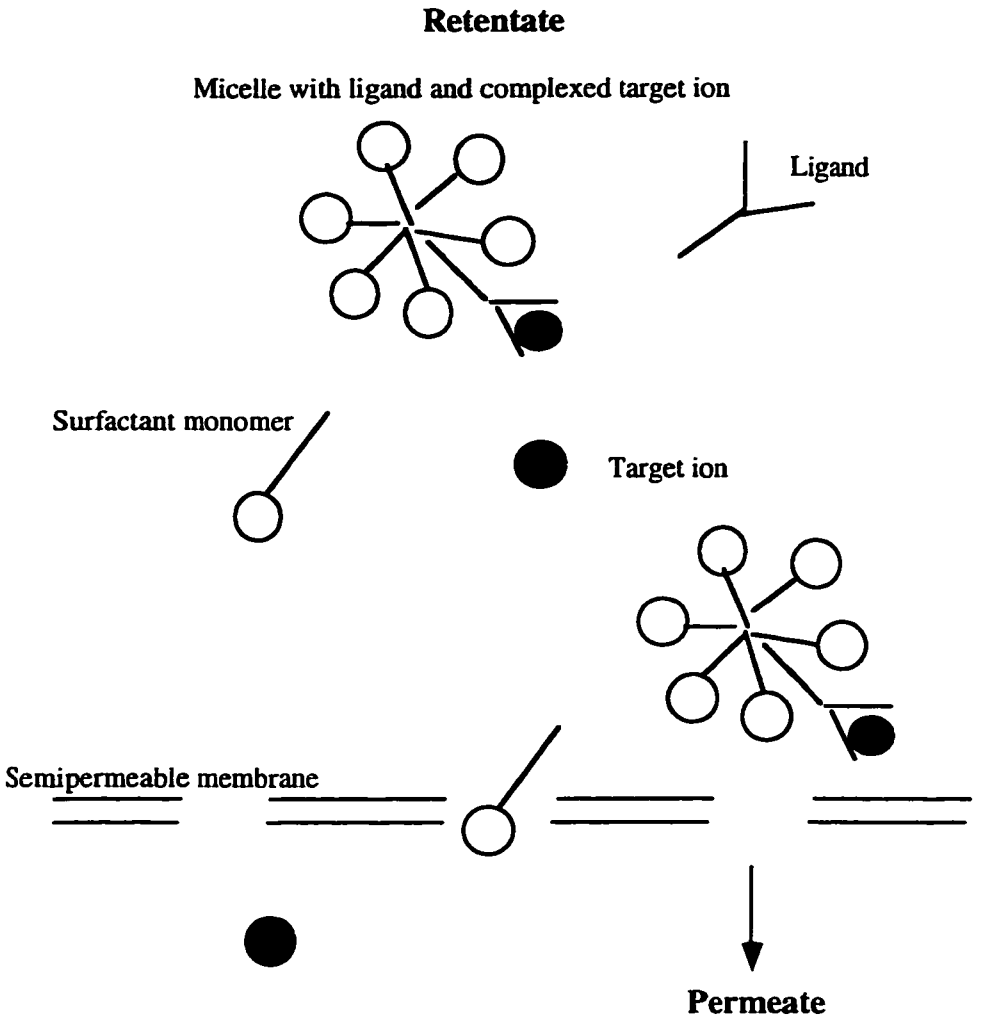

Figure I.6 Diagram of the LM-MEUF process

Experiments with different combinations of metal, ligand and surfactant have established the effectiveness of LM-MEUF. Klepac et al. (27) demonstrated the selectivity of an iminodiacetic acid ligand for copper in the presence of calcium. Copper was rejected up to 99.8% with no rejection of calcium in cationic surfactant. Subsequent sudies showed that iminodiacetic acid

ligands were capable of greater than 98% rejections of copper in nonionic surfactant solutions. Copper could also be targeted in mixtures of Cd^{2+}, Cu^{2+} and Zn^{2+} with no rejection of the competing ions (35,49). Later work was done with a commercial alkyl-β-diketone extractant as a ligand which again showed greater than 99% rejection of copper with no rejection of calcium (29). Some efforts have been made to target metals other than copper. Pramauro et al. (28) used derivatized salicylic acid ligands in nonionic and nonionic/cationic surfactants to preconcentrate iron with more than 98% rejection and Roach (50) used ligands derived from nitrilotriacetic acid with $CPNO_3$ cationic surfactant or polyelectrolyte to separate lead with 99.9% rejection. The work presented here is the first which examines the effectiveness of ligands targeting cadmium and mercury for use with LM-MEUF.

Semi-Equilibrium Dialysis (SED)

Laboratory screening and characterization of LM-MEUF systems require repetitive analyses. In order to more easily reproduce test conditions as well as run multiple experiments simultaneously, a small volume laboratory scale technique known as semi-equilibrium dialysis (SED) is employed. A schematic representation of an SED cell is shown in Figure I.7. Studies have shown that results obtained from SED experiments can be used to accurately predict results of LM-MEUF experiments (33, 34). A small volume of solution containing surfactant, ligand, target ion and any additional electrolytes or competitor ions is introduced into one side of an SED cell through a small hole at the top. This is

the retentate solution. A semipermeable membrane separates this retentate solution from a second chamber which contains the permeate solution, usually deionized water with buffer at the expermental pH. The cell is sealed and allowed to sit undisturbed for 20-24 hours after which the solutions are removed and analyzed. During the course of the experiment all species present which are able to pass across the semipermeable membrane come to equilibrium. (30) The molecular weight cutoff (6000 MWCO) of the membrane is selected to be smaller than the effective molecular weight of the micelle so micelles and any solutes which are partitioned into the micelle are held on the retentate side of the cell. Percent rejection of target ion is calculated using Equation I.1 in the same manner that is described for LM-MEUF experiments.

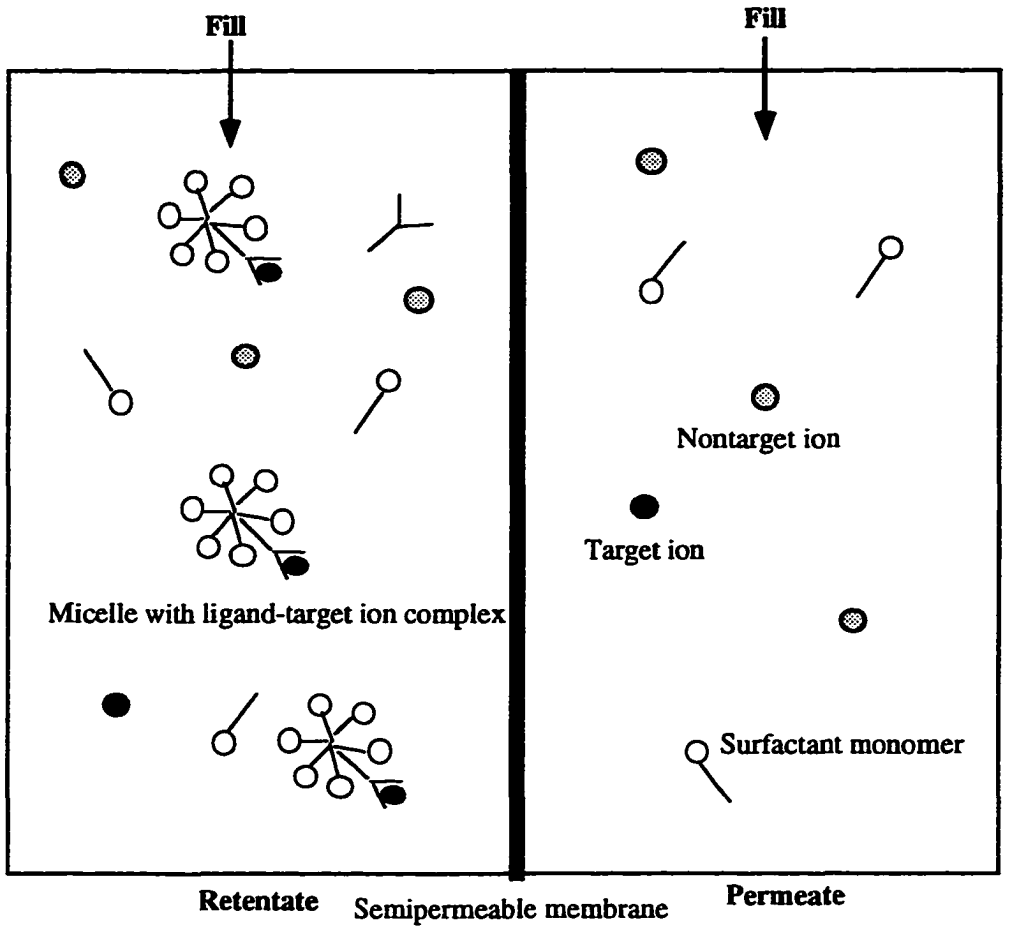

Figure I.7 Diagram of an SED cell

Chemistry of mercury and cadmium in water

Cadmium and mercury are group 12 metals which possess full outer d and s orbitals. They both readily form M^{2+} cations by losing electrons from the outer s orbital. Cadmium is almost exclusively divalent but mercury also occurs in a monovalent form (Hg_2^{2+}) as a dimer. In solution, mercury (I) disproportionates to a small extent, forming mercury (II) and elemental mercury (Equation I.2). Though fairly stable to disproportionation, the equilibrium is

$$Hg_2^{2+} \rightleftharpoons Hg^0 + Hg^{2+} \qquad \text{Log } K = -1.94 \qquad \textbf{Equation I.2}$$

easily shifted to the right by anything that will reduce the activity of the Hg^{2+} ion relative to the Hg_2^{2+} ion, including complexation. The ease with which Hg^0 is vaporized also serves to shift the equilibrium from the left to the right, so little Hg_2^{2+} is present without an excess of Hg^0. The ionic radius of Cd^{2+} is 0.97 Angstroms and that of Hg^{2+} is 1.05 Angstroms. Both Cd^{2+} and Hg^{2+} form 6-coordinate, octahedral aquo complexes. Complexes with larger ligands are commonly tetrahedral or, in the case of mercury, linear. Though similar in size to Ca^{2+}, the inefficient shielding of the nucleus by the full d or d and f subshells make Cd^{2+} and Hg^{2+} softer and more easily polarized than Ca^{2+}. Therefore, most compounds of Cd^{2+} and Hg^{2+} are largely undissociated in water with significant covalent character. The solubility of many compounds is low. Exceptions are

compounds of nitrate, perchlorate and fluoride which are extensively dissociated and hydrolyzed. Chloride compounds are moderately soluble, though once again, largely undissociated. Both cations form complexes readily with nitrogen and sulfur donating ligands. Tables I.5 and I.6 show equilibria for Cd^{2+} and Hg^{2+}, respectively, in water with those ligands which may be present at high concentrations (equal to or greater than the concentration of the metal) in LM-MEUF solutions.

Table I.5 Equilibria and cumulative formation constants for cadmium and common anions in water.

$iM^{2+} + jX^{-} \rightleftharpoons M_iX_j^{2i-j}$	Log β_{ij}, μ=0.1[a]
$Cd^{2+} + OH^{-} \rightleftharpoons CdOH^{+}$	3.48 (b)
$Cd^{2+} + 2OH^{-} \rightleftharpoons Cd(OH)_2$	6.07 (b)
$Cd^{2+} + 3OH^{-} \rightleftharpoons Cd(OH)_3^{-}$	8.67 (b)
$Cd^{2+} + Cl^{-} \rightleftharpoons CdCl^{+}$	1.6 (c)
$Cd^{2+} + 2Cl^{-} \rightleftharpoons Cd(Cl)_2$	2.0 (c)
$Cd^{2+} + 3Cl^{-} \rightleftharpoons Cd(Cl)_3^{-}$	1.8 (c)
$Cd^{2+} + 4Cl^{-} \rightleftharpoons Cd(Cl)_4^{2-}$	1.3 (c)
$Cd^{2+} + NO_3^{-} \rightleftharpoons CdNO_3^{+}$	0.08 (d)
$Cd^{2+} + 2NO_3^{-} \rightleftharpoons Cd(NO_3)_2$	-0.4 (d)

(a) at 25°C (b) Ref. 59 (c) Ref. 58 (d) Ref. 60

Table I.6 Equilibria and cumulative formation constants for mercury and common anions in water.

$iM^{2+} + jX \rightleftharpoons M_iX_j^{2i-j}$	Log β_{ij}, μ=0.1[a]
$Hg^{2+} + OH^- \rightleftharpoons HgOH^+$	10.18 (b)
$Hg^{2+} + 2OH^- \rightleftharpoons Hg(OH)_2$	21.16 (b)
$Hg^{2+} + 3OH^- \rightleftharpoons Hg(OH)_3^-$	20.27 (b)
$2Hg^{2+} + OH^- \rightleftharpoons Hg_2OH^{3+}$	10.70 (b)
$3Hg^{2+} + 3OH^- \rightleftharpoons Hg_3(OH)^{3+}$	34.97 (b)
$Hg^{2+} + Cl^- \rightleftharpoons HgCl^+$	5.79 (c)
$Hg^{2+} + 2Cl^- \rightleftharpoons Hg(Cl)_2$	12.85 (c)
$Hg^{2+} + 3Cl^- \rightleftharpoons Hg(Cl)_3^-$	14.1 (c)
$Hg^{2+} + 4Cl^- \rightleftharpoons Hg(Cl)_4^{2-}$	15.0 (c)
$Hg^{2+} + NO_3^- \rightleftharpoons HgNO_3^+$	1.06 (d)
$HgOHCl + H^+ \rightleftharpoons HgCl^+$	3.1 (c)
$HgCl_2 + OH^- \rightleftharpoons HgOHCl + Cl^-$	4.09 (c)
$Hg(OH)_2 + Cl^- \rightleftharpoons HgOHCl + OH^-$	3.77 (c)

(a) at 25°C (b) Ref. 59 (c) Ref. 58 (d) Ref. 60

Ligand Characteristics

Two ligand characteristics are important for a successful separation. The first is that the ligand must have a high affinity for the target metal. For example, in order to achieve 99% rejection of the metal ($[ML]_{mic} \geq 0.99[M]_{Tot}$), the conditional binding or formation constant (K_{ML}') must be at least 1×10^7 M^{-1} for a solution initially containing 1 mM ligand and 1 mM metal. Furthermore, to ensure selectivity of the ligand for the target metal, the binding constant of the ligand-target metal complex must be at least 1×10^6 higher than that of any competing metals (35). The second criteria is that the ligand should have a high solubility in the chosen surfactant but very low solubility in water. This minimizes the amount of ligand, as well as complexed metal, which will be lost through the membrane during the ultrafiltration. A ligand concentration of 1-2% of the total surfactant concentration is desirable so for a typical surfactant concentration of 0.03-0.05 M, at least 0.3-0.5 mM ligand should be solubilized. Other characteristics of the ligand and its target metal complex are considered in order to get the best separation efficiency with the minimum material costs. The ligand is often the most expensive reagent used in the LM-MEUF system. In order to use the minimum quantity of ligand, the metal to ligand ratio (M:L) should be as high as possible. Generally, this could be expected to be 1:1. Ligand use would also be minimized by "recycling" the ligand and surfactant. The ligand should be chemically stable to withstand stripping the metal from the complex and reusing it through several LM-MEUF cycles. Mild pH conditions (4-9) for stripping would reduce the tendency for the ligand and surfactant to

degrade. In addition, less corrosion resistant hardware could be used and material costs for the acid and base needed for pH adjustment could be minimized. Finally, the ligand should be available commercially or easily synthesized.

Ligands employed for LM-MEUF studies

7-(4-Ethyl-1-methyloctyl)-8-hydroxyquinoline (Kelex 100)

7-(4-Ethyl-1-methyloctyl)-8-hydroxyquinoline is available as the commercial metal extractant Kelex 100 (Figure I.8). It was originally developed for use as a hydrometallurgical extractant for copper (II) but has found more extensive use commercially for other metals including gallium, germanium and copper (I) (36, 55). Research has also been conducted into numerous other extraction applications including precious metals such as gold, palladium and platinum (56, 57), the lanthanides, cerium and lanthanum, (51) and numerous other economically useful metals including rhodium (53), nickel (54) and cobalt (52). It is commonly dissolved in an organic solvent such as kerosene, and the metal removed by extraction into an acid phase. The chelating head group, 8-

hydroxyquinoline (8HQ), also known as oxine, is a common analytical

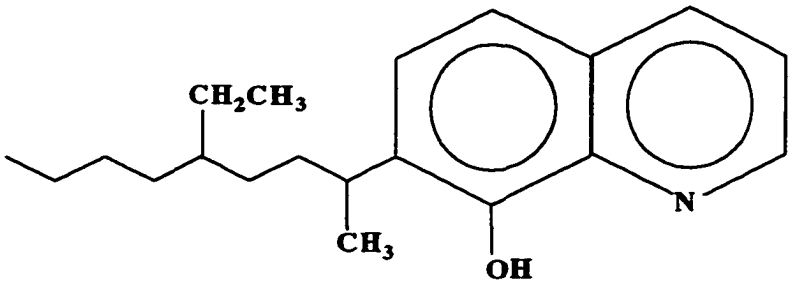

Figure I.8 Structure of 7-(4-Ethyl-1-methyloctyl)-8-hydroxyquinoline

reagent. 8HQ is used for photometric determinations, solvent extractions and as a metal precipitant for a wide range of metal ions. It is bidentate and complexes most polyvalent metal ions through coordination of both the oxygen and nitrogen. The cadmium-8HQ complex (CdL_2) is neutral and four coordinate. Some selectivity is achieved through careful selection of working pH range. Kelex 100 was selected for potential use as a ligand for LM-MEUF because of its low water solubility and affinity for a wide range of metal ions. A preliminary estimate of the affinity of Kelex 100 for the metal may be made based on the formation constants of the unalkylated chelating agent in water. (Table I.7) The cumulative formation constant for complexation of cadmium by 8HQ, β_{ML3}, is 9.1×10^{17}, indicating a strong affinity for cadmium. The only other potential competing metal which has a formation constant of a similar magnitude is zinc ($\beta_{ML2} = 6.3 \times 10^{15}$). It is possible that adjustment of the pH range selected for the separation may allow discrimination between zinc and cadmium;

however, zinc is also an EPA priority pollutant and so simultaneous removal of zinc and cadmium would not necessarily be a disadvantage.

The protonation constants, K_H, are shown for 8HQ dissolved in water; however, these values may be expected to shift when dissolved in surfactant. Previous studies (40, 41, 42) have shown that incorporation into micelles will cause predictable shifts in K_H's due to the microenvironment at the micelle surface. These shifts may be particularly dramatic with charged ligands in ionic surfactant due to either charge stabilization or charge repulsion between ligand and micelle. Spectrophotometric titrations were performed with Kelex in each of the experimental surfactants to determine the conditional log K_H's.

Table I.7 Relevant equilibria and equilibrium constants for 8HQ.

$iM^{2+} + jX \rightleftharpoons M_iX_j^{2i-j}$	Log β_{ij}, μ=0.1 [a, b]
$H^+ + L^- \rightleftharpoons HL$	9.65 (a)
$2H^+ + L^- \rightleftharpoons H_2L^+$	4.97 (a)
$Cd^{2+} + L^- \rightleftharpoons CdL^+$	7.34 (a)
$Cd^{2+} + 2L^- \rightleftharpoons CdL_2$	13.44 (a)
$Cd^{2+} + 3L^- \rightleftharpoons CdL^-$	17.96 (a)
$Ca^{2+} + L^- \rightleftharpoons CaL^+$	2.82 (a)
$Zn^{2+} + L^- \rightleftharpoons ZnL^+$	8.52 (a)
$Zn^{2+} + 2L^- \rightleftharpoons ZnL_2$	15.8 (a)
$Pb^{2+} + L^- \rightleftharpoons PbL^+$	9.02 (a)
$Mg^{2+} + L^- \rightleftharpoons MgL^+$	4.31 (a)

(a) at 25°C (b) Ref. 61

Table I.8 Solubility equilibria and log Ksp's for metal-8HQ complexes

$iM^{2+} + jX \rightleftharpoons M_iX_j^{2i-j}$	Log K_{sp}, μ=0.1 [a, b]
$CdL_2(s) \rightleftharpoons Cd^{2+} + 2L^-$	-21.4
$ZnL_2(s) \rightleftharpoons Zn^{2+} + 2L^-$	-23.5
$PbL_2(s) \rightleftharpoons Pb^{2+} + 2L^-$	-22.0

(a) at 25°C (b) Ref. 61

Alkylthiourea

Thiourea (tu) is a common complexing and analytical reagent. It has a

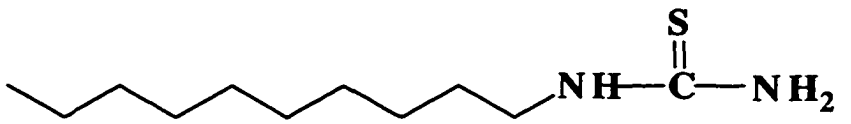

Figure I.5 Structure of 1-decyl-2-thiourea

high affinity for soft (class b) metals including mercury but forms only weak complexes with cadmium (62, 63). Formation constants for complexes of cadmium and mercury with tu are shown in Table I.9. It was selected for potential use as a LM-MEUF ligand because, based on the difference in the formation constants, thiourea should be quite selective for mercury. Akylated thiourea compounds are available commercially with varying alkyl chain lengths. Decylthiourea, shown in Figure I.9, was selected for most of the separation experiments because it had a low solubility in water and was expected to partition strongly into micelles.

Though thiourea has the potential to act as a bidentate ligand, studies of complexes in aqueous solution have shown that mercury is complexed by sulfur alone, probably owing to mercury's preference for linear complexes (64). Complexes of cadmium may be four coordinate, though one or two coordinate complexes are more stable. It has no detectable basic properties (64) and is a very weak monobasic acid with a log K_H ~15 at 25°C, making it insensitive to pH changes.

Table I.9 Equilibria and cumulative formation constants for mercury and cadmium complexes of thiourea.

$iM^{2+} + jX \rightleftharpoons M_iX_j^{2i-j}$	Log β_{ij}, μ=0.1[a]
$Hg^{2+} + 2L \rightleftharpoons HgL_2^{2+}$	21.3 (b)
$Hg^{2+} + 3L \rightleftharpoons HgL_3^{2+}$	24.2 (b)
$Hg^{2+} + 4L \rightleftharpoons HgL_4^{2+}$	25.8 (b)
$Cd^{2+} + 2L \rightleftharpoons CdL_2^{2+}$	2.6 (c)

(a) at 25°C (b) Ref. 65 (b) Ref. 64

In order to determine preliminary experimental conditions of metal and ligand concentration as well as pH, species distribution calculations were carried out using the program COMICS (87) for each ligand and target metal. The species distribution curves are shown in Figures I.10 and I.11. The concentration of different species were plotted as a function of pH. The maximum amount of mercury is complexed by thiourea at any pH below pH 11 for 0.10 mM Hg and 0.30 mM thiourea. Thiourea is insensitive to pH change due to its high pKa, so its useful range is wide. Competition from hydroxide species is not significant until about pH 13. It is also worth noting that the 3:1 excess of ligand allows formation of significant concentrations of the 1:3 and 1:4

mercury-thiourea complexes. Calculations for 0.30 mM 8HQ and 0.15 mM Cd show that complexation of cadmium shows a maximum between pH 5.5 and 12 for the 1:2 metal-ligand complex. This is particularly useful because it indicates a wide range of working pH but also indicates that the cadmium may be stripped from the ligand at relatively moderate pH values of 2-3.5.

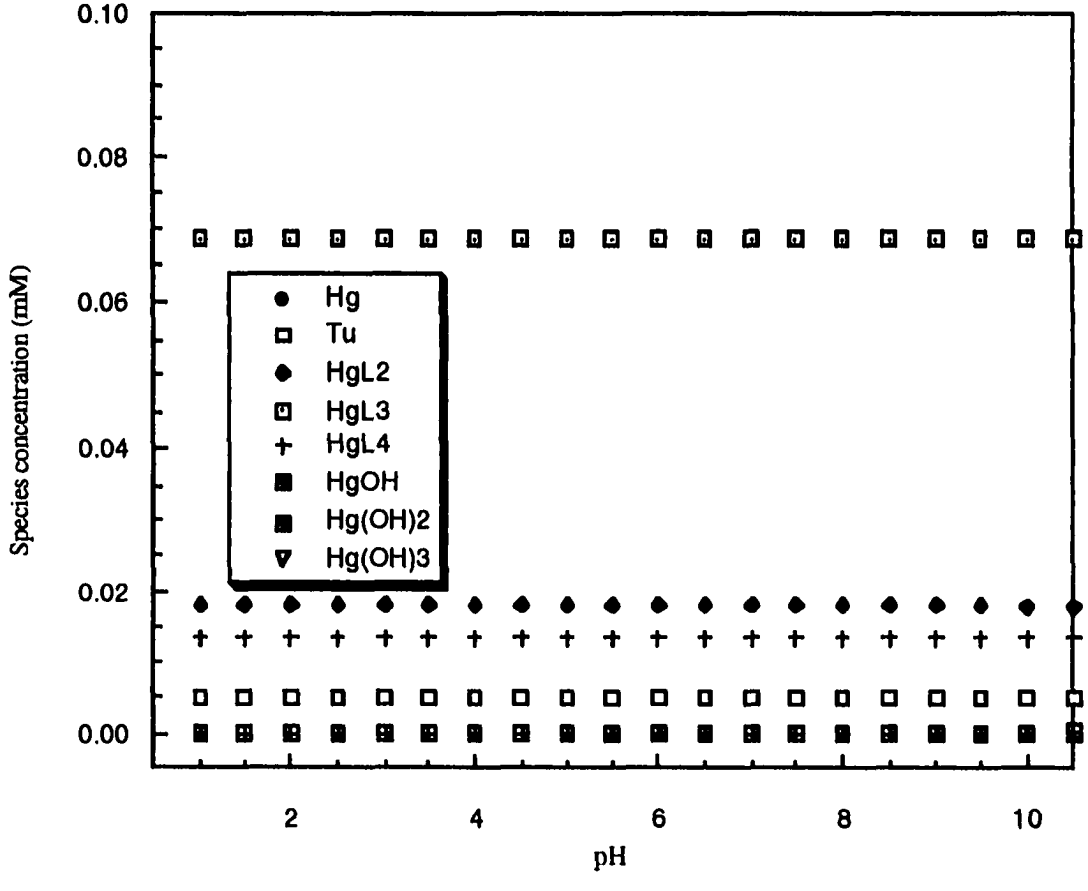

Figure I-10 Species distribution diagram for 0.3 mM thiourea and 0.1 mM Hg^{2+}.

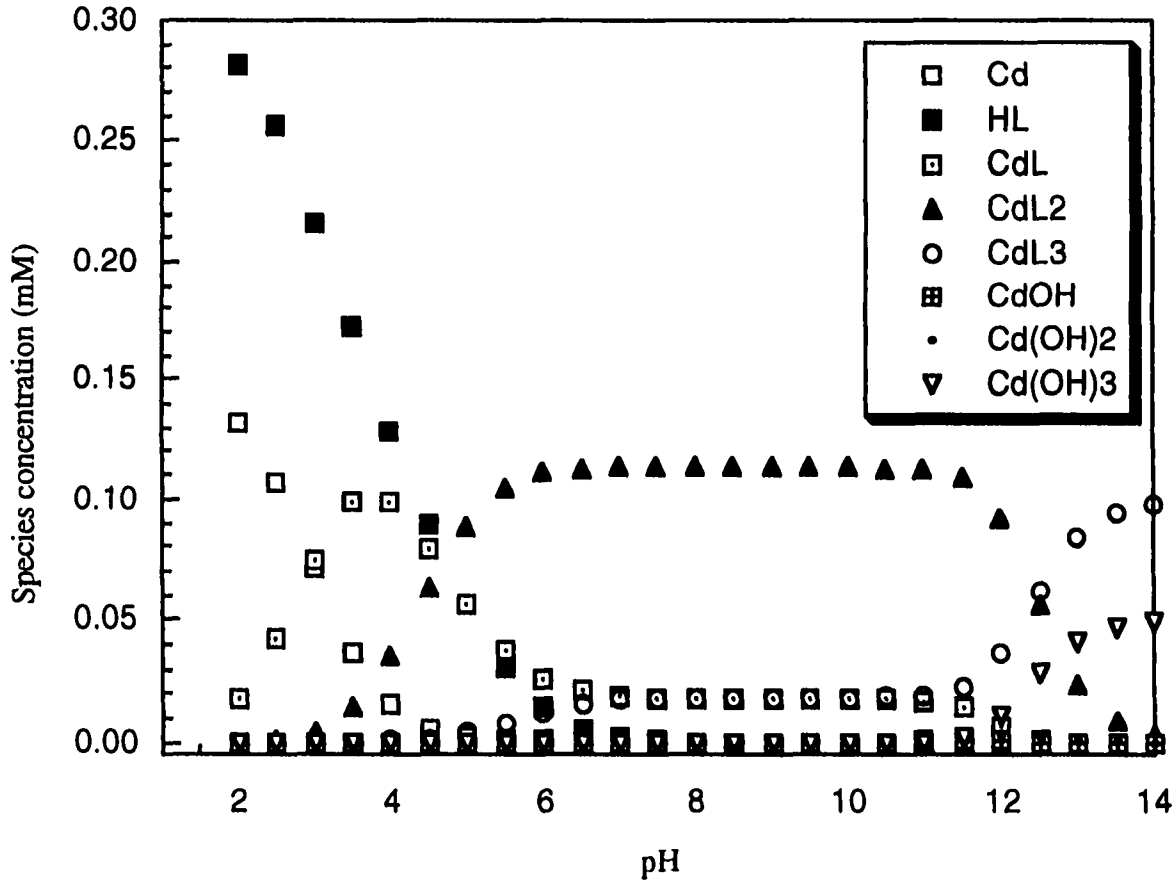

Figure I-11 Species distribution diagram for 0.3 mM 8HQ and 0.15 mM Cd^{2+}.

Objectives

The objective of the work presented is to examine the potential use of Kelex 100 as a ligand for separation of cadmium and a commercially available alkylated thiourea compound as a ligand for the separation of mercury using LM-MEUF. The conditions for optimum separation will be identified as well as conditions which will allow the ligand to be regenerated. Ligands will be characterized with the following experiments:

1. Spectrophotometric titration of Kelex 100 in surfactant solution for the purpose of determining conditional protonation constants (log K_H).

2. Spectrophotometric titration of Kelex 100 in surfactant solution for the purpose of determining metal:ligand stoichiometry .

3. Separation studies utilizing SED and UF to determine the effects of variations in pH, ligand, metal and surfactant concentration, and competing metal ions for Kelex 100 and thiourea.

Chapter II

Experimental

Reagents

Distilled deionized water - D.D. H_2O. All aqueous solutions were prepared with water which was purified by distilling deionized water with a Corning Model MP-3A Mega-Pure distillation apparatus.

Hydrochloric acid - HCl, reagent grade, Mallinckrodt Co.

Sulfuric acid - H_2SO_4, trace metal grade, Fisher Scientific Co.

Ammonium hydroxide - NH_4OH, reagent grade, Mallinckrodt Co.

Nitric acid - HNO_3, trace metal grade, Fisher Scientific Co.

Sodium Hydroxide - NaOH, low CO_2 0.1 M "Dilut-it" concentrate, J.T. Baker Co., and NaOH pellets, 97.4%, reagent grade, Fisher Scientific Co.

Chloroform - $CHCl_3$, reagent grade, 99.9% pure, Mallinckrodt Co.

Calcium carbonate - $CaCO_3$, primary standard grade, Mallinckrodt Co.

Cadmium perchlorate - $Cd(ClO_4)_2 \cdot 6H_2O$, reagent grade, 99.9% pure, Alfa Products.

Cadmium metal - Cd, 99.99% , J.T. Baker Chemical .

Mercuric nitrate - $Hg(NO_3)_2 \cdot H_2O$, reagent grade, Fisher Scientific Co.

Lead nitrate - $Pb(NO_3)_2$, reagent grade, Matheson, Coleman & Bell.

Copper chloride - $CuCl_2$, anhydrous, reagent grade, Fluka A.G.

Sodium chloride - NaCl reagent grade, Mallinckrodt Co.

Zinc metal - Zn, reagent grade, 20 mesh granular, Mallinckrodt Co.

Potassium permanganate - $KMnO_4$, reagent grade, Fisher Scientific Co.

Stannous chloride - $SnCl_2 \cdot H_2O$, reagent grade, Mallinckrodt Co. A fresh 1%(w/v) solution was prepared for each set of analyses by dissolving in 1 mL of concentrated HCl and diluting with D.D. H_2O.

Disodium dihydrogenethylenediaminetetraacetate - Na_2H_2EDTA, primary standard grade, 99+%, Fisher Scientific Co.

Hydroxylamine hydrochloride - $NH_2OH \cdot HCl$, 97%, Aldrich Chemical Co.

1-Butanol - C_4H_9OH, 99+%, spectrophotometric grade, Aldrich Chemical Co.

Kerosene - obtained from Hollywood Corners, retail service station.

Sodium lauryl sulfate (sodium dodecyl sulfate) - SDS, electrophoresis grade, Fisher Scientific Co., used without further purification.

Hexadecyl pyridinium chloride - CPC, Hexcel Co., used without further purification.

Hexaoxyethylene *n*-dodecyl ether - $C_{12}(EO)_6$, Nikko Chemical Co. used without further purification.

N,N-Dimethyl-(*n*-dodecyl)-amine-*N*-oxide - DDAO, 30% aqueous solution, Fluka A.G., purified as described below.

Polyoxyethylene nonylphenyl ether - $NP(EO)_{10}$ or CO660, GAF Corp. used without further purification.

2-(*N*-Cyclohexylamino)ethanesulfonic acid - CHES, pH buffer with pK_a = 9.3 at 25 °C, Sigma Chemical Co., stock solutions (5-100 mM) prepared by weight.

N-[2-Hydroxyethyl]piperazine-*N*-[2-ethanesulfonic acid] - HEPES, pH buffer with pK_a = 7.5 at 25°C, Sigma Chemical Co., stock solutions (5-100 mM) prepared by weight.

2-(*N*-Morpholino)-2-ethanesulfonic acid - MES, pH buffer with pK_a = 6.15 at 25 °C, Sigma Chemical Co., stock solutions (5-100 mM) prepared by weight.

Diphenylthiocarbazone - Dithizone, Matheson Co., 0.01% stock solution (w/v) prepared in carbon tetrachloride and then diluted 1:10 for extraction.

4-(2-Pyridylazo)resorcinol, monosodium salt hydrate - PAR, 98%, Aldrich Chemical Co., indicator solution prepared in D.D. H_2O.

1-(2-Pyridylazo)-2-naphthol - PAN, indicator grade, GFS Co., prepared in 0.05 M DDAO surfactant solution.

Eriochrome Black T - EBT, reagent grade, J.T. Baker Co., indicator solution prepared in 75% triethanolamine and 25% absolute ethanol (v/v).

Xylenol Orange, sodium salt - XO, ACS reagent grade, Aldrich Chemical Co., indicator solution prepared in D.D. water.

Fast Sulphon Black - FSB, 65%, Sigma Co., indicator solution prepared in D.D. water.

Phosphorus pentoxide - P_2O_5, purified, obtained from Fisher Scientific Co.

Hexamethylenetetramine - Hexamine buffer, obtained from Eastman Kodak, 20%(w/v) solution prepared using D.D. water.

7-(4-Ethyl-1-methyloctyl)-8-quinolinol - Kelex 100, crude, Sherex Corp., purified as described below.

1-Decyl-2-thiourea - Dtu, 98%, Trans World Chemicals, Inc.

1-Hexyl-2-thiourea - Htu, Trans World Chemicals, Inc.

Purification and preparation of selected compounds

Purification of Dithizone

Solid dithizone was purified to remove oxidized impurities according to a procedure published by Sandell and Onishi (71). A 10% (w/v) solution was prepared in chloroform and filtered through a fritted glass filter. It was then extracted with four 50 mL portions of a 1:100 ammonium hydroxide solution. The fractions were combined and extracted with 10 mL of chloroform. The chloroform was discarded and the aqueous phase transferred to a flask. Sulfur dioxide gas was generated and bubbled through the extracted aqueous phase until the dithizone precipitated as a solid. The solids were then filtered onto a sintered glass crucible and dried under vacuum over potassium hydroxide.

Purification of Dimethyldodecylamine-*N*- Oxide (DDAO)

DDAO was purified prior to use by freeze-drying to remove the water and then recrystallizing several times from acetone. After purification it was stored in a tightly sealed container at 0° C.

Preparation of Cetylpyridinium Nitrate ($CPNO_3$)

In order to prevent side reactions of the chloride counterion with either

cadmium or mercury, the surfactant cetylpyridinium chloride (CPC) was modified to replace the chloride with nitrate counterions, forming cetylpyridinium nitrate ($CPNO_3$). $CPNO_3$ was prepared by mixing 250 mL of 0.1 M CPC with 250 mL of 1 M sodium nitrate ($NaNO_3$). A white precipitate was formed which was filtered through an ice cooled Buchner funnel, rinsed with cold water and then redissolved in 250 mL of warm water. An additional 250 mL of 1 M $NaNO_3$ was then added and the resulting precipitate filtered again. The nitrate form of the surfactant was then recrystallized a minimum of four times until chloride was no longer observed using silver nitrate.

Purification of Kelex 100

The commercial product Kelex 100 has been manufactured by three different companies using at least two different processes since its introduction in 1968. It has also attracted considerable attention for research purposes. Therefore, there have been a number of studies of the composition of Kelex 100 and attempts to identify the best procedure for its purification (36, 37). The crude material contains only about 85% of the active component, 7-(4-ethyl-1-methyloctyl)-8-hydroxyquinoline, as received. The structure is shown in Figure I.10. The remaining 15% contains both active and inert impurities. The presence of these impurities creates two important problems for quantitative studies. First, spectrophotometric studies are complicated by the absorbance changes of these minor compounds, particularly with changes in pH. In addition, lower molecular weight compounds which are capable of complexing

metal ions can affect separation studies by competing with the parent ligand for metal ions and then carrying them across the dialysis or ultrafiltration membrane.

Kelex 100 was purified using a procedure published by Cote and Bokobza (37). Several grams were initially dissolved in toluene and then extracted repeatedly (8-10x) with 1 M HCl to remove unalkylated 8-hydroxyquinoline. When the aqueous phase was no longer yellow, the organic phase was extracted repeatedly with D.D. H_2O until no chloride was detected with $AgNO_3$. The remaining organic phase was then degassed and toluene was removed under reduced pressure. Five distillations were done under vacuum (0.1 mm Hg) to obtain a single, pale yellow product which distilled at approximately 153 °C. This fraction was then dissolved in 50% (v/v) ethanolic 3M NH_4OH and the lead complex precipitated with an equal volume of aqueous 1 M $Pb(NO_3)_2$. The bright yellow precipitate was stirred for about 3 hours and then filtered, rinsed with a 0.1 M HNO_3 solution, followed by D.D. H_2O, and then ethanol. The resulting solids were dried over P_2O_5 and recrystallized from ethanol. After recrystallization, the lead complex was dissolved in a 30:70 mixture of 1-butanol and kerosene and extracted with 2 M H_2SO_4 to remove lead and regenerate the ligand. Finally, two additional vacuum distillations were done to remove solvent and isolate the product. Thin layer chromatography of the product with silica gel plates (J.T. Baker Inc.) (Figure II.1) shows a single fraction, mass spectrometry results verify a molar mass of 299 and the ^1H NMR spectrum, shown in Figure II.2, agrees with published results (37). Peak assignments are shown in Table II.1.

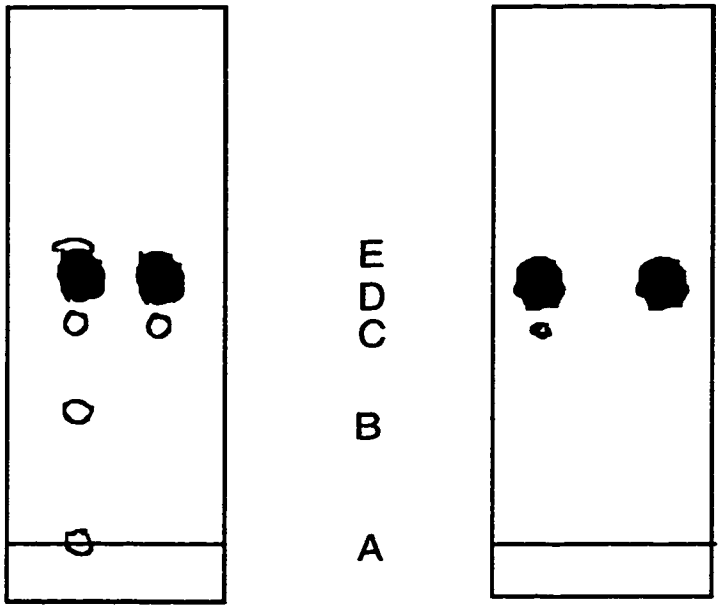

Figure II.1 Diagram of thin layer chromatography plates. Solvent system was 80:20 mixture of hexane and ethyl acetate. Plate 1) Separation of crude Kelex 100 on the left side shows a large spot of 7-(4-ethyl-1-methyloctyl)-8-hydroxyquinoline, $R_f = 0.58$ (D), unalkylated 8HQ, $R_f = 0.60$ (E) and smaller spots of unidentified, fluorescent impurities, $R_f = 0.42$(C), 0.24(B), 0.0(A). Following extraction with acid and the first distillation, the fluorescent impurities at $R_f = 0$ (A) and 0.24 (B), as well as the 8HQ (E) are no longer present (right side). Plate 2) After three distillations some of the fluorescent material at $R_f = 0.42$ (C) is still present (left side) but is no longer visible on the right following precipitation of the lead complex.

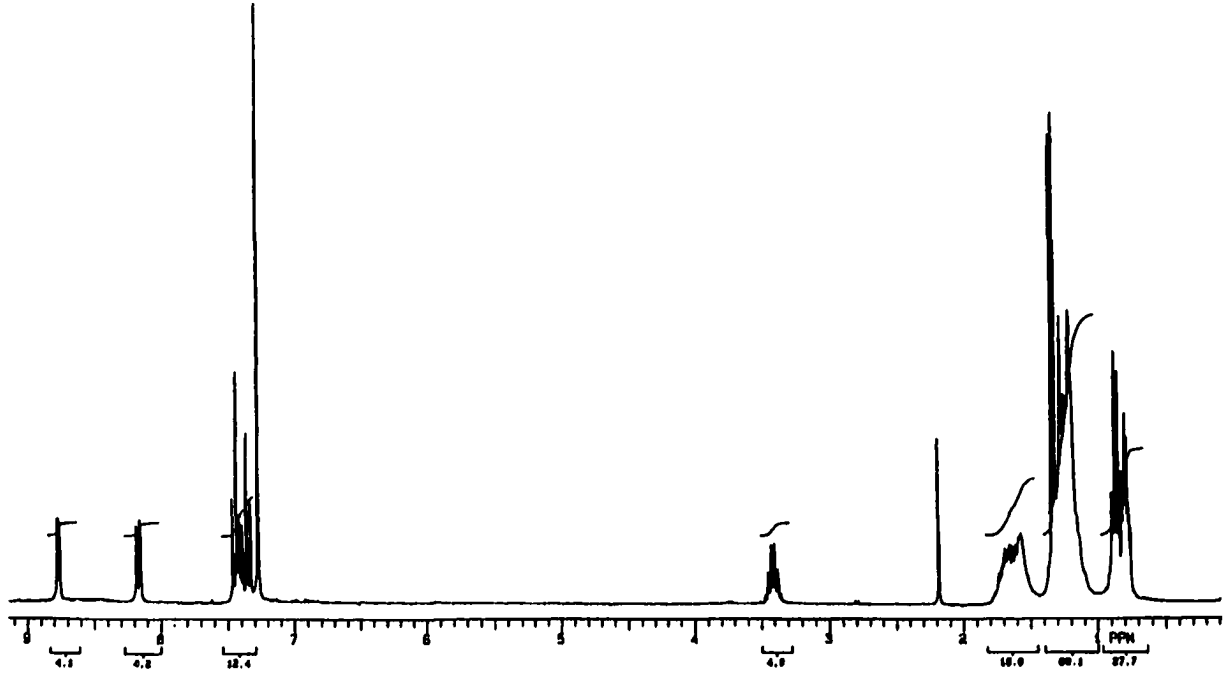

Figure II.2 ^{1}H-NMR spectrum of purified Kelex 100 in $CDCl_3$.

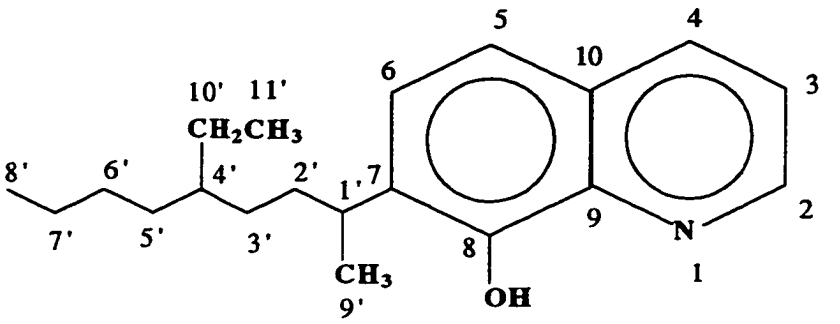

Chemical shift (ppm)			Peak assignment
doublet	8.17	1H	H_4
doublet	8.79	1H	H_2
multiplet	7.40	3H	H_6, H_3, H_5
sextuplet	3.42	1H	H_1'
singlet	2.18		(acetone)
multiplet	1.63	3H	aliphatic protons[a]
multiplet	1.25	15H	aliphatic protons[a]
multiplet	0.85	5H	aliphatic protons[a]

a) The presence of solvent made peak integrations unreliable.

Figure II.3 Peak assignments for ^{1}H-NMR spectrum of purified Kelex 100.

Preparation and Standardization of Kelex Stock Solutions

Concentrated stock solutions of 1 x 10^{-2} M Kelex were prepared by weighing purified compound into a teflon beaker and then quantitatively transferring it to a volumetric flask by washing with chloroform. The solution was brought to volume with chloroform and stored out of light and under refrigeration. Surfactant solutions of ligand were prepared by pipetting the stock solution and evaporating the chloroform under nitrogen, adding surfactant and other reagents and then stirring for several hours, usually overnight. Solutions were standardized by spectrophotometric titration with standard copper (II) chloride solution. Results were plotted as absorbance versus millimoles of copper (II) and the separate linear segments were fitted with a linear least-squares routine included with the Kaleidagraph graphing program. Millimoles of Kelex 100 was determined from the intersection of the two line segments based on a 1:1 Cu^{2+}:Kelex 100 stoichiometry. Titrations were performed in triplicate.

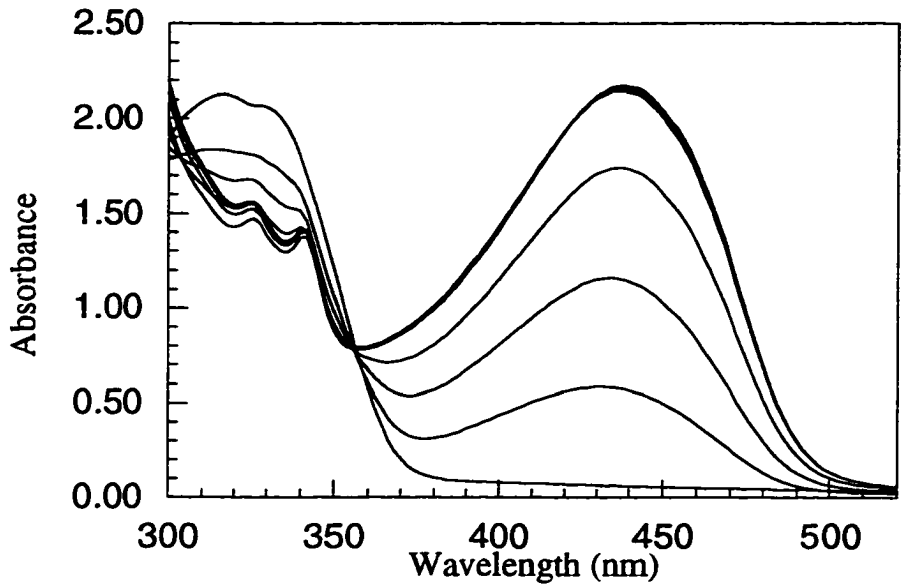

Figure II.4 UV-visible spectrum of 3.0 mL of 0.5 mM Kelex 100 in 5 mM $C_{12}(EO)_6$ solution titrated with 3.5 μL aliquots of 0.1062 M $CuCl_2$ solution.

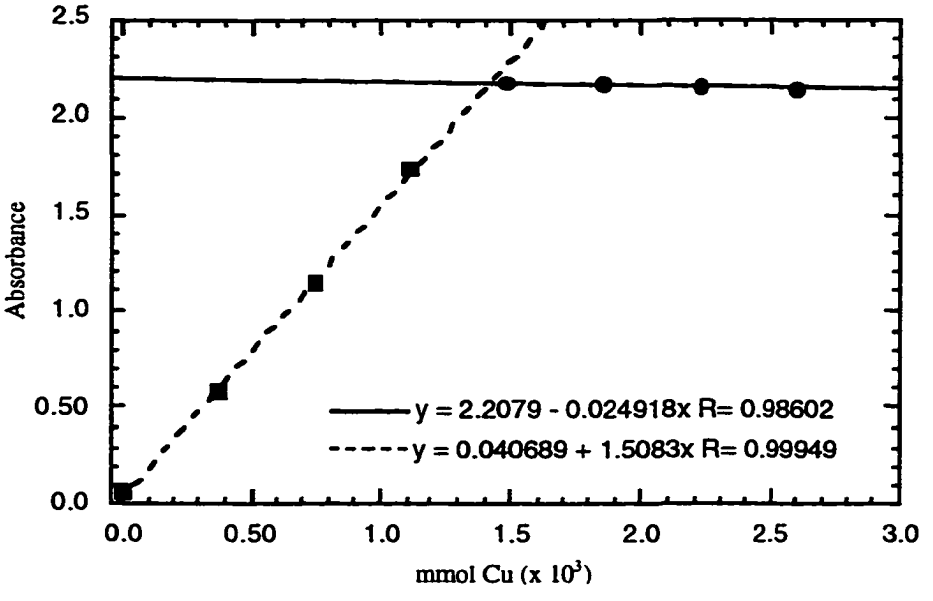

Figure II.5 Plot of absorbance versus mmoles of copper titrant for standardization of Kelex 100 stock solution.

Methods

Spectrophotometric analysis (UV-vis)

Spectrophotometric titrations were performed to determine protonation constants (log K_H) for Kelex in surfactant solution and to investigate the stoichiometry of Kelex complexes with cadmium, mercury and lead. Spectra were recorded using a Hewlett Packard model 8452A diode array UV-vis spectrophotometer with 1 cm pathlength cuvets. Generally, three milliters of solution was titrated and the volume and concentration of titrant were adjusted to create 1% or less volume increase through the course of a titration. The pH of solutions was monitored with the a semimicro glass pH electrode placed in the cuvet. Solutions were stirred with a magnetic stirbar until a stable pH was achieved and then the spectrum was recorded between 190 nm and 800 nm. All titrations were performed at 22-24 °C without temperature control.

pH Measurements

Measurements and adjustments of pH were made with either an Orion Sure-Flow Ross semi-micro combination electrode model 8175BN or a Sensorex pHASE combination electrode model S1021CD with a Fisher Scientific Accumet model 825MP or model 420 pH meter. Three point calibrations were performed with 4.01, 6.86 and 9.18 pH buffer solutions prepared from Fisher Scientific Gram-Pac commercial buffers.

Semi-Equilibrium Dialysis

Semi-equilibrium dialysis (SED) was used as a laboratory-scale model system for LM-MEUF (33, 35, 46). It allowed rapid screening of ligands and surfactants as well as optimization of experimental conditions with minimal use of reagents. A diagram of a typical SED cell is shown in Figure I.9. A 5000-6000 MWCO cellulose membrane obtained from Fisher Scientific was placed between the two halves of the cell, taking care to smooth any wrinkles, and then secured with bolts and wing nuts. A permeate solution buffered at the desired pH was added to one side of the cell cavity through the filling hole at the top. The retentate solution containing the ligand, surfactant, buffer and target metal ion was then added to the other side and the two sides of the cell were sealed with screws wrapped in parafilm to prevent leakage. The flexibility of the membrane allowed for a volume difference of $\pm$10%, so a reproducible technique for filling the cells was necessary to minimize this difference between cells. The cells were then allowed to sit undisturbed for 20-24 hours at room temperature (30). Cells were unloaded by removing the permeate solution first, followed by the retentate solution. Precipitation of metal hydroxides was prevented by immediately adding 10-20 μL of 1:1 nitric acid to the solutions prior to analysis.

Preliminary experiments showed that adsorption of target metal ions onto the dialysis membranes was a problem but that it could be reduced under most experimental conditions by pretreatment of the membranes. Therefore,

membranes were soaked in doubly distilled water for several hours (usually overnight) and then rinsed. Soaking was repeated in a low concentration solution of the target metal ion. Since most experiments were performed at relatively high pH, concerns about metal hydroxide precipitation and membrane degradation precluded adjusting the pH of the soaking solutions. Stable pH was maintained by buffering both permeate and retentate solutions with 10 mM of the appropriate buffer and adjusting the pH with either concentrated sodium hydroxide or 1:1 nitric acid prior to loading the cells.

Ultrafiltration

Ultrafiltration (UF) experiments were performed with a 600 mL stirred cell apparatus obtained from Fisher Scientific with 5000 MWCO cellulose membranes. Generally, 250 mL of the retentate solution containing surfactant, ligand, buffer and target metal ion was placed in the cell and 55 psi nitrogen pressure was applied to force the solution through the membrane. Fractions of 25 mL each were collected until 150 mL total permeate was collected. Prior to introduction of the retentate solution the membrane was conditioned by rinsing with 50-100 mL of D.D. water, followed by 50 mL of pH adjusted solution containing the same concentration of metal ion as the retentate.

Separation for both UF and SED experiments was expressed as either percent rejection or percent expulsion of the metal ion as shown in Equations II.1 and II.2. A high value for percent rejection indicates that most of the target ion was held by the ligand in the retentate. When percent expulsion is high,

most of the target ion was expelled into the permeate as a result of charge repulsion from the cationic surfactant.

Percent rejection is defined as:

$$\%R = \left(1 - \frac{\left[M^{2+}\right]_P}{\left[M^{2+}\right]_R} \right) \times 100 \qquad \textbf{Equation II.1}$$

where $[M^{2+}]_P$ is the analyzed concentration of metal ion in the permeate and $[M^{2+}]_R$ the concentration of metal ion in the retentate. Similarly, percent expulsion is defined as:

$$\%E = \left(1 - \frac{\left[M^{2+}\right]_R}{\left[M^{2+}\right]_P} \right) \times 100 \qquad \textbf{Equation II.2}$$

Preparation and Standardization of Metal Stock Solutions

Concentrated stock solutions of cadmium, mercury, zinc, copper and calcium were prepared for use in SED, UF and titrations. The stock cadmium solutions were prepared from either cadmium metal or cadmium perchlorate and were standardized by titration with a standard EDTA solution and EBT indicator at pH 10 (48). Mercury solutions prepared from metal were also standardized with EDTA after being adjusted to pH 5.0 to 5.5 using 20% hexamine buffer and xylenol orange indicator (47). Stock copper solutions, prepared from copper (II) chloride, were standardized with EDTA and Fast Sulphon Black

indicator (47). Calcium solutions were prepared from primary standard grade calcium carbonate. Oven dried $CaCO_3$ was dissolved in concentrated hydrochloric acid and heated to drive off CO_2, then used without standardization. Zinc solutions were also prepared by dissolving high purity zinc metal and used without standardization.

Atomic Absorption Analysis

Analysis of cadmium, zinc, calcium and mercury were performed on a Varian SpectrAA20 atomic absorption spectrophotometer (AA). Analysis of mercury required a specialized routine for cold vapor analysis which will be described later. Cadmium, zinc and calcium were analyzed using flame atomization with an air/acetylene flame for cadmium and zinc and a nitrous oxide/acetylene flame for determination of calcium. Internal calibration curves were generated by the instrument software using three or four standards. Standards were prepared by matching the expected sample matrix as closely as possible to allow for the appropriate dilution. Samples were diluted so that metal concentrations would fall within the optimum working range of the most sensitive wavelength. The analytical wavelengths and typical detection limits are shown in Table II.1.

Table II.1 Analytical wavelengths, typical detection limits and optimum working range for metals determined by atomic absorbtion.

Analyte	Wavelength (nm)	AA technique	Detection limit (μg/L)	Optimum working range
Cd	228.8	flame	1	0.1-1.0 μg/mL
Zn	213.9	flame	1	0.4-1.6 μg/mL
Ca	422.7	flame	1	1-4 μg/mL
Hg	253.7	CVAA	0.02	0.1-0.4 μg/L

The concentration of surfactant in SED retentates was assumed to be the same as that of the stock solution, while surfactant concentration in the permeate solutions was assumed to be at the surfactant CMC. These assumptions are based on previous studies showing that within the 20-24 hour SED experimental time, surfactant monomer is equilibrated across the membrane but micelles are not (27, 33, 46). Permeate solutions are prepared with the concentration equal to that of the retentate. Therefore, for a stock solution of 0.25 mM Cd^{2+}, 0.5mM ligand, 5 mM surfactant and 5 mM buffer, the concentration of Cd^{2+} in the permeate, assuming 99% rejection, would be 0.002475 mM (0.157 μg/mL) and the retentate concentration would be 0.2475 mM (15.73 μg/mL). The permeate solution would be within the optimum working range without dilution, so standards would be prepared with 5 mM buffer and the surfactant concentration equal to the CMC. The retentate solution would require approximately a 1:30 dilution for a final concentration of 0.5 μg/mL, the middle of the optimum working range. The final concentration of surfactant and buffer in the retentate standards would then be 0.167 mM each. No ligand is added to the standards

due to its very low concentration in both permeate and retentate and the need to conserve the purified ligand. Samples analyzed for calcium were diluted with sufficient KCl to give a final concentration of 0.067 M. KCl was added to suppress ionization of the vaporized calcium atoms.

Cold Vapor Atomic Absorption and Digestion

Mercury is unique among metals because in its elemental state it has an appreciable vapor pressure. This precludes the use of normal AA techniques because it is quickly lost under flame conditions. To prevent this, a modified Perkin Elmer mercury analyzer cold vapor apparatus was used as shown in Figure II.5. The sample is held in a BOD (biological oxygen demand) flask fitted with a sparger attached to a small air pump. Stannous chloride is added to the sample to reduce mercury (II) to elemental mercury. The resulting vapor is swept into a 10 cm flow-through absorbance cell which is in the beam path of the mercury hollow cathode lamp. The peak absorbance at 253.7 nm is measured and compared to a calibration curve to determine concentration. Surfactant present in the sample causes foaming and the presence of the ligand retards the rate at which the mercury is reduced, contributing to peak broadening. Each sample was subjected to digestion prior to analysis in order to obtain the maximum reproducibility and peak height. Initially, a procedure supplied by the Oklahoma Geological Society was used which called for 300 mL BOD bottles to be used for sample preparation and analysis. In order to streamline the process and allow for more samples to be analyzed at a time, the

procedure was modified to use 60 mL BOD bottles. An extensive comparison was done of the two procedures and sample calibration curves are shown for each (Figures II.6 and II.7). The absorbances measured for standards and samples varied between the two procedures due to changes in both the sample size and the decreased dead space in the smaller flasks. Also, a comparison of the recovery of mercury using both hot and cold digestion techniques was done. There was some concern that hot digestion would create vaporization losses of the mercury. However, the data indicated that hot digestion gave the best recovery of mercury from standards and that results were reproducible (44,45). Complete results for the experimental comparison of the two techniques are presented in Chapter III.

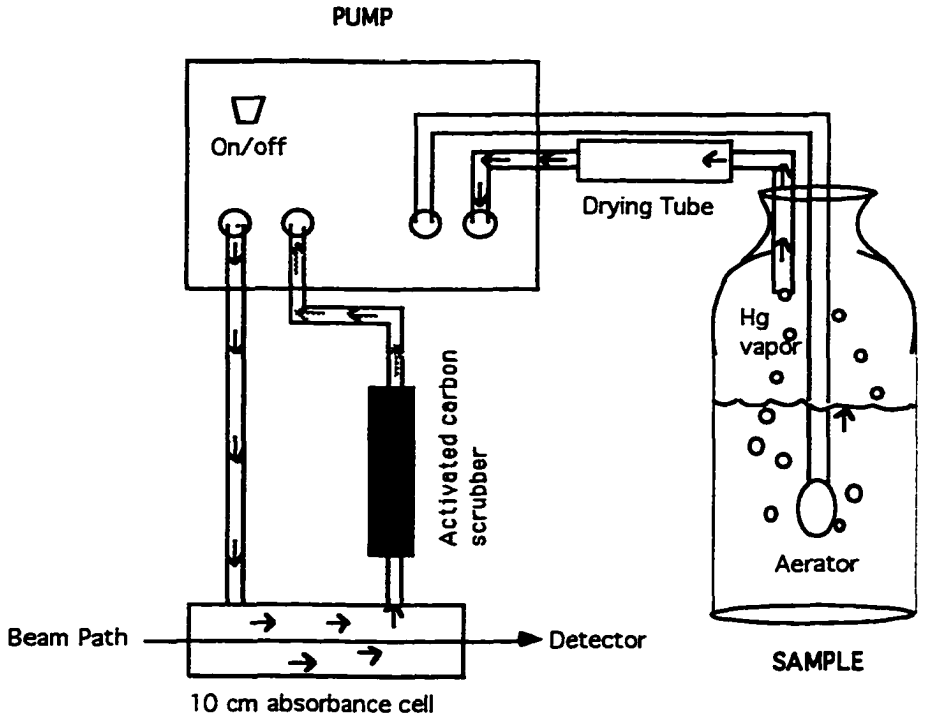

Figure II.6 Cold vapor apparatus for atomic absorbtion analysis of mercury. Solid arrows indicate the direction of mercury vapor flow.

Cold digestions were performed by addition of 0.2 mL of concentrated sulfuric acid to 1 mL of sample in a 300 mL BOD bottle. The flask was cooled in an ice bath and 1.5 mL of 6% $KMnO_4$ solution added. The solution was mixed carefully and left loosely stoppered overnight. Excess $KMnO_4$ was then reduced with 0.3 mL of 20% hydroxylamine hydrochloride prior to analysis.

Hot digestions were performed by placing 0.5 mL aliquots of sample in a 60 mL BOD bottle with 15 mL D.D. water. Volumes of reagents for the 300 mL

literand the 60 mL BOD flask procedures are shown in Table II.2. The larger volumes were used for the comparison of the hot and cold procedures, but later experiments were performed with the smaller volumes. One milliter of 5% potassium persulfate, 2.5 mL of 5% potassium permanganate and 4 mL of a mixture of concentrated sulfuric and nitric acids (2:1) were added and the samples placed in a boiling water bath for two hours. Marbles placed at the mouth of the BOD bottle prevented loss of the solution from bumping without pressurizing the flasks. Following digestion, enough hydroxylamine hydrochloride was added to reduce the remaining potassium permanganate. Freshly prepared 1% (w/v) stannous chloride was added (3.5 mL) immediately before the samples were analyzed. Standards and blanks were prepared with D.D. water and a surfactant concentration which was matched to either the retentate or permeate concentrations. They were also digested and analyzed simultaneously with samples. Sample concentration was determined from the curve fitted by a linear least-squares routine contained in the Kaleidagraph software package. Because total mercury is analyzed, the mercury content of each sample is determined as μg of total Hg^{2+} per 0.5 mL aliquot and then corrected to millimolar concentration units.

Table II.2 Volumes of reagent for CVAA sample digestion using 300 mL BOD and 60 mL BOD flasks.

Reagent	Volume for 300 mL BOD (mL)	Volume for 60 mL BOD (mL)
Sample	1.0	0.5
D.D. H_2O	100	15
2:1 mixture conc. H_2SO_4 + conc. HNO_3	7.5	4.0
5% $KMnO_4$	5.0	2.5
5% $K_2S_2O_8$	2.0	1.0
$NH_2OHxHCl$	about 4 mL	1 mL
SnCl2	5.0	3.5

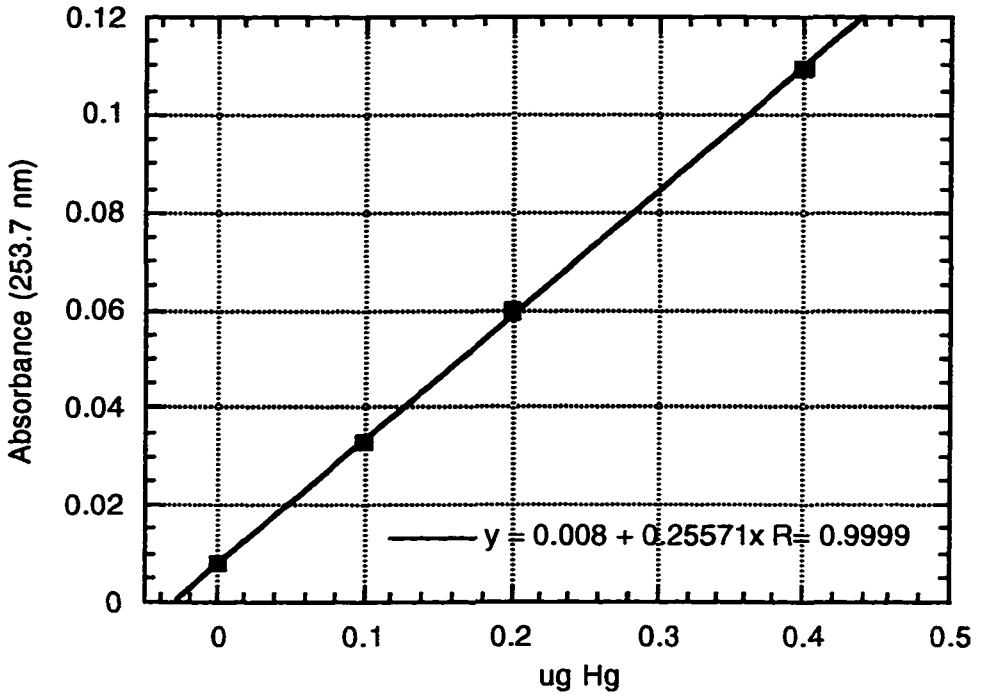

Figure II.7 Calibration curve for CVAA analysis of mercury using 60 mL BOD flasks.

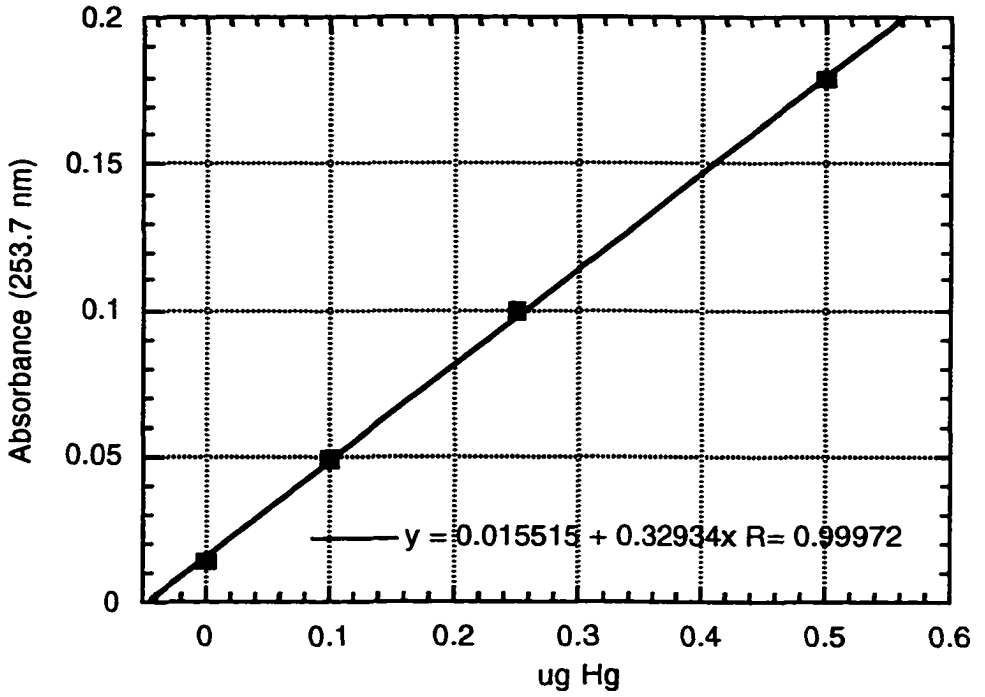

Figure II.8 Calibration curve for CVAA analysis of mercury using 300 mL BOD flasks.

Samples containing mercury must be handled with extreme care due to the ease with which low concentrations of mercury are lost. Because of the high reduction potential of the mercury (II)/mercury (I) pair the presence of almost any reducing agent, including carbon, creates low levels of mercury (I). Mercury (I) then easily disproportionates and the resulting elemental mercury is lost through vaporization. Oxidizing agents in the digestion process minimized losses by preventing the formation of mercury (I).

$$Hg_2^{2+} \rightarrow Hg^0 + Hg^{2+} \qquad \textbf{Equation II.3}$$

Samples are also readily contaminated due to the ease with which mercury adsorbs onto glassware. To preclude these problems, all glassware was acid washed, rinsed in D. D. H_2O and air dried prior to use.

Chapter III

Results

Results are presented for experiments investigating the use of Kelex 100 as a ligand for separation of cadmium and 1-decyl-2-thiourea as a ligand for separation of mercury using the LM-MEUF method. The Kelex 100/cadmium experiments are presented in two parts: (1) results of spectrophotometric metal and pH titrations and (2) SED and UF separation studies. The third section describes the results of a variety of experiments for analysis of mercury and preliminary separation studies with 1-decyl-2-thiourea.

Spectrophotometric pH studies of Kelex 100 in surfactant solutions

8-Hydroxyquinoline (8HQ), the chelating head group of Kelex 100, can exist in three protonation states (Figure III.1). The unprotonated compound is negatively charged due to the loss of the dissociable proton from the aromatic hydroxyl group and the doubly protonated form is a monovalent cation due to the charge on the quinolinic nitrogen. The charged species are soluble in water but the neutral molecule has very low solubility and the akylated form is almost completely insoluble in water in any protonation state. Therefore, protonation constants (K_{Hi}) in aqueous solution cannot be determined directly. Protonation constants have been determined in mixed aqueous and nonaqueous solvents and the values are listed Table IV.1. However, values for K_{Hi} have not been determined in surfactant solutions, such as those used for SED and UF separations. Constants determined in

surfactant solution are conditional due to their dependence on the surfactant concentration and its subsequent effect on the amount of ligand partitioning into the micelle.

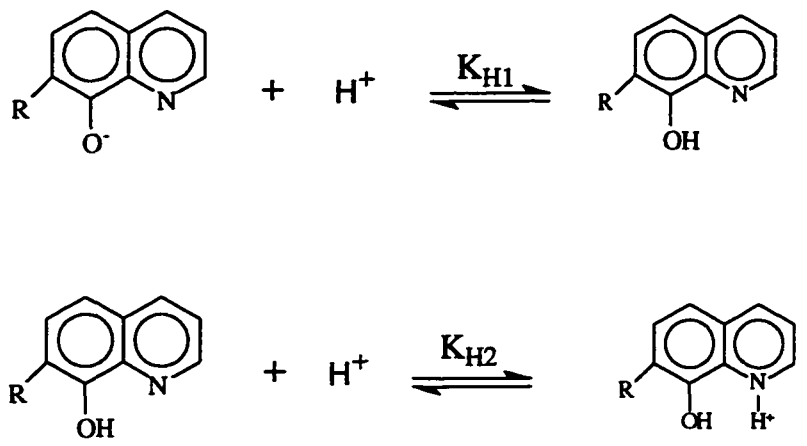

Figure III.1 Protonation equilibria of alkylated 8-hydroxyquinoline.

As discussed in Chapter 1, protonation and complexation constants determined in water provide only a rough estimate of the behavior of the ligand in surfactant solution due to the partitioning of the ligand into the micellar psuedophase. This is particularly true when the ligand is partitioned into charged micelles. Shifts of two to three log units have been observed for conditional protonation constants which result from the tendency of the charged ligand to be either stabilized or destabilized by the attraction to or repulsion by, respectively, the charged micelle surface. (41, 42) The extent of metal ion complexation at a given pH will be affected by the direction and magnitude of

the shifts in the protonation equilibria as illustrated by the coupled reaction equilibria shown in Figure III.2

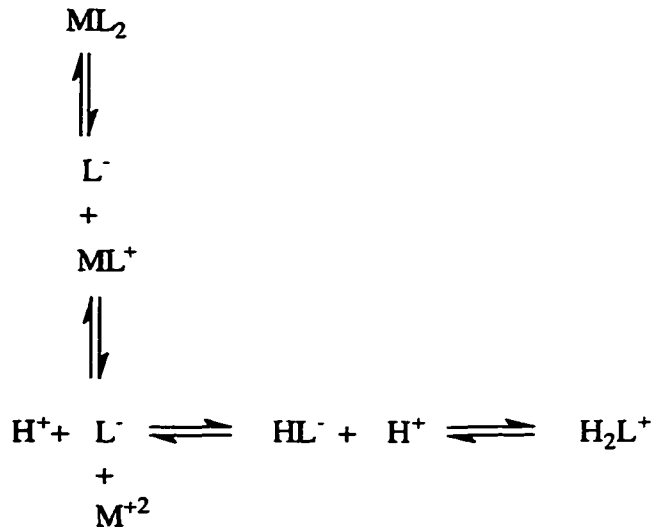

Figure III.2 Schematic diagram of ligand equilibria.

Conditional protonation constants were determined for Kelex 100 in surfactant solutions by spectrophotometric pH titration. The surfactant solutions chosen were representative of the three surfactant charge types: cationic (0.05 M $CPNO_3$), anionic (0.1 M SDS) and nonionic (0.05 M $C_{12}(EO)_6$). Figures III.5, III.6, III.11, III.13, III.14 show the spectra of 0.5 mM Kelex 100 as a function of pH (~2-12) in each of these surfactant solutions. All solutions contained 10 mM each HEPES, CHES and MES buffers to stabilize pH during the titration. In addition, 0.25 mM EDTA was added to prevent interference from trace metal ions that might be present. Titrations were performed on

surfactant solutions which contained all reagents except Kelex 100 to check for spectrophotometric changes which were not attributable to the ligand. Spectra of these blank titrations are shown for $CPNO_3$ (Figure III.3) and SDS (Figure III.9). No blank titration was performed with the neutral surfactant $C_{12}(EO)_6$. For the results of blank titrations of $CPNO_3$ and SDS, plots of absorbance as a function of pH are shown in Figures III.4 and III.10, respectively. The wavelengths selected for these plots of the corresponding solutions containing ligand. Generally, this was the wavelength (λ_{max}) where the maximum absorbance change occured during the titration. High absorbances (>2.5) are common for surfactant solutions at wavelengths below 300 nm, so titration of blanks also determined whether this background absorbance would overlap the wavelength range where the ligand absorbs. Plots of absorbance (λ_{max}) versus pH for titrations of Kelex 100 in $CPNO_3$, SDS and $C_{12}(EO)_6$ solutions are shown in Figures III.7, III.12 and III.15, respectively. For Kelex 100 in $CPNO_3$ (Figure III.7) spectral changes are observed at high pH (K_{H1}) and at low pH(K_{H2}). The spectral change at high pH is essentially complete; however only the initial part of the absorbance change associated with the second protonation step is observed. For the titration in SDS, the plot of absorbance versus pH (Figure III.12) reveals only a single process that occurs in the pH range from 4 to 8. The direction of the absorbance change, high to low as pH increases, indicates that the observed process is associated with the second protonation equilibrium (K_{H2}). For the titration of Kelex 100 in $C_{12}(EO)_6$, absorbance changes are observed at the lower and upper pH limits. However, neither spectral change is complete. For titrations where a complete absorbance

neither spectral change is complete. For titrations where a complete absorbance change was observed, the equilibrium constant may be evaluated for the nth protonation step,

$$H_{n-1}L^{n-2} + H^+ \rightleftharpoons H_nL^{n-1} \ (n=1,2) \qquad \textbf{Equation III.1}$$

$$K_{H_n} = \frac{[H_nL_{n-1}]}{[H_{n-1}L_{n-2}]a_H} \qquad \textbf{Equation III.2}$$

where:

$a_H = H^+$ acitivity ($=10^{-pH}$)

$K_{Hn} = n^{th}$ mixed-mode protonation constant for the nth step of the protonation equilibrium (Eq. III.1)

Values of K_{HL} were obtained using non-linear least squares program to fit the absorbance-pH (a_H) data to the following expression:

$$Abs(\lambda) = \frac{Abs_L + Abs_{HL}K_{H_n}a_n}{1 + K_{Hn}a_n} \qquad \textbf{Equation III.3}$$

where for any given pair $H_nL/H_{n-1}L$:

Abs_L = limiting absorbance of basic form of the ligand at λ

Abs_{HL} = limiting absorbance of acidic form of the ligand at λ

Experimental data are shown as individual points with a solid curve representing the calculated curve. Values for both K_{H1} and K_{H2} in $C_{12}(EO)_6$

because these parameters could not be determined from the incomplete titration curve in $C_{12}(EO)_6$. A summary of calculated values for the conditional constants determined in surfactant solutions are shown in Table III.1. Protonation constant values for both Kelex 100 and 8HQ determined in 80% (w/w) methanol:water (80% MeOH) were determined for comparison. Plots of absorbance versus pH are shown in Figures III.16 and III.17 for Kelex 100 and 8HQ, respectively, in 80% MeOH.

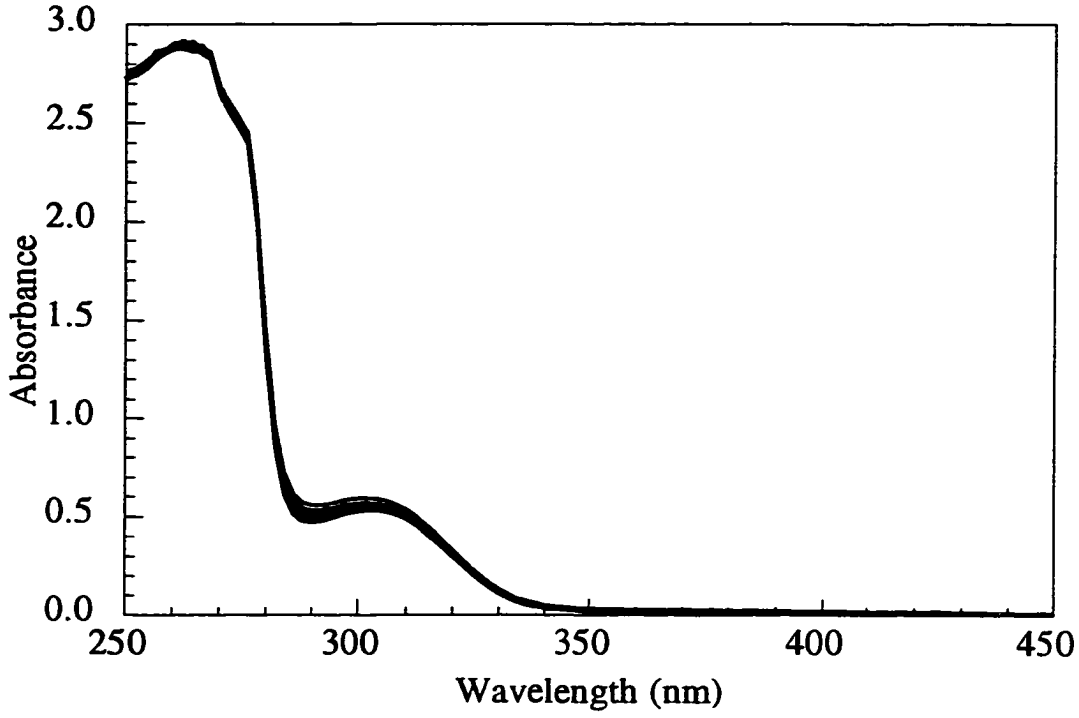

Figure III. 3 UV-visible spectra of 0.05 M $CPNO_3$ solution blank containing 0.25 mM EDTA, 5 mM HEPES, 5 mM CHES, and 5 mM MES. The pH was adjusted with concentrated sodium hydroxide from pH 2.0 to pH 13.0.

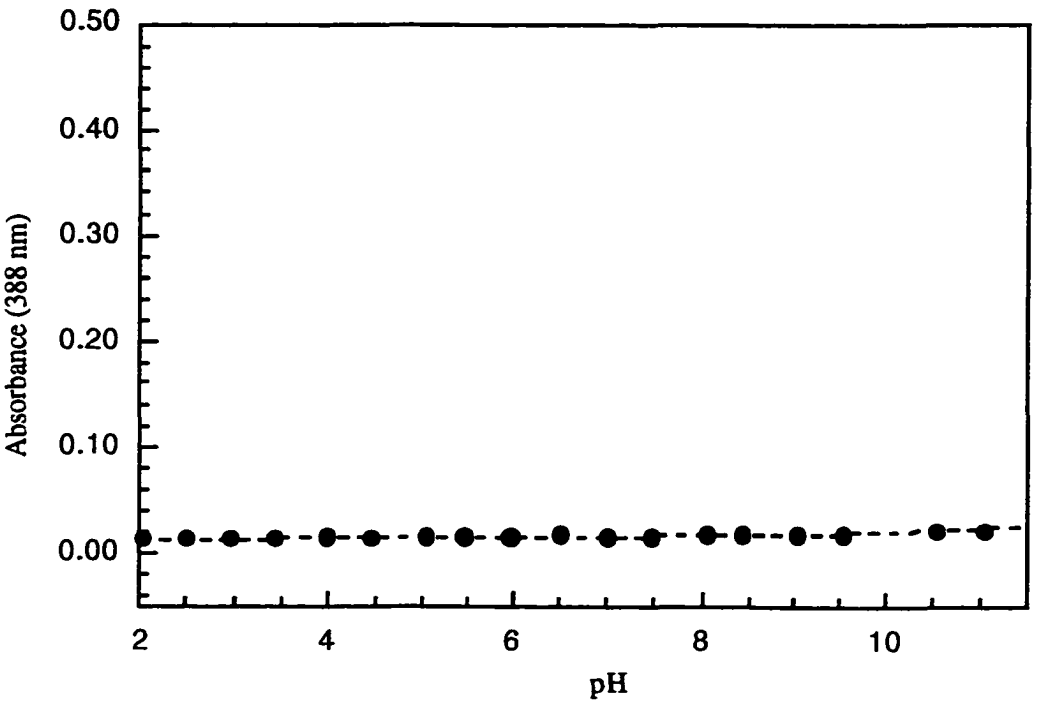

Figure III.4 Plot of absorbance versus pH at 388 nm for titration of 0.05 M $CPNO_3$ solution blank with 0.25 mM EDTA, 5 mM HEPES, 5 mM CHES, and 5 mM MES. The pH was adjusted with concentrated sodium hydroxide from pH 2.0 to pH 13.0.

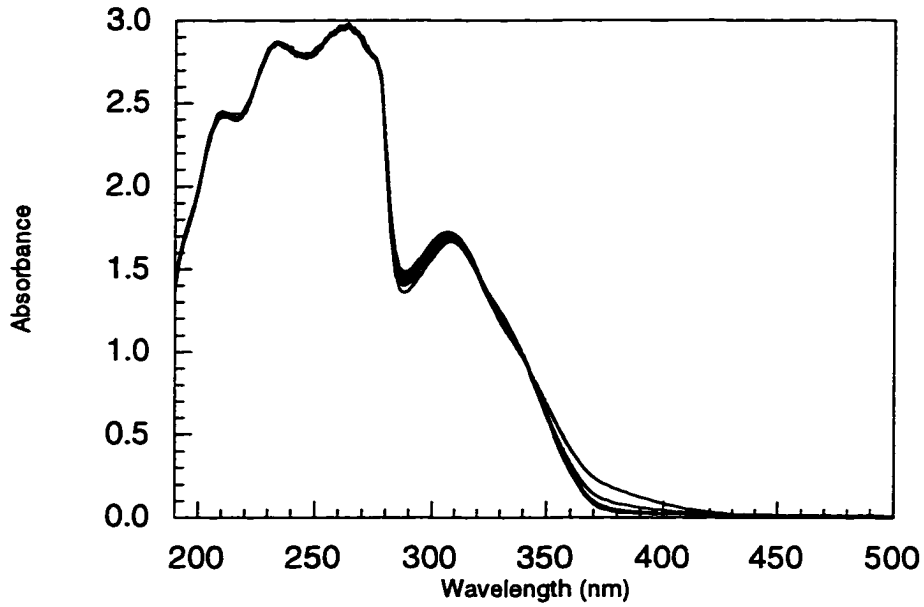

Figure III. 5 UV-visible spectra of 0.5 mM Kelex 100 in 0.05 M $CPNO_3$ solution containing 0.25 mM EDTA, 5 mM HEPES, 5 mM CHES, and 5 mM MES. The pH was adjusted with concentrated sodium hydroxide from pH 2.0 to pH 7.0.

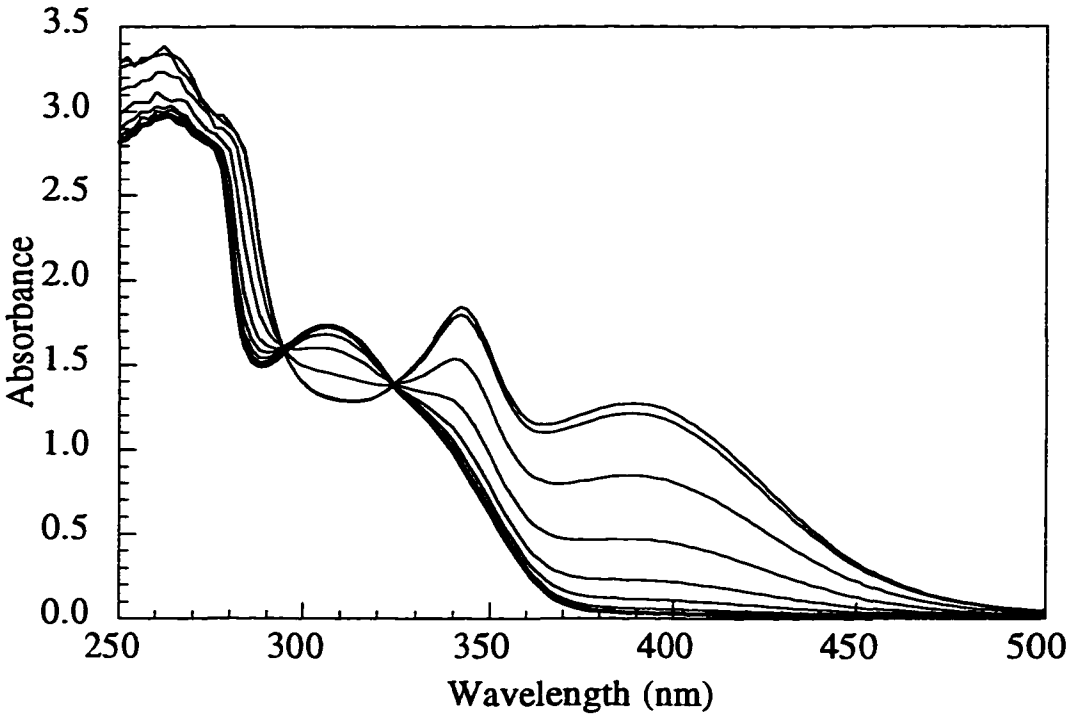

Figure III.6 UV-visible spectra of 0.5 mM Kelex 100 in 0.05 M $CPNO_3$ solution containing 0.25 mM EDTA, 5 mM HEPES, 5 mM CHES, and 5 mM MES. The pH was adjusted with concentrated sodium hydroxide from pH 7.5 to pH 12.5.

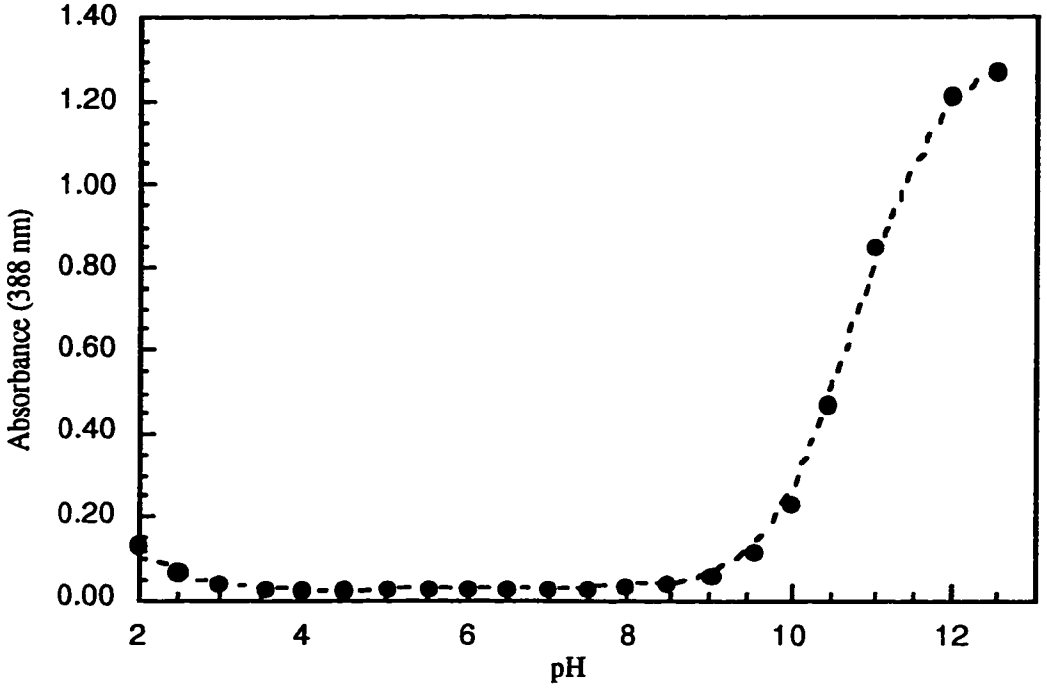

Figure III.7 Plot of pH versus absorbance at 388 nm for 0.5 mM Kelex 100 in 0.05 M $CPNO_3$ solution with 0.25 mM EDTA, 5 mM HEPES, 5 mM CHES, and 5 mM MES titrated with concentrated sodium hydroxide from pH 2 to pH 12.5. Individual data points are shown connected with dashed curve.

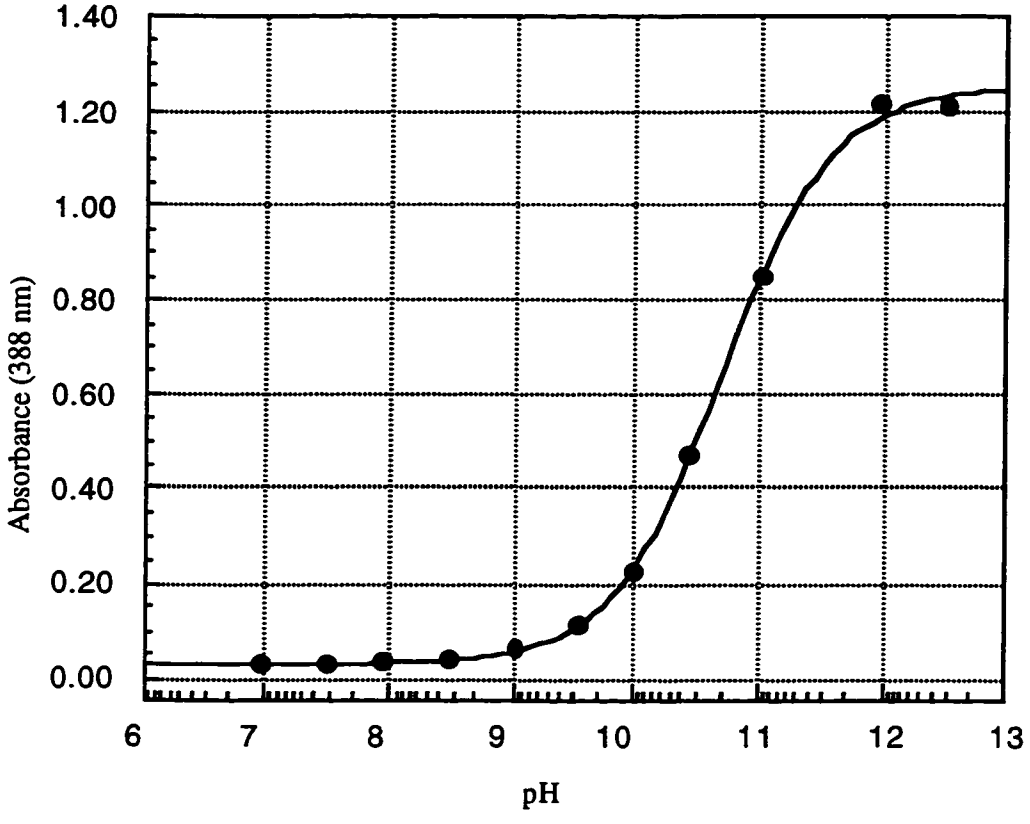

Figure III.8 Plot of pH versus absorbance at 388 nm for titration of 0.5 mM Kelex in 0.05 M $CPNO_3$ solution with 5 mM each MES, CHES and HEPES buffers and 0.25 mM EDTA between pH 7.0 and pH 12.5. The calculated value for log K_{H1} is 10.70 ± 0.02.

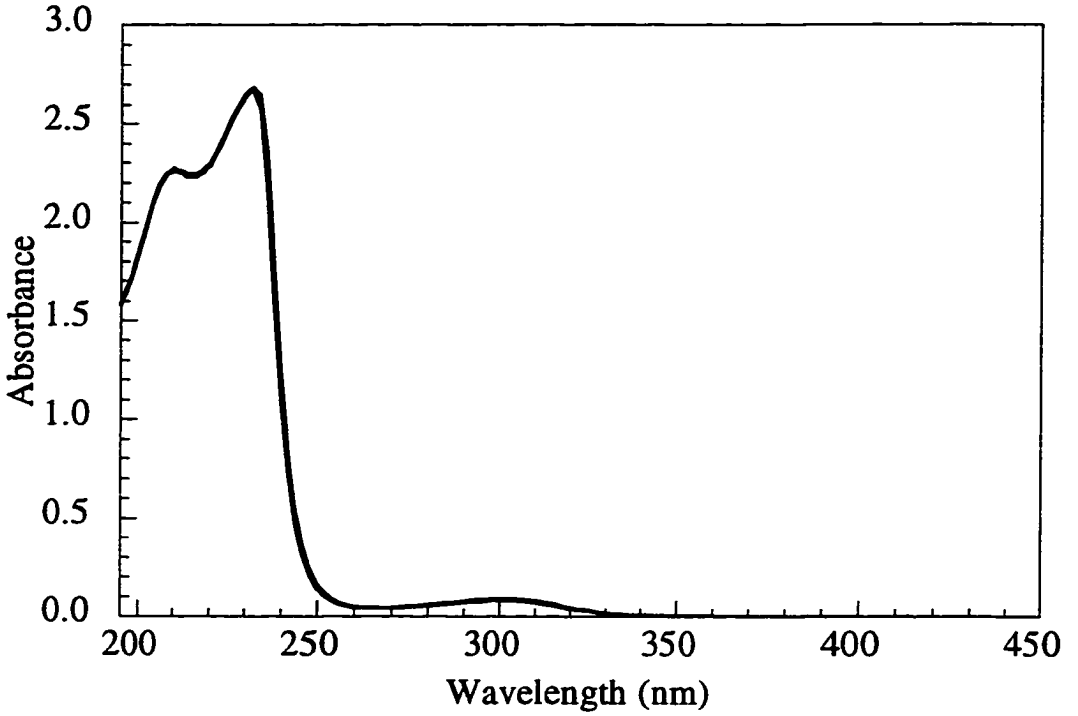

Figure III. 9 UV-visible spectra of 0.1 M SDS solution blank containing 0.25 mM EDTA, 5 mM HEPES, 5 mM CHES, and 5 mM MES. The pH was adjusted with concentrated sodium hydroxide from pH 2.5 to pH 13.0.

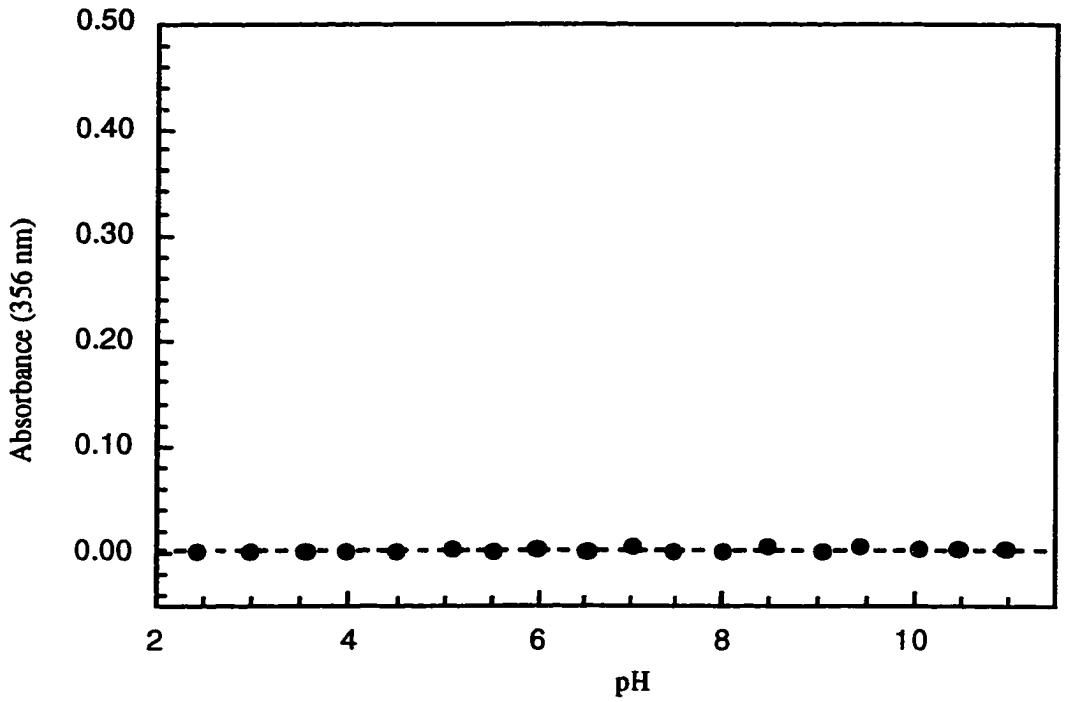

Figure III.10 Plot of pH versus absorbance at 356 nm for 0.1 M SDS solution blank containing 0.25 mM EDTA, 5 mM HEPES, 5 mM CHES, and 5 mM MES. The pH was adjusted with concentrated sodium hydroxide from pH 2.5 to pH 11.0. Individual data points are shown connected with dashed line.

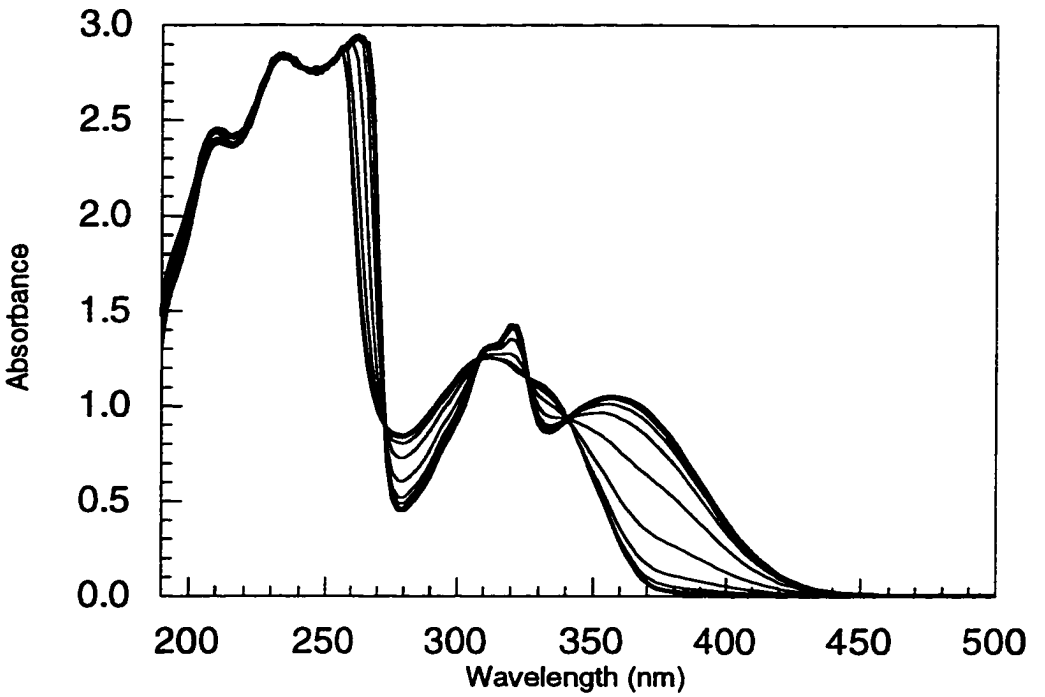

Figure III. 11 UV-visible spectra of 0.5 mM Kelex 100 in 0.1 M SDS solution containing 0.25 mM EDTA, 5 mM HEPES, 5 mM CHES, and 5 mM MES. The pH was adjusted with concentrated sodium hydroxide from pH 2.4 to pH 12.6.

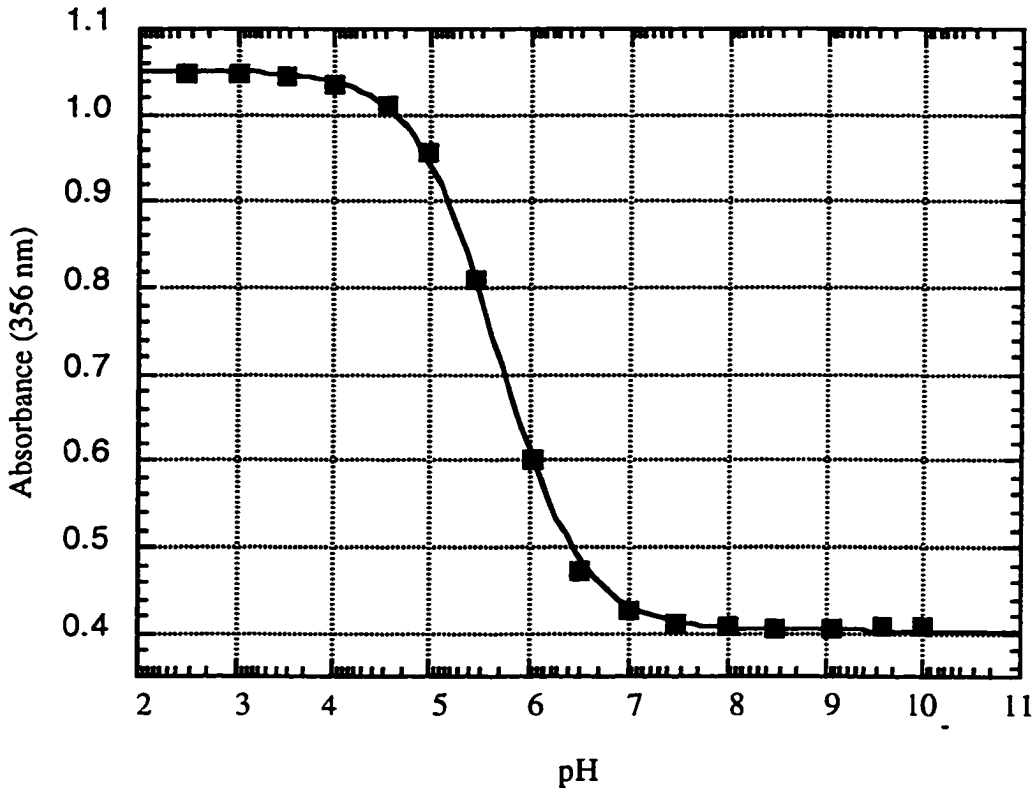

Figure III.12 Plot of pH versus absorbance at 356 nm for titration of 0.5 mM Kelex in 0.1 M SDS solution containing 5 mM each MES, CHES and HEPES buffers and 0.25 mM EDTA between pH 2.4 and pH 12.4. The calculated value for the log K_{H2} is 5.68 $\pm$ 0.01

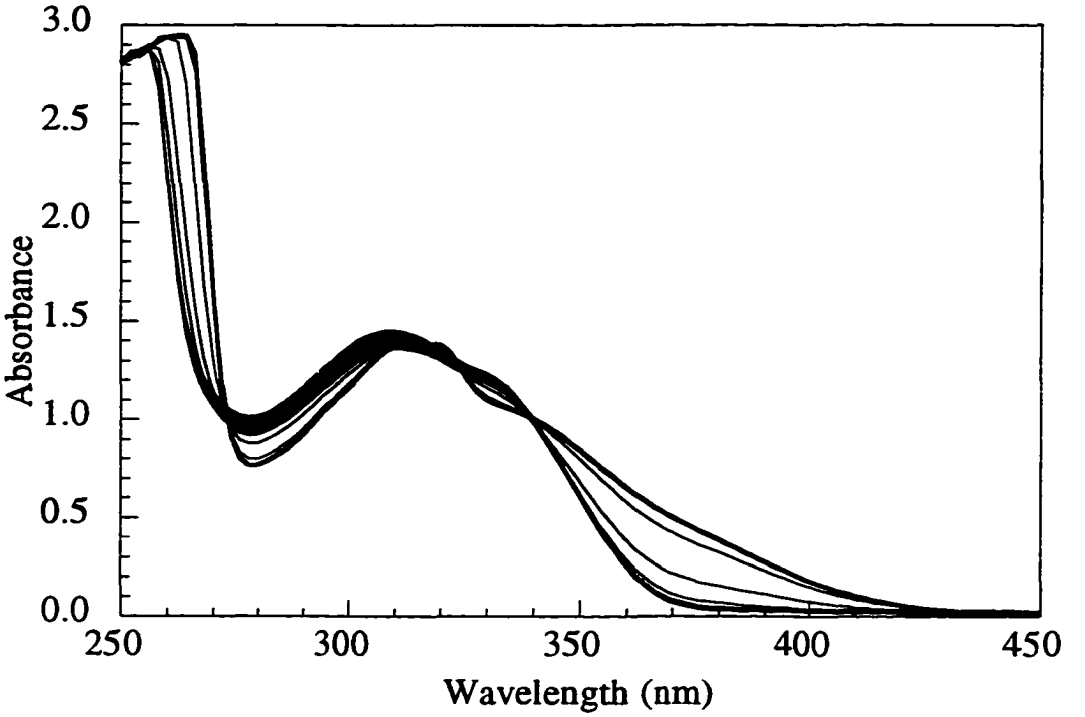

Figure III. 13 UV-visible spectra of 0.5 mM Kelex 100 in 0.05 M $C_{12}(EO)_6$ solution containing 0.25 mM EDTA, 5 mM HEPES, 5 mM CHES, and 5 mM MES. The pH was adjusted with concentrated sodium hydroxide from pH 2.0 to pH 10.5.

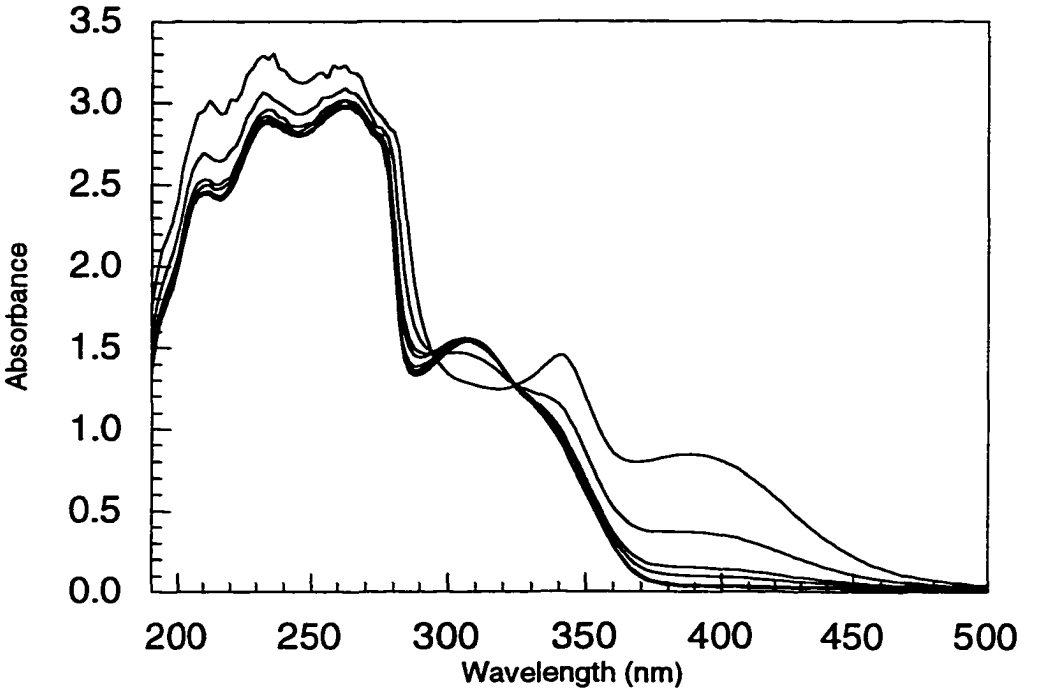

Figure III. 14 UV-visible spectra of 0.5 mM Kelex 100 in 0.05 M $C_{12}(EO)_6$ solution containing 0.25 mM EDTA, 5 mM HEPES, 5 mM CHES, and 5 mM MES. The pH was adjusted with concentrated sodium hydroxide from pH 11.0 to pH 13.0.

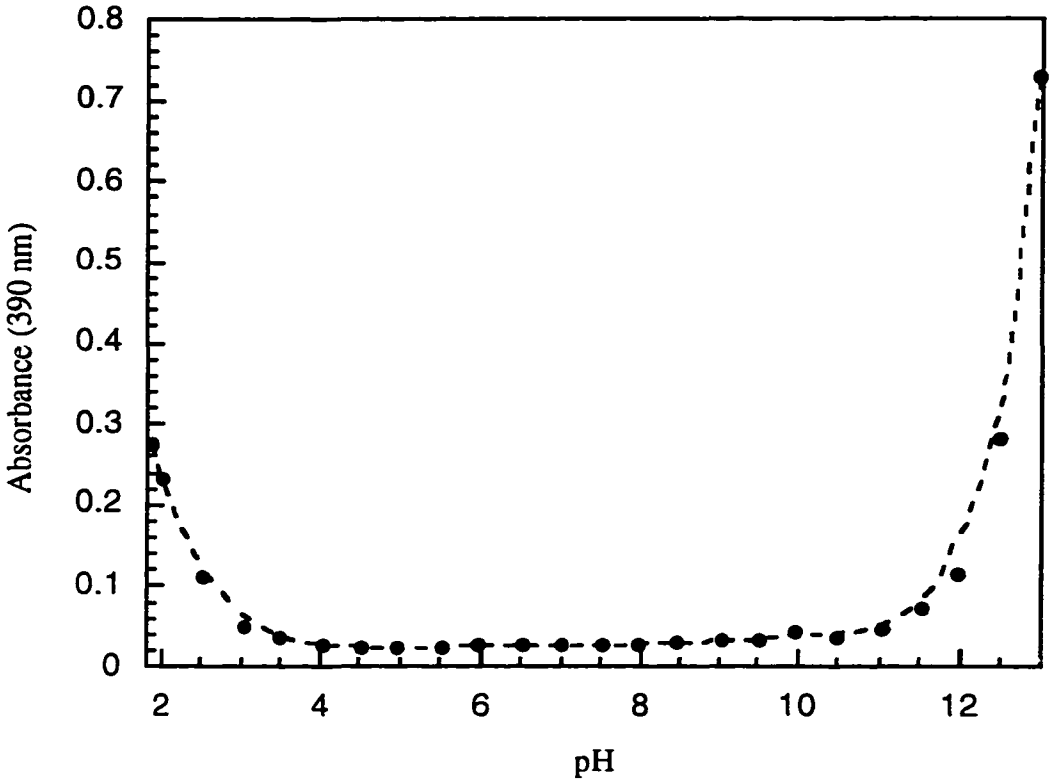

Figure III.15 Plot of pH versus absorbance for spectrophotometric study of 0.5 mM Kelex 100 in 50 mM $C_{12}(EO)_6$ containing 5 mM each MES, CHES and HEPES buffers and 0.25 mM EDTA. Individual data points are shown connected by a smooth curve.

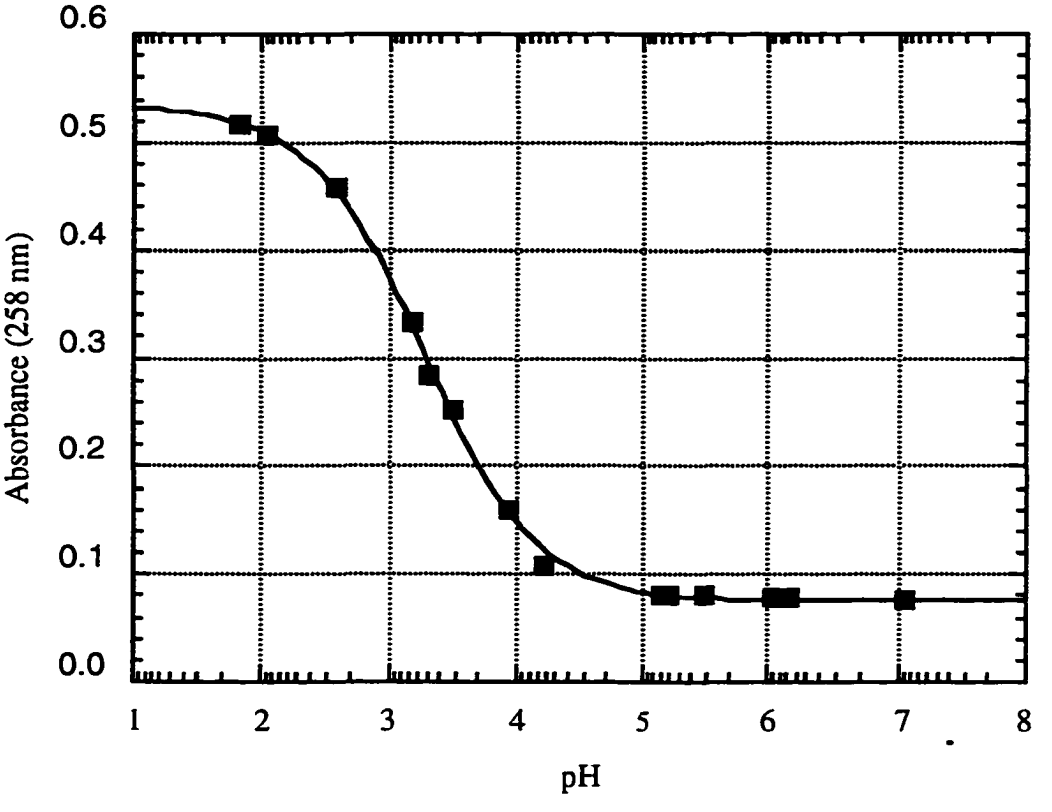

Figure III.16 Plot of pH versus absorbance at 258 nm for spectrophotometric study of 0.125 mM Kelex 100 in 80% methanol:water containing 1 mM each MES, CHES and HEPES buffers and 0.25 mM EDTA. The calculated value for the log K_{H2} is 3.26 ± 0.02

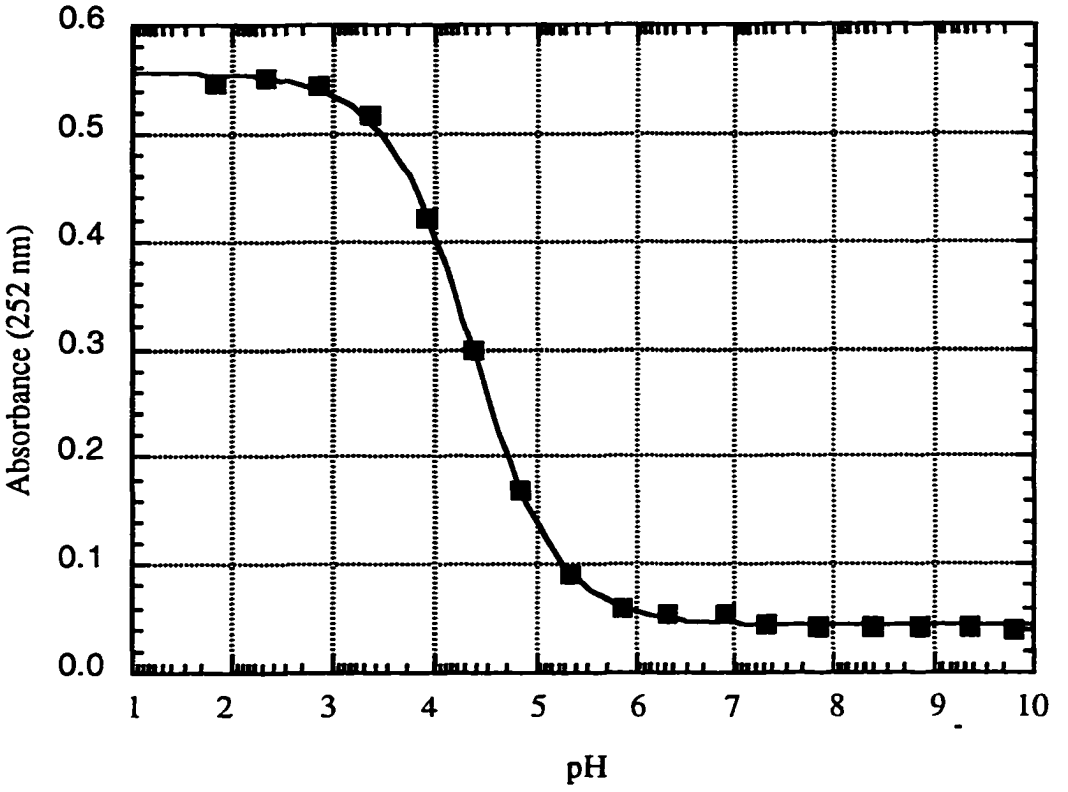

Figure III.17 Plot of pH versus absorbance at 252 nm for spectrophotometric study of 0.125 mM 8-hydroxyquinoline in 80% (w/w) methanol:water containing 1 mM each MES, CHES and HEPES buffers and 0.25 mM EDTA. The calculated value for the log K_{H2} is 4.36 $\pm$ 0.01

Table III.1 Summary of mixed-mode conditional protonation constants at 25 °C for 0.5 mM Kelex 100 (new formulation) determined in surfactant solution. Protonation constants for 0.125 mM 8-hydroxyquinoline and 0.125 mM Kelex 100 in 80% (w/w) methanol:water were also determined.

Solution	Surfactant charge	Log K_{H1}	Log K_{H2}
0.05 M $CPNO_3$	+	10.70 ± 0.02	<2.0
0.05 M $C_{12}(EO)_6$	0	12.8 ± 0.5	1.4 ± 0.5
0.1 M SDS	-	>13.0	5.68 ± 0.01
Kelex 100 in 80% MeOH		>12	3.26 ± 0.02
8HQ in 80%MeOH		>12	4.36 ± 0.01

Spectrophotometric studies of metal complexation with Kelex 100 in surfactant solutions

The stoichiometry of metal ion complexes of Kelex 100 in the presence of different surfactant types was determined by spectrophotometric titration. Studies were carried out with Cd^{2+}, Hg^{2+} and Pb^{2+} in the presence of $CPNO_3$, CO660 and DDAO. In addition, the Cd^{2+}-Kelex system was evaluated in solution with the neutral surfactant $C_{12}(EO)_6$. In each case a solution of the surfactant (0.05 M), ligand (0.17 - 0.53 mM) and buffers (5 mM) was titrated by addition of aliquots of a standardized stock solution of the metal of interest. The pH was controlled ($\pm$ 0.3 pH units) by addition of buffers: CHES (pK_a = 9.3), HEPES (pK_a = 7.5) and MES (pK_a = 6.1), used alone or in combination. For each system spectra were recorded of Kelex alone and after each quantitative addition of metal solution. At low metal to ligand ratios absorbance increased linearly with addition of metal ions. Absorbance showed no further increase at higher metal to ligand for Cd^{2+} titrations and little additional increase for Hg^{2+} titrations. Spectra for Cd^{2+} titrations are shown in Figures III.18, III.20, III.22, III.23 and III.25. Spectra for Hg^{2+} titrations are shown in Figures III.28, III.30 and III.32. Spectra of Hg^{2+} additions in D.D. H_2O are shown in Figure III.27 to show the wavelength range in which Hg^{2+} absorbs. Investigations with Pb^{2+} were terminated due to increases in baseline absorbance resulting from precipitation as the metal to ligand ratio approached 1:2. Figures III.34, III.36 and III.37 show spectra recorded for Pb^{2+} titrations performed at pH 7.5-7.7 in $CPNO_3$, CO660 and DDAO with the dashed line indicating increased baseline absorbance. Spectra for a titration performed at pH 5.7 are shown in Figure III.35. No precipitation occurred but the absorbance did

not level out at higher metal to ligand ratios (up to $[Pb^{2+}]$:[Kelex] = 1.4) indicating that complexation was not quantitative at this pH.

The absorbance for each titration at the wavelength of maximum absorbance change (λ_{max}) was plotted versus the metal to ligand ratio ($[M^{2+}]$:[Kelex]). Plots showed two linear regions which were then fitted with the linear-least squares routine in the Kaleidagraph graphing program, generating separate equations. The point of intersection of the two lines was calculated and the metal to ligand ratio which corresponded to this point wastaken as the complex stoichiometry. Plots for titrations with Cd^{2+} are shown in Figures III.19, III.21, III.24 and III.26. Figures III.21, III.24 and III.26 show that in solutions of neutral surfactant (CO660, $C_{12}(EO)_6$ and DDAO) absorbance essentially levels off for high metal to ligand ratios. More complicated behavior was observed for formation of the Cd^{2+}-Kelex complex in cationic surfactant solution ($CPNO_3$), as shown in Figure III.18. At least two different isosbestic points can be seen between 320 nm and 360 nm and the λ_{max} can be seen to shift between about 395 nm and 420 nm. Absorbance versus $[Cd^{2+}]$:[Kelex] was plotted at two different wavelengths as shown in Figure III.19. An isosbestic point occurs at 404 nm so at this wavelength the plot at high metal to ligand ratio is flat. The plot of absorbance versus $[Cd^{2+}]$:[Kelex] at 440 nm shows a negative slope with increasing metal to ligand ratio. Only the data from the 404 nm plot are fitted. The complex stoichiometry was determined to be 1:3 Cd^{2+}-Kelex from data at this wavelength.

Plots of absorbance versus metal to ligand ratio for Hg^{2+} titrations are shown in Figures III.30, III.32 and III.34. All plots of Hg^{2+} titrations show two regions where the absorbance increases linearly with added Hg^{2+}. A distinct break

occurs between the linear absorbance increase at low metal to ligand ratio and the smaller linear absorbance increase at higher metal to ligand ratios. Both linear segments were fitted and the equations are shown for each with the complex stoichiometry determined from the calculated intersection of the two lines. Complete results for all three metals are summarized in Table III.2.

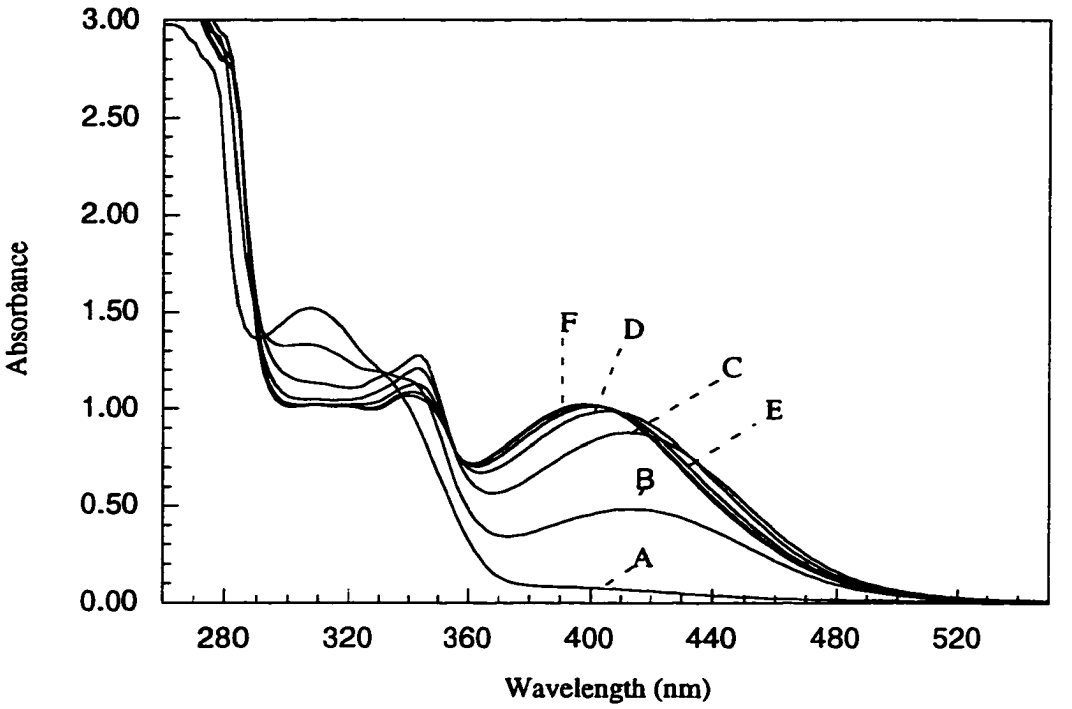

Figure III.18 UV-visible spectra of 0.518 mM Kelex 100 in a solution containing 0.05 M $CPNO_3$ and 5.0 mM CHES at pH 8.6 titrated with 0.1467 M Cd^{2+} The total volume of Cd^{2+} added (in μL) A) 0; B) 1.35; C) 2.70; D) 4.05; E) 5.40; F) 6.75.

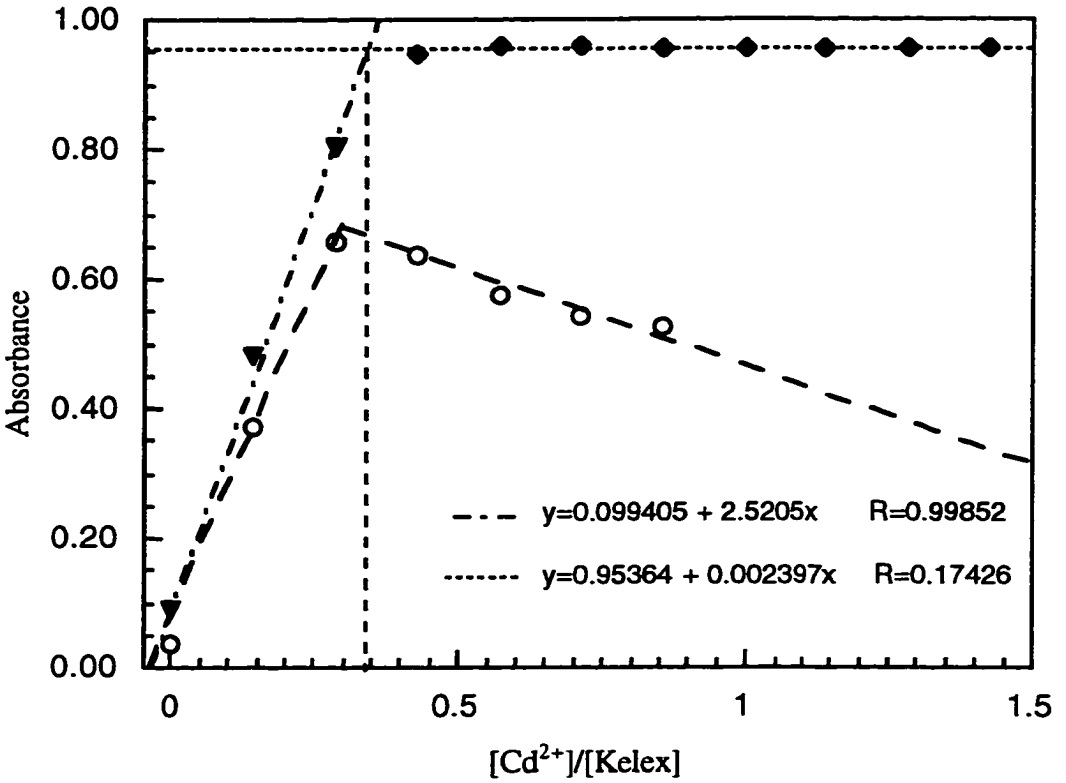

Figure III.19 Plot of absorbance versus ratio of moles Cd^{2+} to moles Kelex 100 for titration of 0.518 mM Kelex 100 in 0.05 M $CPNO_3$ at pH 8.6. (F,P) Absorbance at 404 nm was plotted and equations are shown for the linear regression fits of the two linear regions. The intersection occurs at x = 0.339 which corresponds to a 1:3 ratio of Cd^{2+} to Kelex 100. (E) Absorbance at 440 nm was also plotted versus ratio of moles Cd^{2+} to moles Kelex 100.

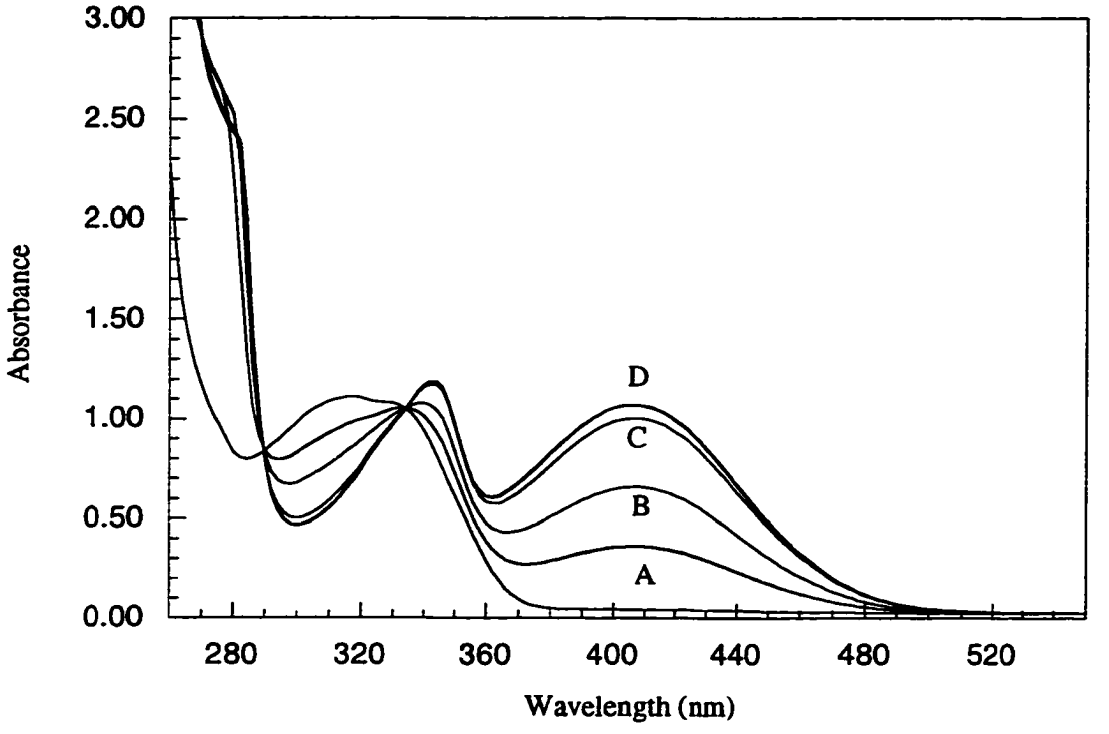

Figure III.20 UV-visible spectra of 0.528 mM Kelex 100 in a solution containing 0.05 M DDAO with 5.0 mM CHES at pH 8.7 titrated with 0.09075 M Cd^{2+}. The total volume of Cd^{2+} added (in μL): A) 0; B) 2.00; C) 4.00; D) 6.00-10.00.

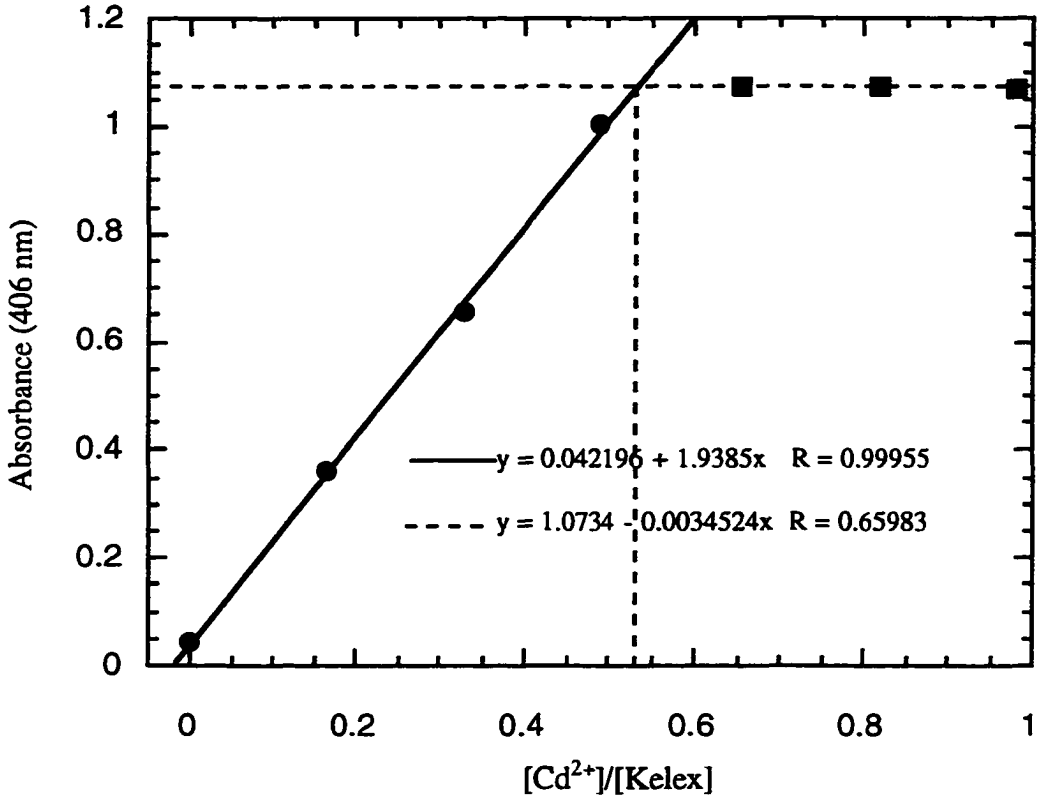

Figure III.21 Plot of absorbance at 406 nm versus ratio of moles Cd^{2+} to moles Kelex 100 for titration of 0.50 mM Kelex 100 in 0.05 M DDAO at pH 8.7. Equations are shown for the linear regression fit of the two linear regions. The intersection of the two lines occurs at x = 0.531 which corresponds to a 1:2 ratio of Cd^{2+} to Kelex 100.

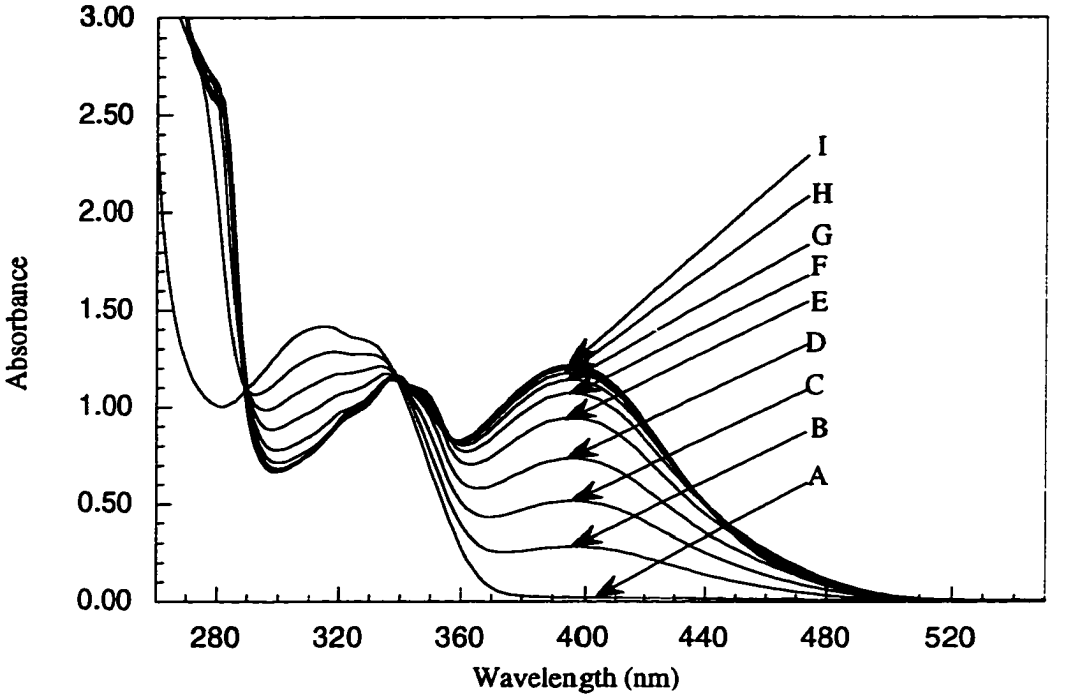

Figure III.22 UV-visible spectra of 0.528 mM Kelex 100 in 0.05 M $C_{12}(EO)_6$ solution with 5.0 mM CHES at pH 9.0 titrated with 0.07320 M Cd^{2+}. The total volume of Cd^{2+} added (in μL) A) 0; B) 2.70; C) 5.40; D) 8.10; E) 10.80; F) 13.50; G) 16.20; H) 18.90; I) 21.60 - 27.00.

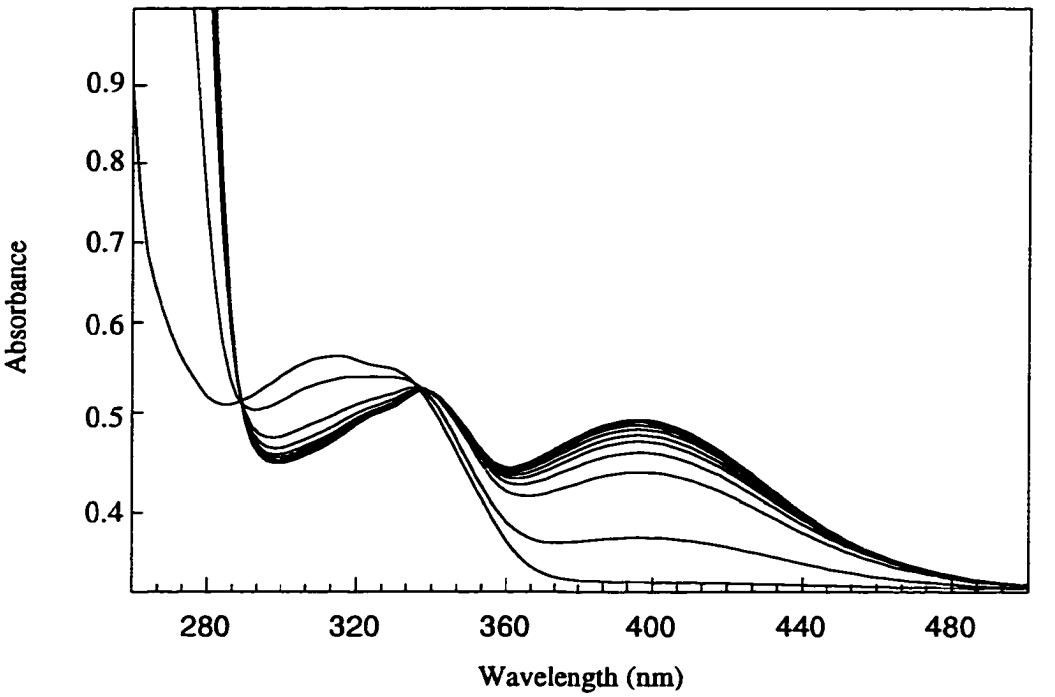

Figure III.23 UV-visible spectra of 0.170 mM Kelex 100 in 0.05 M $C_{12}(EO)_6$ solution with 5.0 mM CHES at pH 9.0 titrated with 0.01464 M Cd^{2+}. The total volume of Cd^{2+} added (in μL) A) 0 B) 4.35 C) 8.70 D) 13.05 E) 17.40 F) 21.75 G) 26.10 H) 30.45 I) 34.80 J) 39.15 K) 43.50.

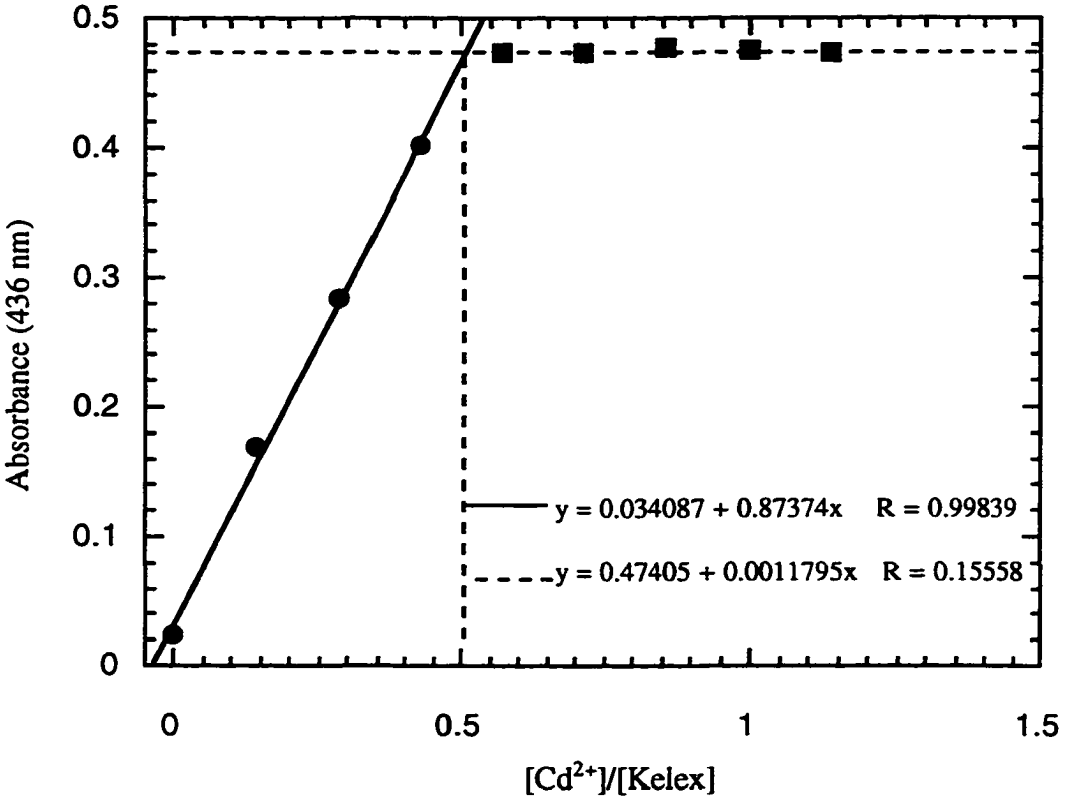

Figure III.24 Plot of absorbance at 406 nm versus ratio of moles Cd^{2+} to moles Kelex 100 for titration of 0.17 mM Kelex 100 in a solution of 0.05 M $C_{12}(EO)_6$ at pH 9.0. Equations are shown for the linear regression fit of the two linear regions. The intersection of the two lines occurs at x = 0.539 which corresponds to a 1:2 ratio of Cd^{2+} to Kelex 100.

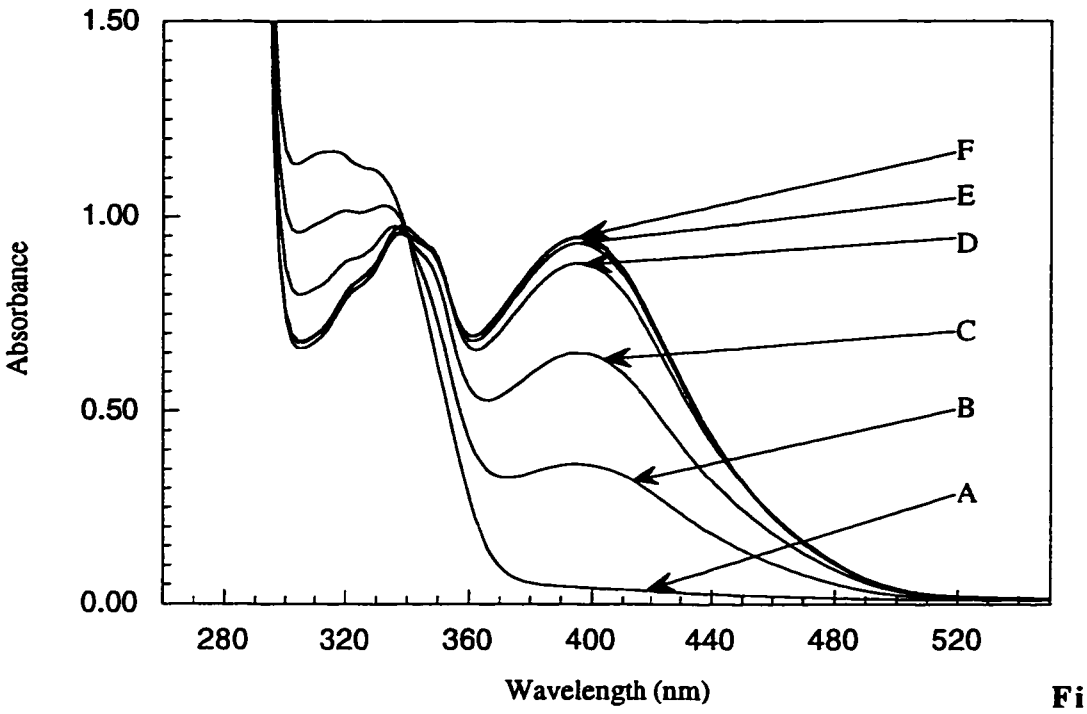

Figure III.25 UV-visible spectra of 0.528 mM Kelex 100 in 0.05 M CO660 solution with 5.0 mM CHES at pH 9.3 titrated with 0.09075 M Cd^{2+}. The total volume of Cd^{2+} added (in μL) A) 0; B) 2.00; C) 4.00; D) 6.00; E) 8.00; F) 10.00.

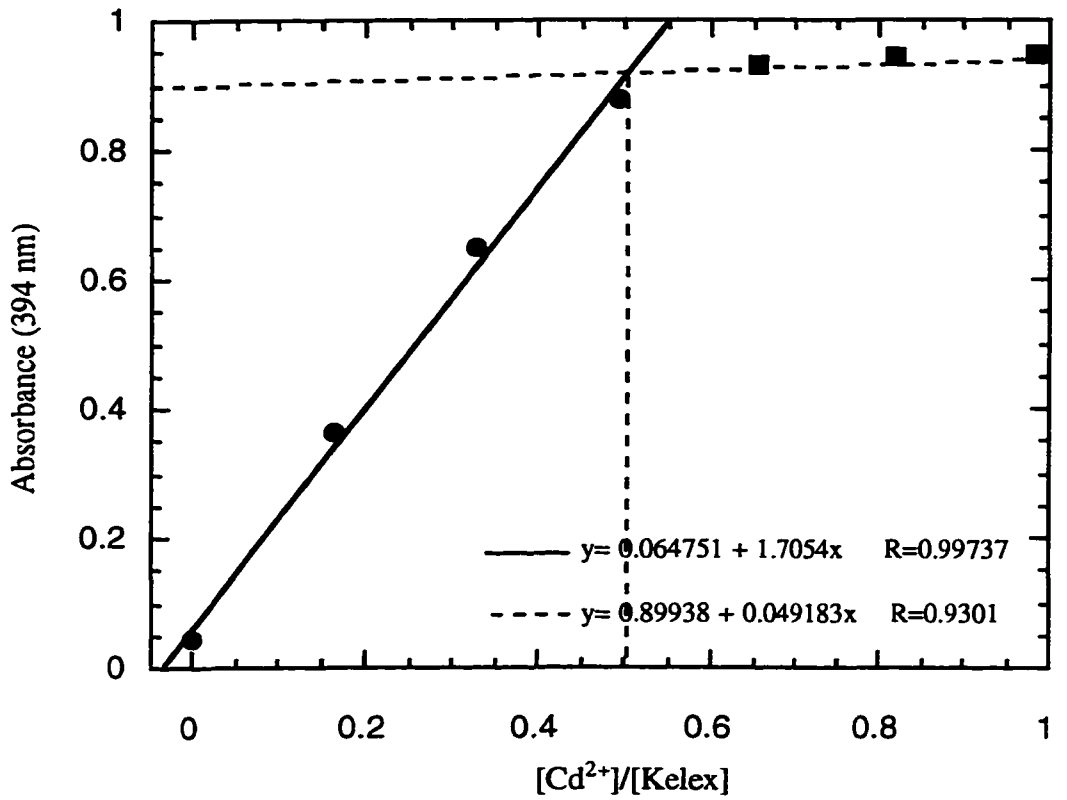

Figure III.26 Plot of absorbance at 394 nm versus ratio of moles Cd^{2+} to moles Kelex 100 for titration of 0.5 mM Kelex 100 in a solution of 0.05 M CO660 at pH 9.3. Equations are shown for the linear regression fit of the two linear regions. The intersection of the two lines occurs at x = 0.504 which corresponds to a 1:2 ratio of Cd^{2+} to Kelex 100.

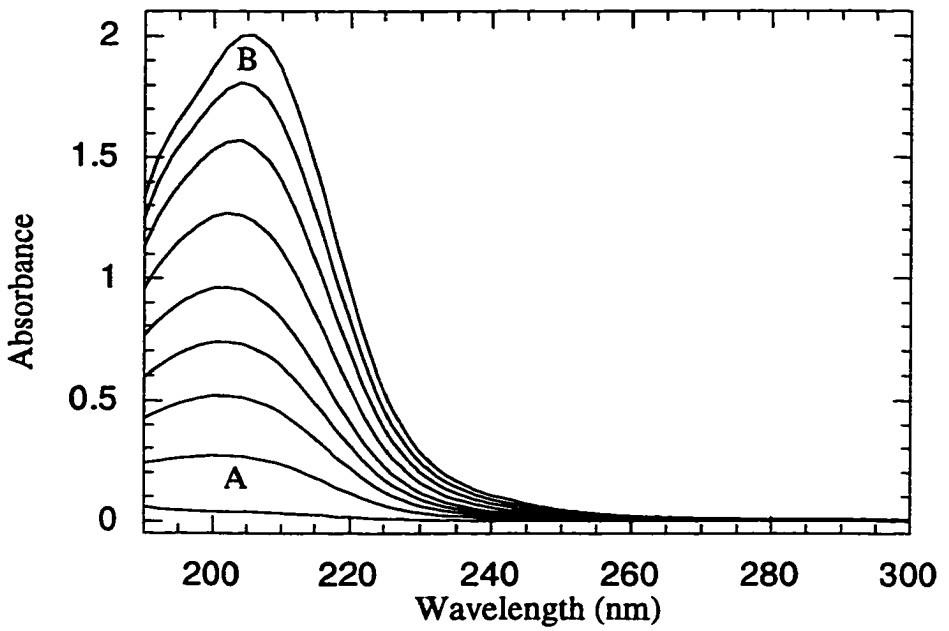

Figure III.27 UV spectra of Hg^{2+} in D.D. H_2O at pH 1.5. A) D.D. H_2O blank at pH 1.; B) after eight 4.0 μL aliquots of 0.1 mM Hg^{2+}

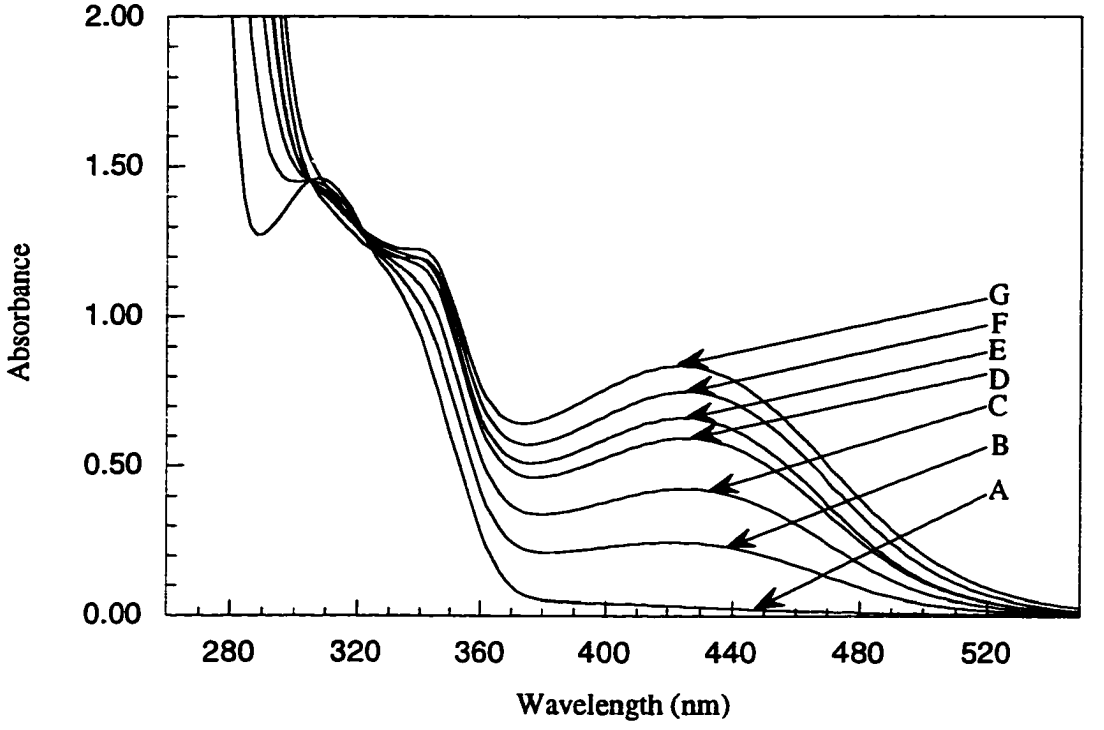

Figure III.28 UV-visible spectrum of 0.528 mM Kelex 100 in a solution of 0.05 M $CPNO_3$ with 5.0 mM CHES buffer at pH 8.4 titrated with 0.04456 M Hg^{2+}. The total volume of Hg^{2+} added (in μL) A) 0; B) 4.00; C) 8.00; D) 12.00; E) 14.00; F) 16.00; G) 18.0.

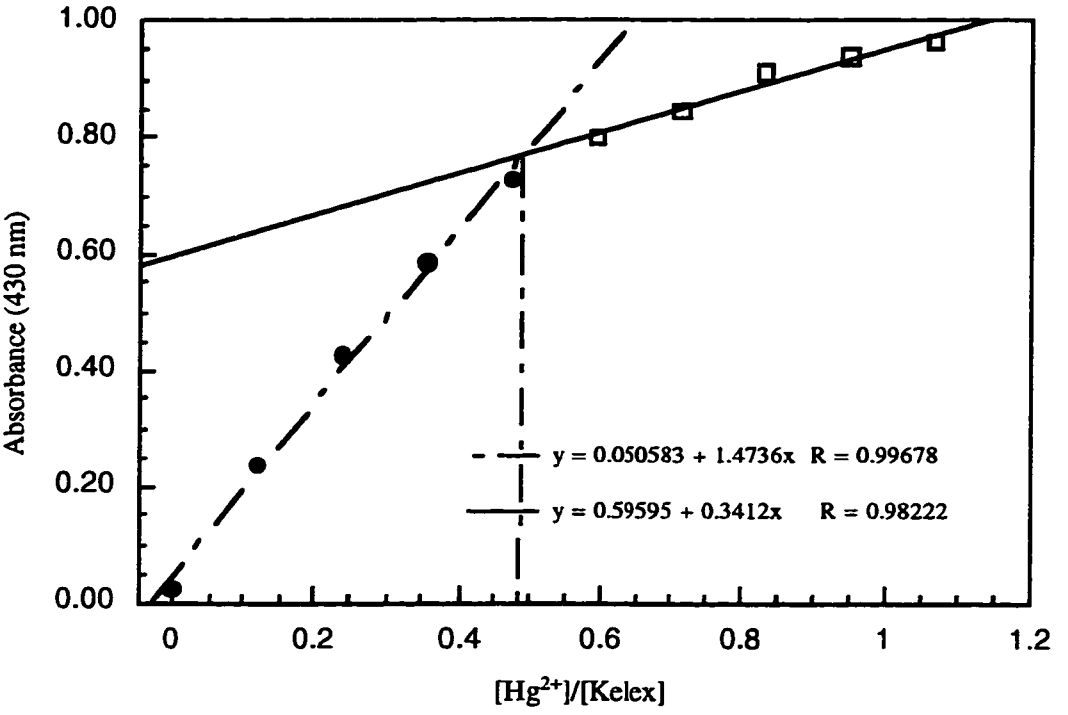

Figure III.29 Plot of absorbance at 430 nm versus ratio of moles Hg^{2+} to moles Kelex 100 for titration of 0.50 mM Kelex 100 in 0.05 M $CPNO_3$ solution at pH 8.4. Equations are shown for the linear regression fit of the two linear regions. The intersection of the two lines occurs at x = 0.487 which corresponds to a 1:2 ratio of Hg^{2+} to Kelex 100.

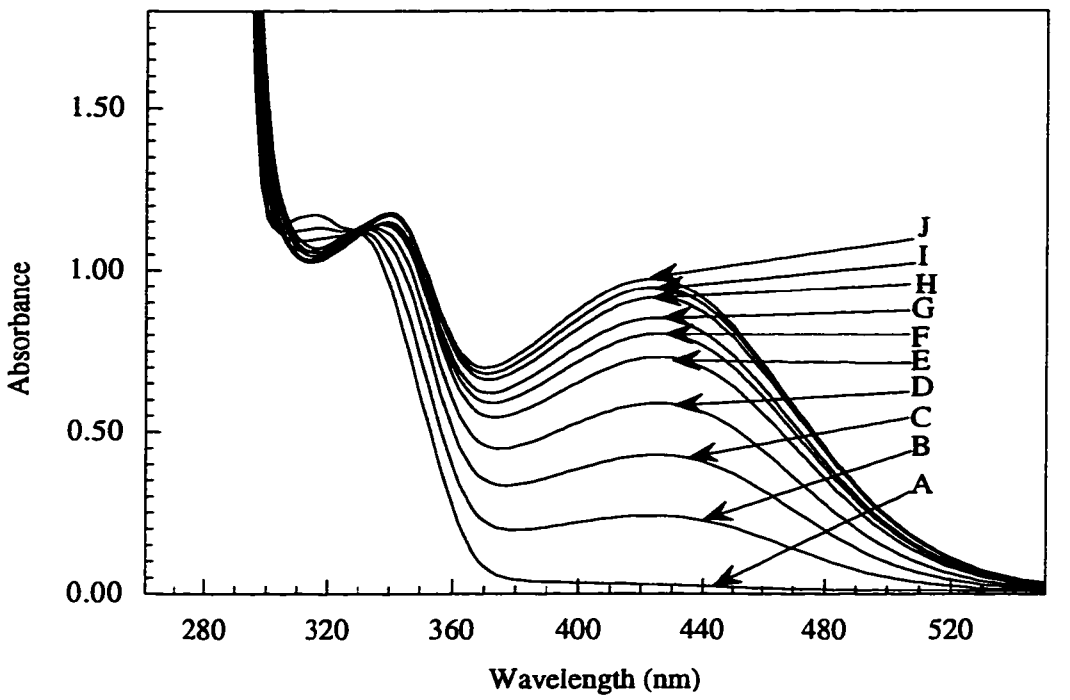

Figure III.30 UV-visible spectra of 0.528 mM Kelex 100 in 0.05 M CO660 solution with 5.0 mM CHES buffer at pH 8.9 titrated with 0.04556 M Hg^{2+}. The total volume of Hg^{2+} added (in μL) A) 0; B) 4.00; C) 6.00; D) 8.00; E) 12.00; F) 16.00; G) 20.00; H) 24.00; I) 28.00; J) 32.00.

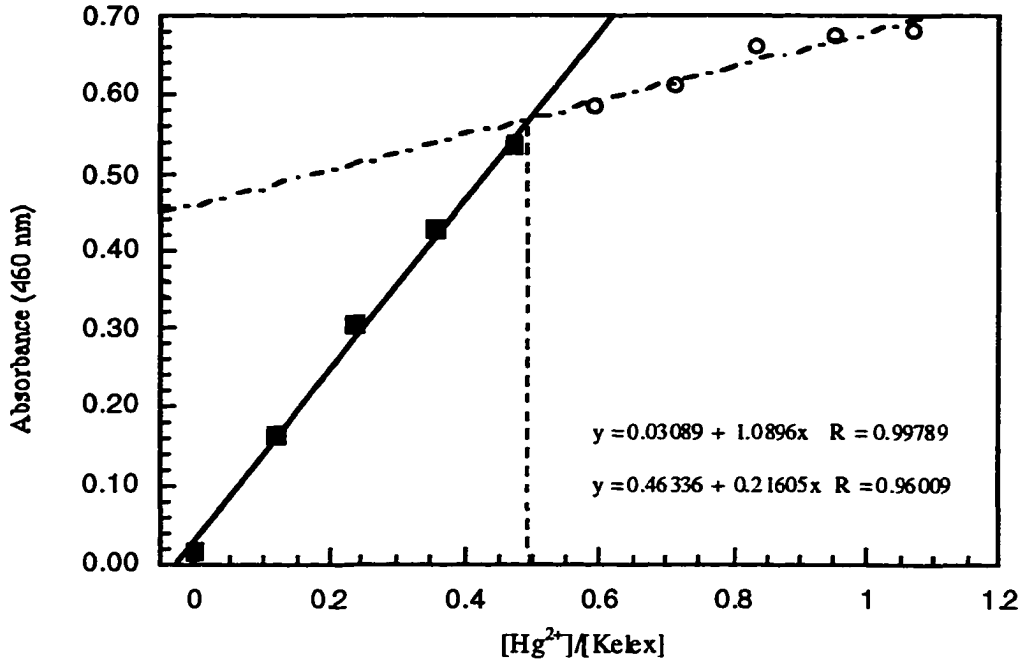

Figure III.31 Plot of absorbance at 460 nm versus ratio of moles Hg^{2+} to moles Kelex 100 for titration of 0.50 mM Kelex 100 in 0.05 M CO660 at pH 8.9. Equations are shown for the linear regression fit of the two linear regions. The intersection of the two lines occurs at x = 0.495 which corresponds to a 1:2 ratio of Hg^{2+} to Kelex 100.

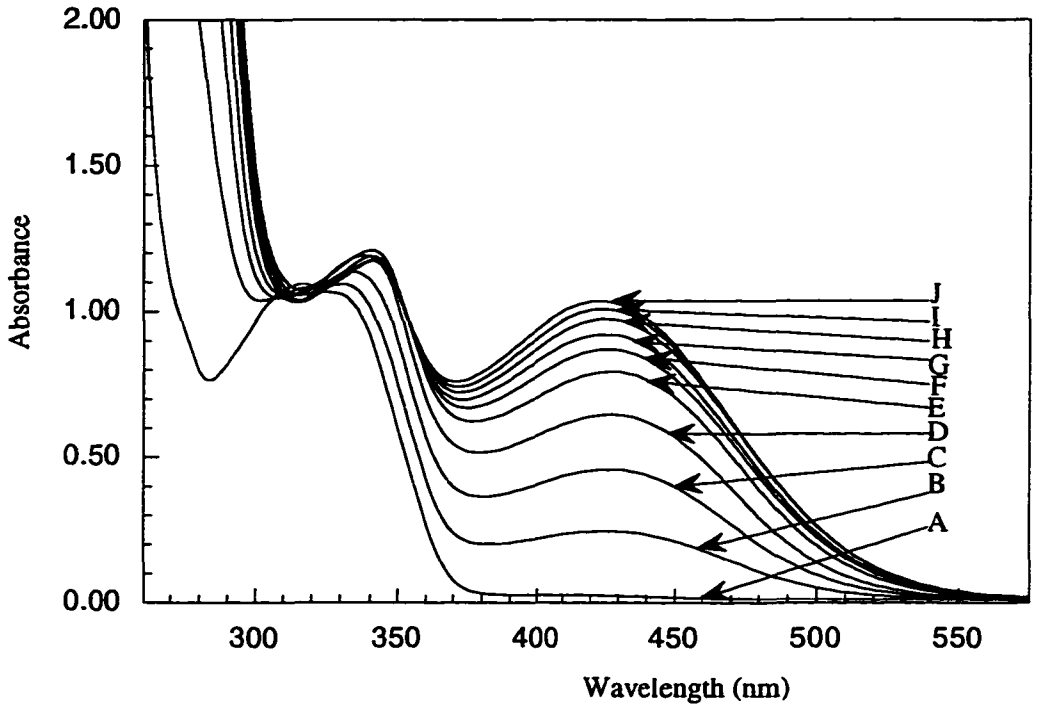

Figure III.32 UV-visible spectra of 0.528 mM Kelex 100 in 0.05 M DDAO solution with 5.0 mM CHES and 5.0 mM HEPES buffers at pH 8.5 titrated with 0.04556 M Hg^{2+}. The total volume of Hg^{2+} added (in μL) A) 0; B) 4.00; C) 8.00; D) 12.00; E) 16.00; F) 20.00; G) 24.00; H) 28.00;I) 32.00; J) 36.00.

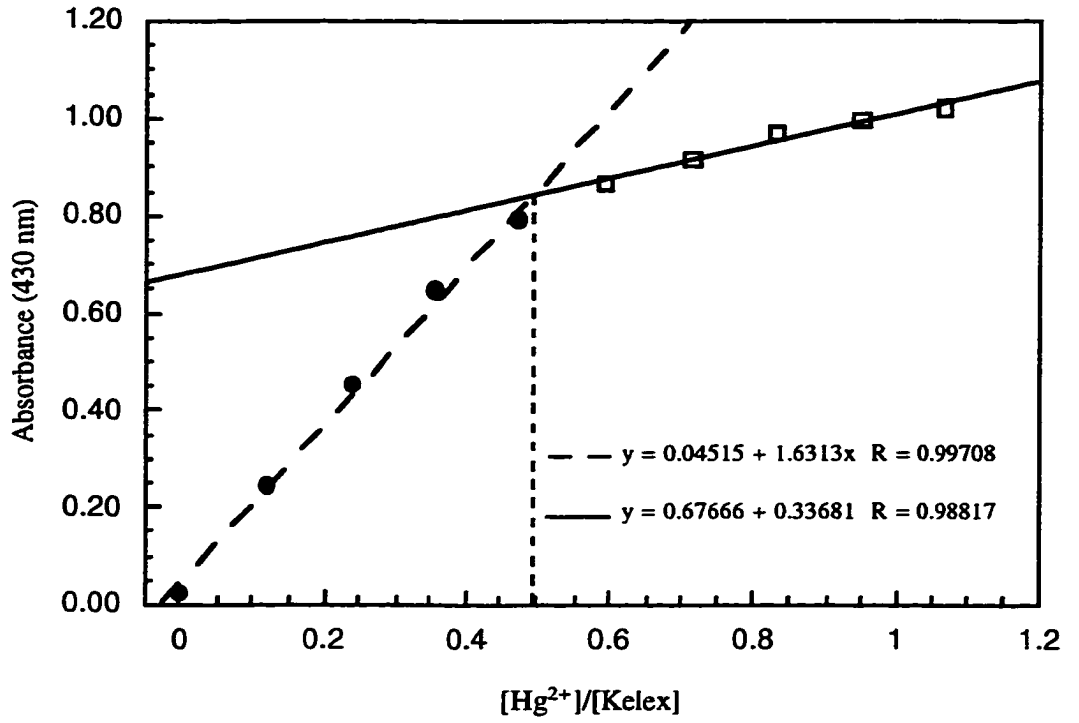

Figure III.33 Plot of absorbance at 430 nm versus ratio of moles Hg^{2+} to moles Kelex 100 for titration of 0.50 mM Kelex 100 in 0.05 M DDAO at pH 8.5. Equations are shown for the linear regression fit of the two linear regions. The intersection of the two lines occurs at x = 0.488 which corresponds to a 1:2 ratio of Hg^{2+} to Kelex 100.

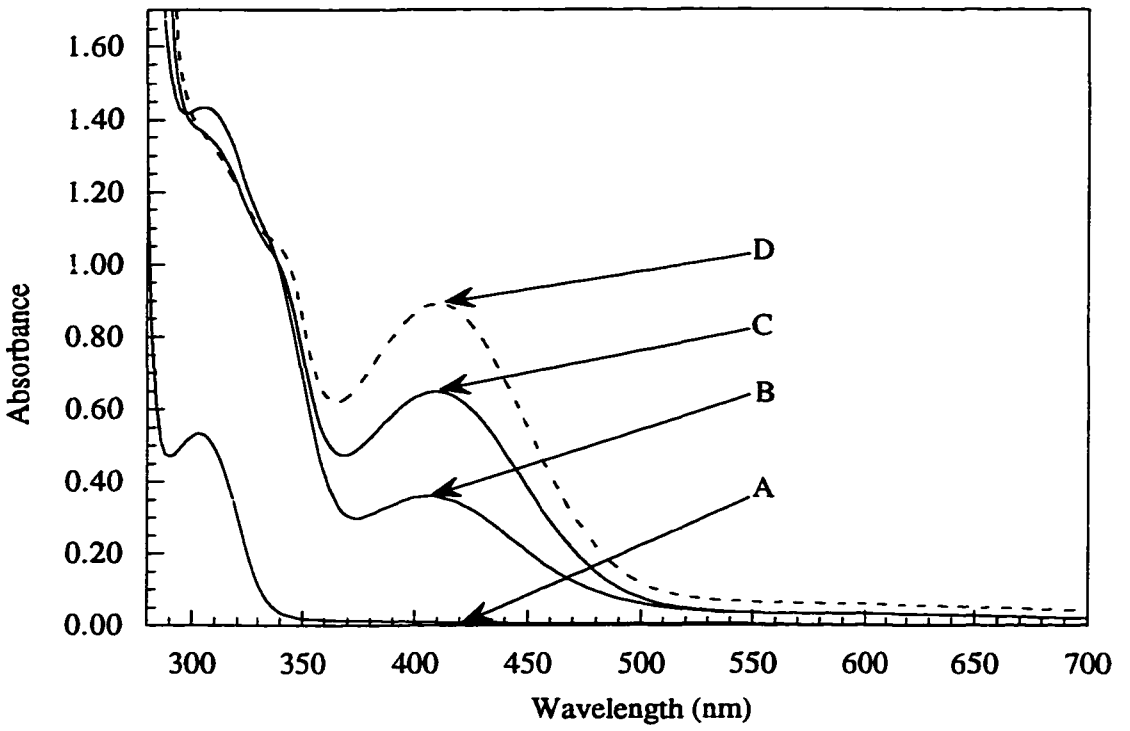

Figure III.34 UV-visible spectra of 0.5 mM Kelex 100 in a solution of 0.05 M $CPNO_3$ solution with 5.0 mM each CHES, MES and HEPES buffers at pH 7.5 titrated with 0.05480 M Pb^{2+}. The total volume of Pb^{2+} added (in μL) A) 0 B) 3.60; C) 7.20; D) 10.80. Formation of a precipitate caused increased baseline absorbance (dashed line).

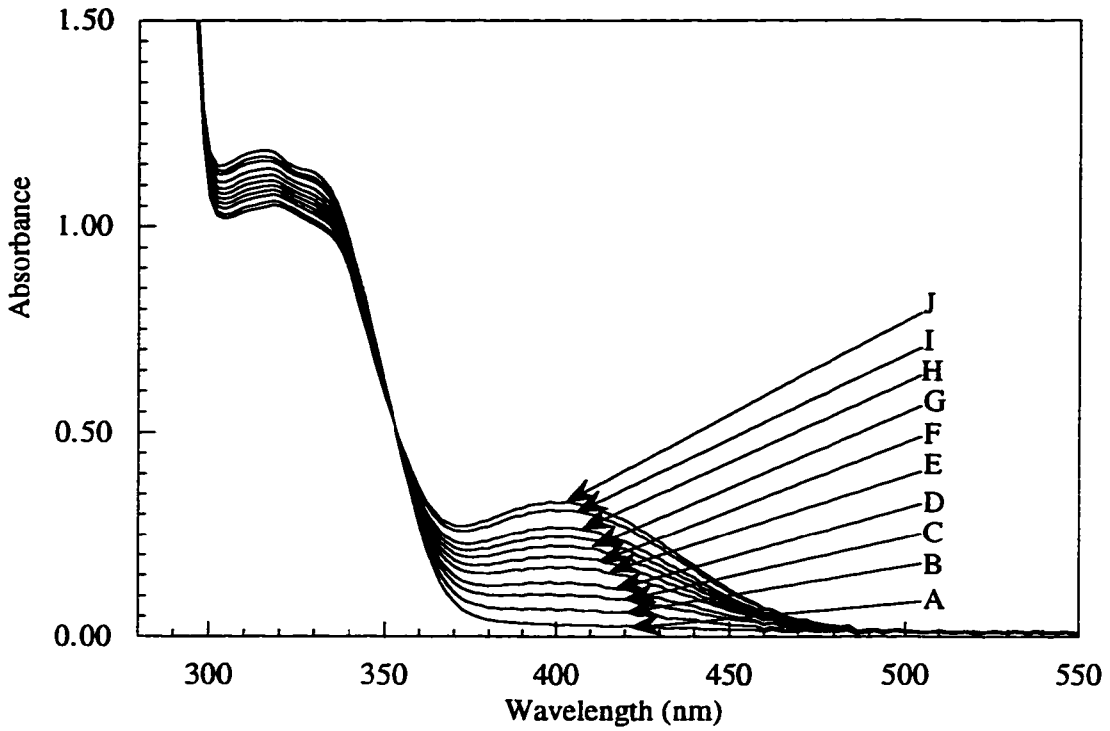

Figure III.35 UV-visible spectra of 0.528 mM Kelex 100 in 0.05 M CO660 solution with 5.0 mM each CHES, MES and HEPES buffers at pH 5.7 titrated with 0.05480 M Pb^{2+}. The total volume of Pb^{2+} added (in μL) A) 0; B) 3.60; C) 7.20; D) 10.80; E) 14.40; F) 18.00; G) 21.60; H) 28.80; I) 28.80; J) 32.40.

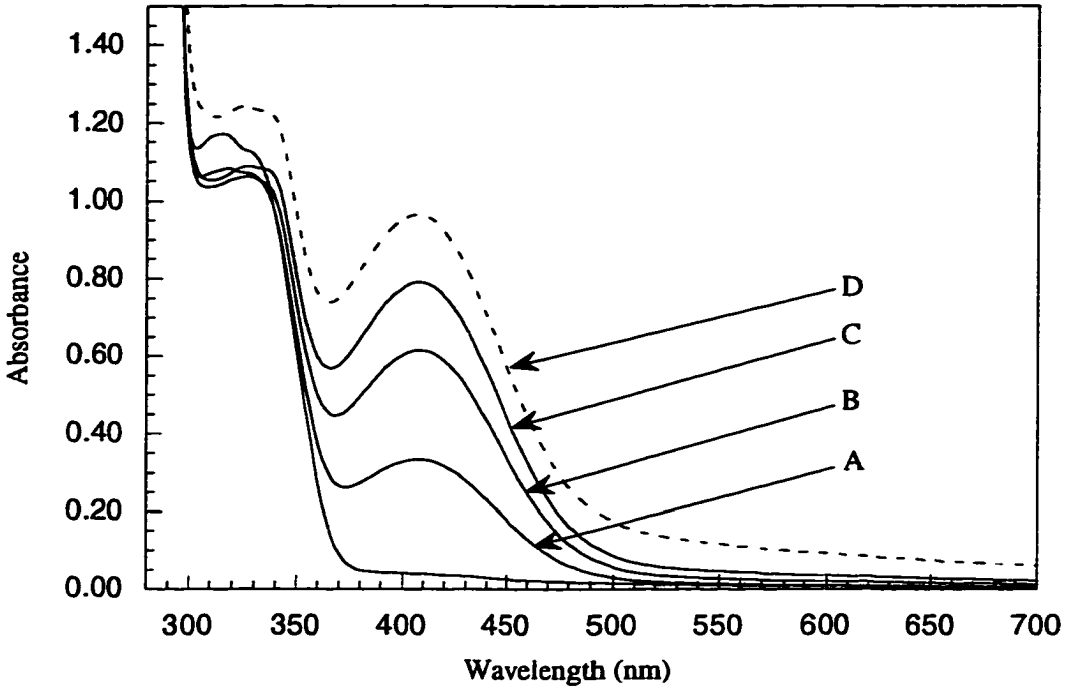

Figure III.36 UV-visible spectra of 0.528 mM Kelex 100 in 0.05 M CO660 solution with 5.0 mM each CHES, MES and HEPES buffers at pH 7.7 titrated with 0.05480 M Pb^{2+}. $^{+}$. The total volume of Pb^{2+} added (in μL) A) 0; B) 3.60; C) 7.20; D) 10.80.

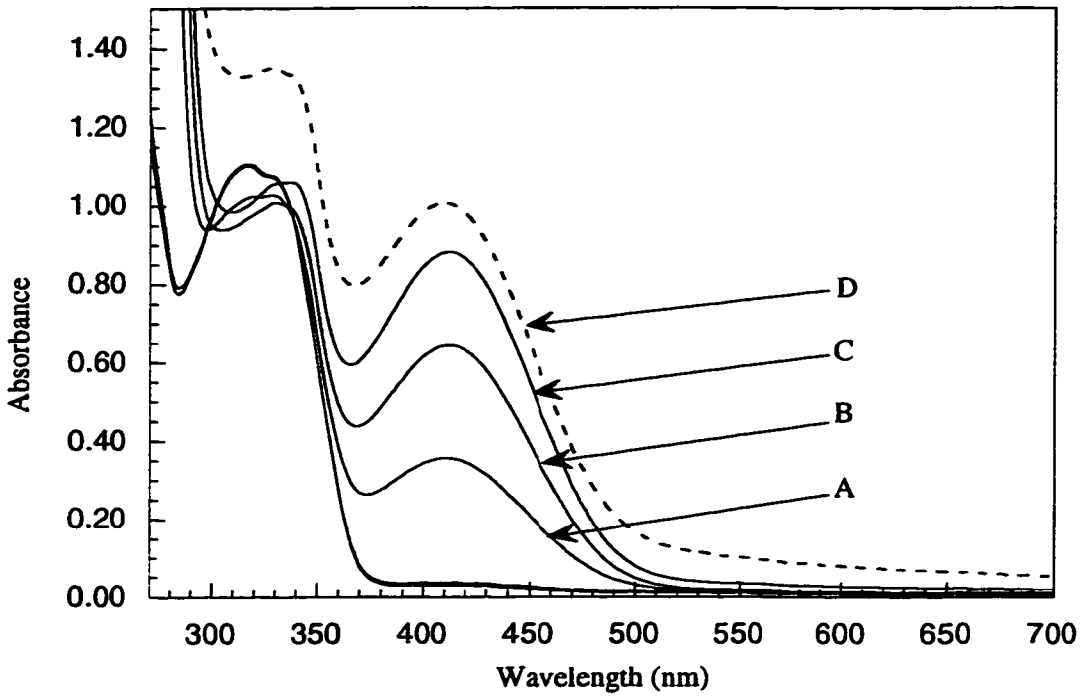

Figure III.37 UV-visible spectra of 0.528 mM Kelex 100 in 0.05 M DDAO solution with 5.0 mM each CHES, MES and HEPES buffers at pH 7.5 titrated with 0.05480 M Pb^{2+}. The total volume of Pb^{2+} added (in μL) A) 0; B) 3.60; C) 7.20; D) 10.80.

Table III.2 Summary of the results of metal ion titrations of Kelex 100 in various surfactant solutions.

Kelex	Metal ion	Surfactant solution	pH	M^{2+}:Kelex
0.5 mM	Cd^{2+}	0.05 M $CPNO_3$	8.6	1:3
0.5 mM	Cd^{2+}	0.05 CO660	9.3	1:2
0.17 mM	Cd^{2+}	0.05 M $C_{12}(EO)_6$	9.0	1:2
0.5 mM	Cd^{2+}	0.05 M $C_{12}(EO)_6$	9.0	1:2
0.5 mM	Cd^{2+}	0.05 M DDAO	8.7	1:2
0.5 mM	Hg^{2+}	0.05 M $CPNO_3$	8.4	1:2
0.5 mM	Hg^{2+}	0.05 CO660	8.9	1:2
0.5 mM	Hg^{2+}	0.05 M DDAO	8.5	1:2
0.5 mM	Pb^{2+}	0.05 M $CPNO_3$	7.5	(a)
0.5 mM	Pb^{2+}	0.05 CO660	5.7	(b)
0.5 mM	Pb^{2+}	0.05 CO660	7.7	(a)
0.5 mM	Pb^{2+}	0.05 M DDAO	7.5	(a)

(a) Precipitation of $Pb(OH)_2$ occurred as Pb^{2+}:Kelex 100 approached 1:2 in each case. (b) Could not be determined because complexation was not stoichiometric at this pH.

SED studies with Cd^{2+}

Semi-equilibrium dialysis (SED) experiments were performed to determine the range of conditions to be employed for LM-MEUF. Previous studies have shown that SED results provide a reasonable prediction of behavior in LM-MEUF and the SED technique is amenable to preliminary studies due to small solution volumes and the ability to run multiple sets of experiments simultaneously.

The first set of experiments was designed to investigate the adsorption behavior of Cd^{2+} on the cellulose dialysis membranes. Results are presented describing the effects of different membrane pretreatment methods. The SED studies were carried out using several types of surfactants (cationic, neutral) in the presence or absence of either metal or ligand at various pH values.

Membrane Treatment Studies

Preliminary experiments with both mercury and cadmium indicated that a significant proportion of the total metal ion in solution would be adsorbed onto the cellulose membrane of the SED cell. In earlier studies with copper and calcium, the membranes were soaked overnight in a solution of copper ion at the experimental pH in order to saturate the available metal binding sites on the membrane and eliminate or significantly reduce the loss of metal ion to the membrane. (26, 33) A series of SED experiments was done to evaluate several methods for reducing adsorption of Cd^{2+} ions by the membrane and to determine whether there was rejection of metal ions without ligand present.

Membranes were prepared by soaking overnight in D.D. water and then soaking an additional 12-24 hours in either D.D. water, 10 mM Ca^{2+}, 0.025 mM Cd^{2+}, 0.25 mM Cd^{2+} or 2.5 mM Cd^{2+}. The presoaking solutions were chosen to determine which metal and concentration would adequately saturate the membranes without introducing excess metal ions that would affect the values obtained for Cd^{2+} rejection or expulsion in the SED and UF systems. Immediately prior to assembling the SED cells, the membranes were rinsed thoroughly with D.D. water and lightly blotted. All SED experiments were performed in duplicate and the AA metal ion analysis of each solution was done in duplicate so results shown are the average of four analyses. Cadmium concentrations indicated as <0.0002 mM are below the detection limit (0.01 absorbance) for flame AA determination. In order to determine whether cadmium was being retained by the membrane, the total concentration of Cd^{2+} in solution was calculated by adding the concentrations (mM) of Cd^{2+} in the permeate and retentate together ($[Cd^{2+}]_{Tot}$) and comparing the sum to the stock concentration ($[Cd^{2+}]_O$), which was the original concentration in the retentate compartment. The volume of permeate and retentate solutions were assumed to be equal.

Results of blank experiments (without ligand) comparing the percent rejection (Eq. II.1) or percent expulsion (Eq. II.2) of Cd^{2+} in different surfactant solutions and membrane treatments at pH 5.0 are shown in Table III.3. Solutions contained approximately 0.20-0.25 mM Cd^{2+} in D.D. water, DDAO (0.05 M), $CPNO_3$ (0.05 M) or CO660 (0.05 M) surfactant. Comparison of the %R or %E for each surfactant shows that results are within 3-5%. However, when the concentration of Cd^{2+} in the stock solution, $[Cd^{2+}]_O$, is compared to the combined

retentate and permeate concentrations, $[Cd^{2+}]_{Tot}$, the value for $[Cd^{2+}]_{Tot}$ is 20-45% lower than that of $[Cd^{2+}]_o$ with untreated membranes in all cases except with DDAO. The $\%Cd^{2+}$ retained by the membrane is calculated according to Equation III.4 and results are shown in Table III.3.

$$\%Cd^{2+}_{lost} = \left(1 - \frac{[Cd^{2+}]_{Tot}}{[Cd^{2+}]_o}\right) \times 100 \qquad \textbf{Equation III.4}$$

The low value for $[Cd^{2+}]_{Tot}$ indicates that up to 45% of the uncomplexed Cd^{2+} is bound to the membrane. In the case of DDAO, the Cd^{2+} may remain in solution due to complexation by amine contaminants present in the surfactant. Generally, pretreatment of membranes with either 2.5 or 0.25 mM Cd^{2+} decreases the loss of the Cd^{2+} in solution to the SED membrane at this pH. In two cases, the loss is less with 0.25 mM Cd^{2+} than it is with 2.5 mM Cd^{2+}; therefore, subsequent experiments were done with 0.25 mM and 0.025 mM Cd^{2+}.

Table III.3 SED results for solution blanks containing Cd^{2+} in D.D. water or surfactant solution at pH 5.0. [a, b]

Membrane treatment	$[Cd^{2+}]_O$	$[Cd^{2+}]_R$	$[Cd^{2+}]_P$	$[Cd^{2+}]_{Tot}$	$\%R_{Cd}$ ($\%E_{Cd}$)[c]
D.D. water	0.234 mM Cd^{2+}	0.0631	0.0645	0.128	(2.1)
D.D. water	0.245 mM Cd^{2+}	0.0682	0.0696	0.138	(2.0)
0.25 mM Cd^{2+}	0.234mM Cd^{2+}	0.0840	0.0838	0.168	0.2
2.5 mM Cd^{2+}	0.234 mM Cd^{2+}	0.0842	0.0842	0.168	0
D.D. water	0.191 mM Cd^{2+} 0.05 M CO660	0.0702	0.0838	0.154	(16)
D.D. water	0.25 mM Cd^{2+} 0.05 M CO660	0.0623	0.0811	0.143	(23)
0.25 mM Cd^{2+}	0.191 mM Cd^{2+} 0.05 M CO660	0.0795	0.0918	0.171	(13)
2.5 mM Cd^{2+}	0.191 mM Cd^{2+} 0.05 M CO660	0.0732	0.0896	0.163	(18)
D.D. water	0.229 M Cd^{2+} 0.05 M DDAO	0.0505	0.171	0.222	(70)
0.25 mM Cd^{2+}	0.229 M Cd^{2+} 0.05 M DDAO	0.0450	0.170	0.215	(73)
2.5 mM Cd^{2+}	0.229 M Cd^{2+} 0.05 M DDAO	0.0523	0.186	0.238	(72)

Table III.3

D.D. water	0.276 mM Cd^{2+} 0.05 M $CPNO_3$	0.0359	0.154	0.190	(75)
0.25 mM Cd^{2+}	0.276 mM Cd^{2+} 0.05 M $CPNO_3$	0.0425	0.159	0.202	(73)
2.5 mM Cd^{2+}	0.276 mM Cd^{2+} 0.05 M $CPNO_3$	0.0304	0.140	0.171	(78)

(a) Concentration expressed as millimoles/liter, with $[Cd^{2+}]_{Tot.} = [Cd^{2+}]_R + [Cd^{2+}]_P$, where $[Cd^{2+}]_R$ is the concentration of Cd^{2+} in the retentate and $[Cd^{2+}]_P$ is the concentration of Cd^{2+} in the permeate. (b) Retentate and permeate results are the average of two SED runs. (c) Values in parentheses indicate %E

Table III.4 Percent Cd^{2+} lost (retained by SED membrane) in studies of solution blanks containing Cd^{2+} in D.D. water or surfactant solution at pH 5.0.

Membrane Treatment	Surfactant[a]			
	None	CO660	DDAO	$CPNO_3$
D.D. H_2O	45.3	19.4	3.1	31.2
	43.7	42.8		
0.25 mM Cd^{2+}	28.2	10.5	6.1	26.8
2.5 mM Cd^{2+}	28.2	14.7	0	38.0

(a) $\%Cd^{2+}$ lost calculated as $[1-([Cd^{2+}]_{Tot}/[Cd^{2+}]_O)] \times 100$ where $[Cd^{2+}]_{Tot}$ is combined $[Cd^{2+}]$ from retentate and permeate and $[Cd^{2+}]_O$ is the original concentration of Cd^{2+} in the stock and retentate solutions.

Table III.5 shows the results of SED experiments for blanks containing only D.D. water in both the retentate and permeate compartments to determine the amount of Cd^{2+} that diffuses from the membrane over the duration of the test at pH 5.0. The concentration of Cd^{2+} in both the retentate and permeate solutions was determined to be below the detection limit (<0.0002 mM) for all three treatment techniques.

Table III.5 Results for SED D.D. water blanks with presoaked membranes at pH 5.0.[a, b]

Membrane treatment	$[Cd^{2+}]_R$	$[Cd^{2+}]_P$
D.D. water	<0.0002	<0.0002
0.25 mM Cd^{2+}	<0.0002	<0.0002
2.5 mM Cd^{2+}	<0.0002	<0.0002

(a) Concentrations expressed as millimoles per liter, $[Cd^{2+}]_R$ is the concentration of Cd^{2+} in the retentate and $[Cd^{2+}]_P$ is the concentration of Cd^{2+} in the permeate. (b) All results are the average of two SED runs.

Pretreatment was examined in greater detail for the two surfactants chosen for further study, $C_{12}(EO)_6$ and $CPNO_3$. The neutral surfactant $C_{12}(EO)_6$ replaced CO660 for study because it is purer, more monodisperse and contains no residues. (81) $CPNO_3$ is the cationic surfactant selected. DDAO was eliminated due to the presence of amine impurities and because the charge and CMC varies with pH (pKa = 5.00). (70) The results of additional blank SED experiments with surfactant but no Cd^{2+} added to the retentate compartment are shown in Tables III.6 and III.7 to determine whether Cd^{2+} is leached out of the treated membrane in the presence of surfactant. $C_{12}(EO)_6$ experiments were performed at pH 6.0, 7.0 and 9.0. $CPNO_3$ experiments were performed at pH 7.0 and 9.0. Some Cd^{2+} was leached from the membrane in all cases with the highest concentrations at pH 9.0 for both $CPNO_3$ and $C_{12}(EO)_6$. Permeate concentrations of Cd^{2+} were higher than retentate Cd^{2+} concentrations in $CPNO_3$. This expulsion effect on unbound metal ions occurs when the retentate solution contains cationic surfactant as a result of the increased Cd^{2+} activity in the permeate relative to that in the retentate. (80) Concentrations of Cd^{2+} in $C_{12}(EO)_6$ were generally lower than in $CPNO_3$ and approximately equal in the permeate and retentate compartments.

Table III.6 SED results for Cd^{2+} in 5 mM $C_{12}(EO)_6$ solution without ligand using different membrane treatment techniques[a, b]

Membrane treatment	pH	$[Cd]_O$	$[Cd]_R$	$[Cd]_P$	$[Cd]_{Tot}$
D.D. H_2O	6.0	<0.0002	<0.0002	<0.0002	---
0.025 mM Cd^{2+}	6.0	<0.0002	0.0080	0.0080	0.0160
0.25 mM Cd^{2+}	6.0	<0.0002	0.0080	0.0090	0.0170
D.D. H_2O	7.0	<0.0002	<0.0002	<0.0002	---
0.025 mM Cd^{2+}	7.0	<0.0002	0.0093	0.0089	0.0182
0.25 mM Cd^{2+}	7.0	<0.0002	0.0069	0.0065	0.0134
D.D. H_2O	9.0	<0.0002	<0.0002	<0.0002	---
0.025 mM Cd^{2+}	9.0	<0.0002	0.0203	0.0204	0.0407
0.25 mM Cd^{2+}	9.0	<0.0002	0.0067	0.0068	0.0135

(a) Concentrationis expressed as millimoles/liter, with $[Cd^{2+}]_{Tot.} = [Cd^{2+}]_R + [Cd^{2+}]_P$, where $[Cd^{2+}]_R$ is the concentration of Cd^{2+} in the retentate, $[Cd^{2+}]_P$ is the concentration of Cd^{2+} in the permeate and $[Cd^{2+}]_O$ is the concentration of Cd^{2+} in the stock solution. (b) Retentate and permeate results reflect the average of two SED runs.

Table III.7 SED results for $[Cd^{2+}]$ in 0.05 M $CPNO_3$ solution without ligand using different membrane treatment techniques.[a, b]

Membrane treatment	pH	$[Cd]_O$	$[Cd]_R$	$[Cd]_P$	$[Cd]_{Tot}$
D.D. H_2O	7.0	<0.0002	<0.0002	<0.0002	<0.0002
0.025 mM Cd^{2+}	7.0	<0.0002	0.00115	0.0253	0.0265
0.25 mM Cd^{2+}	7.0	<0.0002	0.0039	0.0201	0.0240
D.D. H_2O	9.0	<0.0002	<0.0002	<0.0002	<0.0002
0.025 mM Cd^{2+}	9.0	<0.0002	0.0020	0.0046	0.0066
0.25 mM Cd^{2+}	9.0	<0.0002	0.0046	0.0154	0.0200

(a) Concentrationis expressed as millimoles/liter, with $[Cd^{2+}]_{Tot.} = [Cd^{2+}]_R + [Cd^{2+}]_p$, where $[Cd^{2+}]_R$ is the concentration of Cd^{2+} in the retentate, $[Cd^{2+}]_p$ is the concentration of Cd^{2+} in the permeate and $[Cd^{2+}]_O$ is the concentration of Cd^{2+} in the stock solution. (b) Retentate and permeate results reflect the average of two SED runs..

Additional studies were done to determine whether pretreatment of the membranes would reduce the amount of Cd^{2+} adsorbed by the membrane. Several methods were tried to saturate the available binding sites on the membranes. As a control, one set was soaked in D.D. water. Two different concentrations of Cd^{2+} solution, low (0.025 mM) and high (0.25 mM), were used in order to identify a balance between providing sufficient Cd^{2+} to reduce loss from the retentate while not releasing significant excesses of Cd^{2+} into the permeate solution. The fourth treatment technique, presoaking in 10 mM Ca^{2+}, was tried in order to prevent introducing additional Cd^{2+}. Experiments were done with both $CPNO_3$ and $C_{12}(EO)_6$ surfactants at varying pH both with and without 0.50 mM Kelex 100. Results are shown for $C_{12}(EO)_6$ at pH 6.0 (Table III.8), pH 7.0 (Table III.9) and pH 9.0 (Table III.10). Experiments in $CPNO_3$ solutions were performed at pH 7.0 (Table III.111) and pH 9.0 (Table III.12).

Table III.8 SED results for Cd^{2+} in 5 mM $C_{12}(EO)_6$ solution at pH 6.0 with different membrane treatment techniques.[a, b]

	without ligand				with 0.50 mM Kelex 100			
Membrane treatment	$[Cd]_O$	$[Cd]_R$	$[Cd]_P$	$[Cd]_{Tot}$	$[Cd]_O$	$[Cd]_R$	$[Cd]_P$	$[Cd]_{Tot}$
D.D. H_2O	0.0502	0.0128	0.0122	0.0250	0.0471	0.0151	0.0155	0.0306
0.025 mM Cd^{2+}	0.0502	0.0240	0.0227	0.0467	0.0471	0.0249	0.0243	0.0492
0.25 mM Cd^{2+}	0.0502	0.0258	0.0258	0.0516	0.0471	0.0230	0.0243	0.0473
10 mM Ca^{2+}	0.0502	0.0146	0.0141	0.0287	0.0471	0.0138	0.0146	0.0284

(a) Concentration expressed as millimoles/liter, with $[Cd^{2+}]_{Tot.} = [Cd^{2+}]_R + [Cd^{2+}]_P$, where $[Cd^{2+}]_R$ is the concentration of Cd^{2+} in the retentate and $[Cd^{2+}]_P$ is the concentration of Cd^{2+} in the permeate, $[Cd^{2+}]_O$ is the concentration in the stock solution (b) Retentate and permeate results reflect the average of two SED runs.

Table III.9 SED results for Cd^{2+} in 5 mM $C_{12}(EO)_6$ solution at pH 7.0 with different membrane treatment techniques. [a, b]

	no ligand				0.5 mM Kelex 100			
Membrane treatment	$[Cd]_O$	$[Cd]_R$	$[Cd]_P$	$[Cd]_{Tot}$	$[Cd]_O$	$[Cd]_R$	$[Cd]_P$	$[Cd]_{Tot}$
D.D. H_2O	0.0616	0.0096	0.0090	0.0186	0.0643	0.0127	0.0115	0.0242
0.025 mM Cd^{2+}	0.0616	0.0233	0.0252	0.0485	0.0643	0.0377	0.0307	0.0684
0.25 mM Cd^{2+}	0.0616	0.0214	0.0194	0.0408	0.0643	0.0283	0.0231	0.0514
10 mM Ca^{2+}	0.0616	0.0110	0.0117	0.0227	0.0643	0.0153	0.0126	0.0279

(a) Concentration expressed as millimoles/liter, with $[Cd^{2+}]_{Tot.} = [Cd^{2+}]_R + [Cd^{2+}]_P$, where $[Cd^{2+}]_R$ is the concentration of Cd^{2+} in the retentate and $[Cd^{2+}]_P$ is the concentration of Cd^{2+} in the permeate, $[Cd^{2+}]_O$ is the concentration in the stock solution (b) Retentate and permeate results reflect the average of two SED runs.

Table III.10 SED results for Cd^{2+} in 5 mM $C_{12}(EO)_6$ solution at pH 9.0 with different membrane treatment techniques. [a,b]

	no ligand				0.50 mM Kelex 100			
Membrane treatment	$[Cd]_O$	$[Cd]_R$	$[Cd]_P$	$[Cd]_{Tot}$	$[Cd]_O$	$[Cd]_R$	$[Cd]_P$	$[Cd]_{Tot}$
D.D. H_2O	0.0596	0.0058	0.0059	0.0117	0.0630	0.0592	0.0001	0.0593
0.025 mM Cd^{2+}	0.0596	0.0245	0.0178	0.0423	0.0630	0.0942	0.0022	0.0964
0.25 mM Cd^{2+}	0.0596	0.0181	0.0178	0.0359	0.0630	0.0901	0.0014	0.0915
10 mM Ca^{2+}	0.0596	0.0085	0.0083	0.0133	0.0630	0.0588	<0.0002	0.0588

(a) Concentration expressed as millimoles/liter, with $[Cd^{2+}]_{Tot.} = [Cd^{2+}]_R + [Cd^{2+}]_P$, where $[Cd^{2+}]_R$ is the concentration of Cd^{2+} in the retentate and $[Cd^{2+}]_P$ is the concentration of Cd^{2+} in the permeate, $[Cd^{2+}]_O$ is the concentration in the stock solution (b) Retentate and permeate results reflect the average of two SED runs.

Table III.11 SED results for Cd^{2+} in 0.05 M $CPNO_3$ solution at pH 7.0 with different membrane treatment techniques [a, b]

	no ligand				0.50 mM Kelex 100			
Membrane treatment	**$[Cd]_O$**	**$[Cd]_R$**	**$[Cd]_P$**	**$[Cd]_{Tot}$**	**$[Cd]_O$**	**$[Cd]_R$**	**$[Cd]_P$**	**$[Cd]_{Tot}$**
D.D. H_2O	0.0409	0.0047	0.0228	0.0275	0.0413	0.0058	0.0225	0.0283
0.025 mM Cd^{2+}	0.0409	0.0073	0.0376	0.0449	0.0413	0.0159	0.0644	0.0803
0.25 mM Cd^{2+}	0.0409	0.0099	0.0504	0.0603	0.0413	0.0111	0.0485	0.0596
10 mM Ca^{2+}	0.0409	0.0046	0.0242	0.0288	0.0413	0.0068	0.0275	0.0343

(a) Concentration expressed as millimoles/liter, with $[Cd^{2+}]_{Tot.} = [Cd^{2+}]_R + [Cd^{2+}]_P$, where $[Cd^{2+}]_R$ is the concentration of Cd^{2+} in the retentate and $[Cd^{2+}]_P$ is the concentration of Cd^{2+} in the permeate, $[Cd^{2+}]_O$ is the concentration in the stock solution (b) Retentate and permeate results reflect the average of two SED runs.

Table III.12 Comparison of SED results with and without Kelex 100 in 0.05 M $CPNO_3$ solution at pH 9.0 with different membrane treatment techniques. [a,b]

	no ligand				0.50 mM Kelex 100			
Membrane treatment	$[Cd]_O$	$[Cd]_R$	$[Cd]_P$	$[Cd]_{Tot}$	$[Cd]_O$	$[Cd]_R$	$[Cd]_P$	$[Cd]_{Tot}$
D.D. H_2O	0.0407	0.0054	0.0014	0.0068	0.0407	0.0398	0.0002	0.0400
0.025 mM Cd^{2+}	0.0407	0.0105	0.0307	0.0412	0.0407	0.0535	0.0006	0.0541
0.25 mM Cd^{2+}	0.0407	0.0126	0.0352	0.0478	0.0407	0.0748	0.0008	0.0756
10 mM Ca^{2+}	0.0407	0.0066	0.0182	0.0248	0.0407	0.0407	0.0002	0.0409

(a) Concentration expressed as millimoles/liter, with $[Cd^{2+}]_{Tot.} = [Cd^{2+}]_R + [Cd^{2+}]_P$, where $[Cd^{2+}]_R$ is the concentration of Cd^{2+} in the retentate and $[Cd^{2+}]_P$ is the concentration of Cd^{2+} in the permeate, $[Cd^{2+}]_O$ is the concentration in the stock solution (b) Retentate and permeate results reflect the average of two SED runs.

The results of experiments shown in Tables III.8-III.12 show that generally there is a decrease in Cd^{2+} adsorption by the dialysis membranes when the membranes are presoaked in Cd^{2+}. At pH 6.0-7.0, presoaking in Cd^{2+} at either high or low concentration reduces the loss of Cd^{2+} to the membrane and the total Cd^{2+} is close to that of the original retentate (stock) solution. In $CPNO_3$, the retentate concentration of Cd^{2+} is much lower than the permeate concentration as a result of expulsion. Presoaking in Ca^{2+} appears to be completely ineffective for experiments with $C_{12}(EO)_6$ since $[Cd^{2+}]_{Tot}$ is approximately the same for the trials which were presoaked in Ca^{2+} as it is for those which were soaked in D.D. water only. Some benefit is seen from the Ca^{2+} presoak with $CPNO_3$ as a result of expulsion. Total Cd^{2+} is higher for membranes soaked in Ca^{2+} than for those soaked in D.D. water but it is much lower than $[Cd^{2+}]_{Tot}$ for membranes soaked in Cd^{2+}.

Experiments with 0.50 mM Kelex 100 in both $CPNO_3$ and $C_{12}(EO)_6$ were performed to determine how much Cd^{2+} could be leached from the membrane. Membranes were presoaked in Cd^{2+} but no Cd^{2+} was added to the retentate compartment. Presoaking in Cd^{2+} is beneficial at pH 9.0 when there is no ligand present. The $[Cd^{2+}]_{Tot}$ is slightly low in $C_{12}(EO)_6$ but it is approximately equal to the stock concentration in $CPNO_3$. However, with ligand present at this pH, $[Cd^{2+}]_{Tot}$ is high by as much as 50%. The excess ligand competes for the membrane-bound Cd^{2+} such that the retentate concentration of Cd^{2+} is increased. Results for experiments in $C_{12}(EO)_6$ are shown in Table III.13 and for experiments in $CPNO_3$ in Table III.14.

Table III.13 SED results for 0.5 mM Kelex 100 in 5 mM $C_{12}(EO)_6$ with pretreated membranes and no Cd^{2+}.[a, b]

pH	Membrane treatment	$[Cd^{2+}]_R$	$[Cd^{2+}]_P$	$[Cd]_{Tot}$
7.0	D.D. water	<0.0002	<0.0002	<0.0002
7.0	0.025 mM Cd^{2+}	0.0034	0.0014	0.0048
7.0	0.25 mM Cd^{2+}	0.0097	0.0044	0.0141
9.0	D.D. water	<0.0002	<0.0002	<0.0002
9.0	0.025 mM Cd^{2+}	0.0252	<0.0002	0.0252
9.0	0.25 mM Cd^{2+}	0.0419	0.0002	0.0421

(a) Concentration expressed as millimoles/liter, with $[Cd^{2+}]_{Tot.} = [Cd^{2+}]_R + [Cd^{2+}]_P$, where $[Cd^{2+}]_R$ is the concentration of Cd^{2+} in the retentate and $[Cd^{2+}]_P$ is the concentration of Cd^{2+} in the permeate, $[Cd^{2+}]_O$ is the concentration in the stock solution (b) Retentate and permeate results reflect the average of two SED runs.

Table III.14 SED results for 0.5 mM Kelex 100 in 0.05 M $CPNO_3$ with pretreated membranes and no Cd^{2+}.[a, b]

pH	Membrane treatment	$[Cd^{2+}]_R$	$[Cd^{2+}]_P$	$[Cd]_{Tot}$
7.0	D.D. water	<0.0002	<0.0002	<0.0002
7.0	0.025 mM Cd^{2+}	0.0027	0.0092	0.0119
7.0	0.25 mM Cd^{2+}	0.0063	0.0221	0.0284
9.0	D.D. water	<0.0002	<0.0002	<0.0002
9.0	0.025 mM Cd^{2+}	0.0174	0.002	0.0194
9.0	0.25 mM Cd^{2+}	0.0363	0.006	0.0423

(a) Concentration expressed as millimoles/liter, with $[Cd^{2+}]_{Tot.} = [Cd^{2+}]_R + [Cd^{2+}]_P$, where $[Cd^{2+}]_R$ is the concentration of Cd^{2+} in the retentate and $[Cd^{2+}]_P$ is the concentration of Cd^{2+} in the permeate, $[Cd^{2+}]_O$ is the concentration in the stock solution (b) Retentate and permeate results reflect the average of two SED runs.

The quantity of Cd^{2+} complexed by the ligand at pH 9.0 is about the same in both $CPNO_3$ and $C_{12}(EO)_6$. When the membranes are presoaked in 0.025 mM Cd^{2+} the total concentration of Cd^{2+} released is about 0.02 mM. When the membrane is presoaked in the more concentrated 0.25 mM Cd^{2+} solution, the total concentration of released Cd^{2+} is 0.042 mM, a two-fold increase. This is the highest maximum concentration leached from the membranes. At pH 7.0, little Cd^{2+} is removed from the membrane because the ligand does not complex Cd^{2+} well at this pH. In $CPNO_3$ the effects of ion expulsion can be seen because the concentration of Cd^{2+} is higher in the permeate than in the retentate. Also, for both Cd^{2+} pretreatment conditions (0.025 mM, 0.25 mM), the total concentration of released Cd^{2+} in the $CPNO_3$ experiements is approximately twice that found in the $C_{12}(EO)_6$ experiments.

Summary of Membrane Studies

The results of membrane studies verified that a significant fraction of the uncomplexed Cd^{2+} initially present in the retentate solution, either with or without ligand present, was retained by the SED membrane. When a low concentration Cd^{2+} solution was used for pretreatment, the amount of Cd^{2+} lost to the membrane could be reduced. Pretreatments using solutions containing different concentrations of Cd^{2+} solution were tested and all were effective.

Another consideration was the effect of the ligand on membrane-bound Cd^{2+}. Experiments with ligand at high pH showed that the analyzed concentration

concentration5of the retentate solution was greater than the original retentate concentration by as much as 50%, presumably due to competition by the ligand for the membrane-bound Cd^{2+}. Total concentrations of Cd^{2+} as high as 0.042 mM were found in experiments where ligand was present and no Cd^{2+} was added to the retentate compartment. Approximately half as much was removed by the ligand when the pretreatment contained 0.025 mM Cd^{2+}. This pretreatment solution was generally as effective at reducing Cd^{2+} loss as the one containing a higher concentration of Cd^{2+} (0.25 mM). It appeared that using the low concentration solution was adequate to saturate the available binding sites on the membrane and that pretreatment with the more concentrated solution only increased the quantity of loosely held Cd^{2+}. For this reason, membranes for later SED experiments were prepared by presoaking in 0.025 mM Cd^{2+} solution.

Because Cd^{2+} was complexed by available ligand at high pH and the ligand remained primarily in the retentate, there was some concern that the values of $\%R_{Cd}$ might be inflated by these higher concentrations. Tables III.15 and III.16 below compare the $\%R_{Cd}$ for 0.50 mM Kelex 100 in $C_{12}(EO)_6$ and $CPNO_3$ solutions for all four of the pretreatment techniques evaluated at pH 9.0. Complete data are shown in Tables III.9 and III.11. The $[Cd^{2+}]_{Tot}$ and $\% Cd^{2+}{}_{\Delta}$ (Eqn III.4) are also shown.

Table III.15 Comparison of $[Cd^{2+}]_{Tot}$ and $\%R_{Cd}$ for SED results at pH 9.0 in $CPNO_3$ with 0.50 mM Kelex 100.[a, b]

Membrane treatment	$[Cd]_O$	$[Cd]_{Tot}$	$\% Cd^{2+}{}_{\Delta}$	$\%R_{Cd}$
D.D. water	0.0630	0.0593	+6	99.8
0.025 mM Cd^{2+}	0.0630	0.0964	-53	97.7
0.25 mM Cd^{2+}	0.0630	0.0915	-45	98.4
10 mM Ca^{2+}	0.0630	0.0590	+6	99.7

(a) Concentrations are expressed as millimoles per liter (b) $[Cd]_O$ is the original concentration of Cd^{2+} in the retentate, $[Cd^{2+}]_{Tot} = [Cd^{2+}]_P + [Cd^{2+}]_R$, $\%Cd^{2+}{}_{\Delta} = (1 - ([Cd^{2+}]_{Tot}/[Cd^{2+}]_O)) \times 100$.

Table III.16 Comparison of $[Cd^{2+}]_{Tot}$ and $\%R_{Cd}$ for SED results at pH 9.0 in $C_{12}(EO)_6$ with 0.50 mM Kelex 100.[a,b]

Membrane treatment	$[Cd]_O$	$[Cd]_{Tot}$	$\% Cd^{2+}_{\Delta}$	$\%R_{Cd}$
D.D. water	0.0407	0.0418	-3	99.5
0.025 mM Cd^{2+}	0.0407	0.0541	-33	98.9
0.25 mM Cd^{2+}	0.0407	0.0756	-86	98.9
10 mM Ca^{2+}	0.0407	0.0409	-0.5	99.5

(a) Concentrations are expressed as millimoles per liter (b) $[Cd]_O$ is the original concentration of Cd^{2+} in the retentate, $[Cd^{2+}]_{Tot} = [Cd^{2+}]_P + [Cd^{2+}]_R$, $\%Cd^{2+}_{\Delta} = (1 - ([Cd^{2+}]_{Tot}/[Cd^{2+}]_O)) \times 100$.

Comparison of these numbers shows that calculated $\%R_{Cd}$ varies by 2% or less even with an 86% increase in analyzed Cd^{2+}.

Concentration Studies of Cd^{2+} with 0.5 mM Kelex 100

A study of the effect of varying Cd^{2+} concentration on percent rejection and expulsion was done in nonionic ($C_{12}(EO)_6$) and cationic ($CPNO_3$) surfactants. The concentration of Kelex 100 was kept constant at 0.50 mM and pH was controlled with 10 mM CHES buffer at pH 9.0 $\pm$ 0.3. Results are shown in Tables III.16 and III.17. Figure III.38 shows a plot of percent rejection Cd^{2+} versus Cd^{2+} concentration in the stock solution ($[Cd^{2+}]_O$) for $C_{12}(EO)_6$ solutions. Rejection is greater than 95% until the Cd^{2+} concentration exceeds 0.25 mM which corresponds to the 1:2 metal to ligand stoichiometry. Cd^{2+} concentration in the stock solution

($[Cd^{2+}]_O$) is plotted versus the percent rejection for $CPNO_3$ solutions in Figure III.39. The $\%R_{Cd}$ calculated for the data at $[Cd^{2+}]_O = 0.476$ appears to be high when compared to the other data. However, the $[Cd^{2+}]_{Tot}$ for this point is lower than $[Cd^{2+}]_O$ by about 50%. This may indicate that a large percentage of the uncomplexed Cd^{2+} was retained by the membrane, causing the $[Cd^{2+}]_P$ to be low and the value calculated for $\%R_{Cd}$ to be high.

Table III.17 SED results for varying concentrations of Cd^{2+} with Kelex 100 in $C_{12}(EO)_6$ at pH 9.0.[a]

$[Cd^{2+}]_O$	$[Cd^{2+}]_R$[b]	$[Cd^{2+}]_P$[b]	$\%R_{Cd}$
0.100	0.0922	<0.0002	≥99.8
0.105	0.125	0.0001	99.9
0.197	0.197	0.0040	99.8
0.216	0.223	0.0016	99.3
0.273	0.245	0.0035	98.6
0.281	0.213	0.0077	96.4
0.319	0.272	0.0114	95.8
0.495	0.310	0.0223	92.8
0.620	0.412	0.0912	77.9

(a) Concentrations expressed as millimoles per liter, $[Cd^{2+}]_o$ is the original concentration of retentate, $[Cd^{2+}]_R$ concentration of retentate after equilibration, $[Cd^{2+}]_P$ concentration of permeate, $[CHES]_{R,O}$ = 10 mM, $[Kelex]_{R,O}$ = 0.50 mM, $[C_{12}(EO)_6]_{R,O}$ = 5.0 mM, pH = 9.00 ± 0.03 (b) Permeate and retentate results are the average of two SED runs.

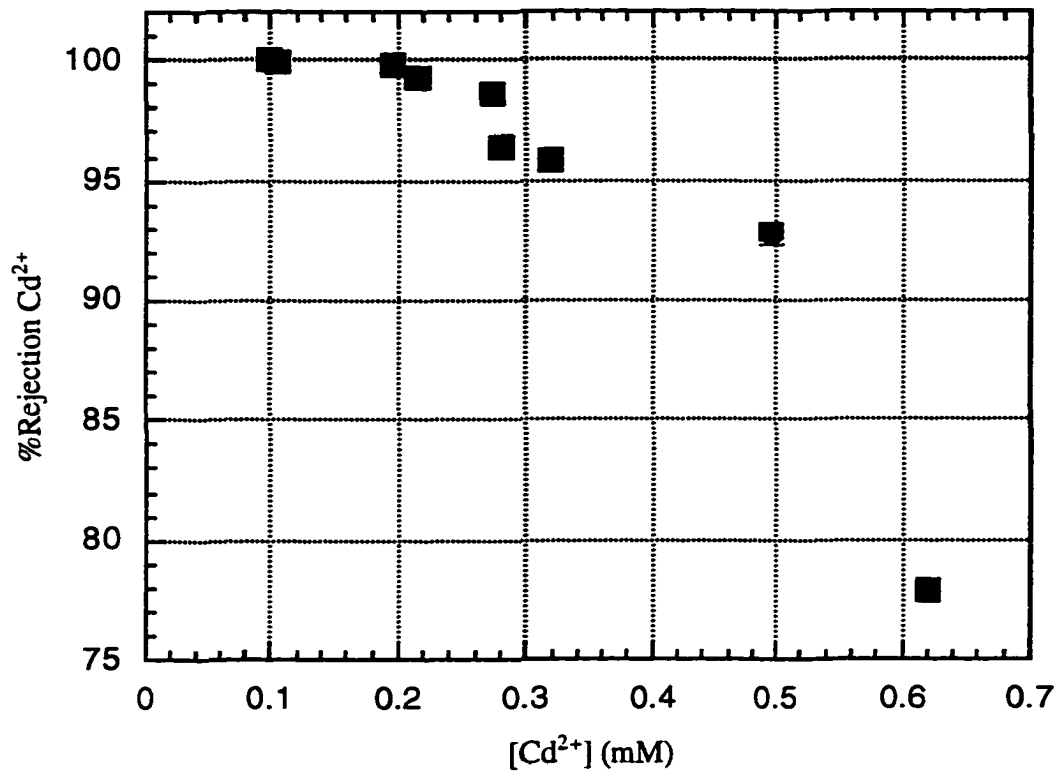

Figure III.38 Plot of Cd^{2+} rejection (%) as a function of $[Cd^{2+}]_o$ for 0.5 mM Kelex 100 in 5 mM $C_{12}(EO)_6$ surfactant solution at pH 9.0.

Table III.18 SED results for varying concentrations of Cd^{2+} in 0.05 M $CPNO_3$ with 0.5 mM Kelex 100 at pH 9.0. [a, b, c]

$[Cd^{2+}]_O$	$[Cd^{2+}]_R$	$[Cd^{2+}]_P$	$\%R_{Cd}$
0.0441	0.0407	0.00015	99.6
0.0864	0.0810	0.0008	99.0
0.1700	0.1974	0.0135	89.8
0.2240	0.1280	0.0333	*74.0*
0.4760	0.2040	0.0284	*86.1*

(a) All solutions contain 10 mM CHES buffer (b) Concentrations expressed as millimoles per liter, $[Cd^{2+}]_O$ is original concentration of retentate, $[Cd^{2+}]_R$ concentration of retentate after equilibration, $[Cd^{2+}]_P$ concentration of permeate (c) Permeate and retentate results are the average of two SED runs.

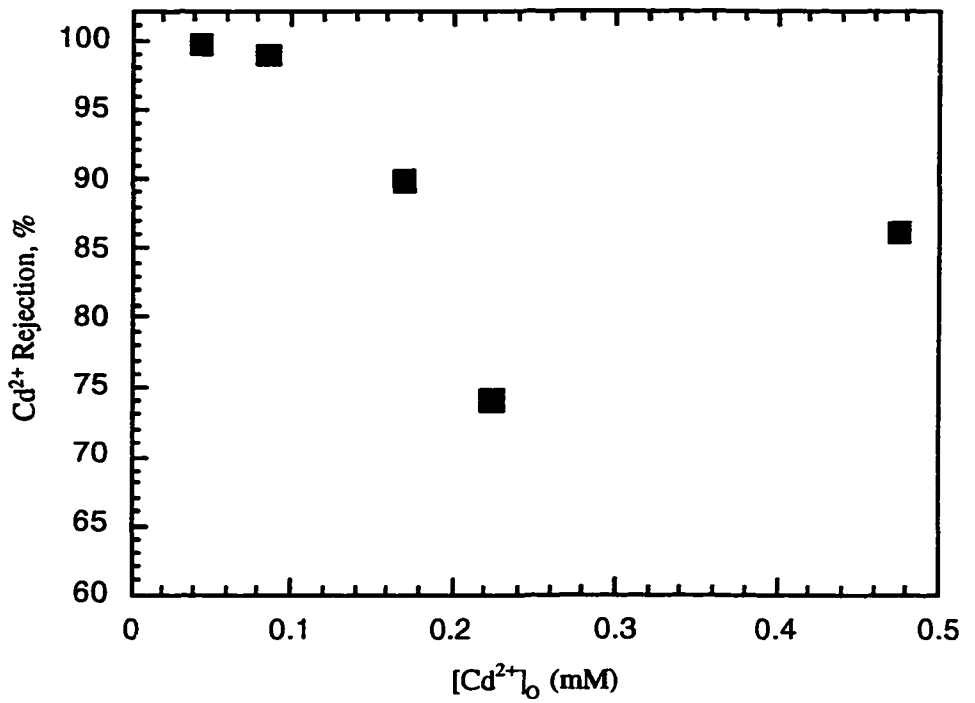

Figure III.39 Plot of rejection of Cd^{2+}, % as a function of $[Cd^{2+}]_o$ in 0.05 M $CPNO_3$ with 0.5 mM Kelex 100 at pH 9.0.

pH Studies of 0.5 mM Kelex 100 with Cd^{2+}

The effect of pH on the percent rejection or expulsion of Cd^{2+} with Kelex 100 was investigated. The concentration of Kelex 100 was held constant at 0.5 mM and the Cd^{2+} concentration was in the range of 0.047-0.064 mM for these experiments. All solutions were prepared with 10 mM CHES, HEPES or MES buffer and the permeate compartments were filled with 10 mM buffer solution which had been adjusted to the experimental pH. Table III.19 shows the results for SED experiments done in 5 mM $C_{12}(EO)_6$ surfactant solution and $\%Cd^{2+}$ rejection is plotted versus pH in Figure III.40. Similarly, results of pH experiments in 0.05 M $CPNO_3$ are shown in Table III.20. A plot of either $\%Cd^{2+}$ rejection (pH 8.0-9.0) or $\%Cd^{2+}$ expulsion (pH 6.0-7.5) versus pH is shown in Figure III.41.

Table III.19 SED results for study of rejection of Cd^{2+} in $C_{12}(EO)_6$ as a function of pH.[a]

(a) $[Kelex]_{R,O}$ = 0.50 mM, $[C_{12}(EO)_6]$ = 5.0 mM. All solutions contain 10 mM

pH	$[Cd]_O$	$[Cd]_P$	$[Cd]_R$	$\%R_{Cd}$[b]
6.0	0.0471	0.0243	0.0249	2 ± 2
6.5	0.0509	0.0253	0.0315	20 ± 4
7.0	0.0643	0.0307	0.0377	19 ± 8
7.5	0.0493	0.0039	0.0586	93.3 ± 0.2
8.0	0.0493	0.0013	0.0867	98.5 ± 0.1
8.5	0.0493	0.0003	0.0801	$99.6_4 \pm 0.02$
9.0	0.0630	0.0002	0.0964	$99.8_0 \pm 0.01$

appropriate buffer. Concentrations expressed as millimoles per liter, $[Cd^{2+}]_O$ is original concentration of retentate, $[Cd^{2+}]_R$ concentration of retentate after equilibration, $[Cd^{2+}]_P$ concentration of permeate. Permeate and retentate results are the average of two SED runs. (b) Uncertainties expressed as average deviation from mean.

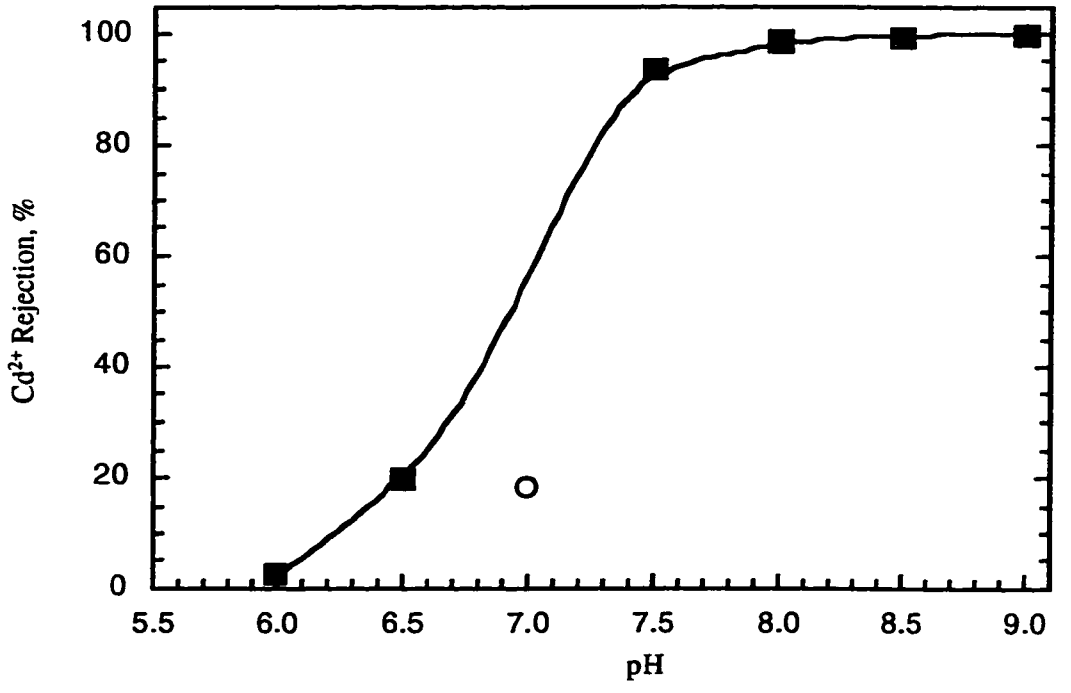

Figure III.40 Plot of % rejection of Cd^{2+} as a function of pH in 5 mM $C_{12}(EO)_6$ for 0.5 mM Kelex 100.

Table III.20 Effect of pH on SED results for Cd^{2+}-Kelex system in $CPNO_3$.[a]

pH	$[Cd]_O$	$[Cd]_P$	$[Cd]_R$	$\%R_{Cd}$[b]	$\%E_{Cd}$[b]
6.0	0.0430	0.0515	0.0236	--	54.2
	0.0438	0.0409	0.0113	--	72.4
					63 ± 9
6.5	0.0430	0.0336	0.0202	--	39.9
	0.0438	0.0372	0.0143	--	61.6
					51 ± 11
7.0	0.0413	0.0485	0.0111	--	77.1
	0.0431	0.0387	0.0101	--	73.9
	0.0385	0.0207	0.0048	--	76.8
					76 ± 2
7.5	0.0431	0.0271	0.0201	--	25.8
	0.0386	0.0154	0.0100	--	35.1
					31 ± 5
8.0	0.0431	0.0075	0.0482	84.4	--
	0.0290	0.0038	0.0180	79.0	--
				82 ± 3	
8.5	(d)	0.0021	0.0618	96.6	--
	0.0442	0.0004	0.0425	99.0	--
				98 ± 1	
9.0	(d)	0.0002	0.0736	99.7_3	--
	0.0442	0.0001	0.0460	99.7_8	--
				99.7_5 + 0.03	

(a) All solutions contain 10 mM appropriate buffer, [Kelex] = 0.50 mM, $[CPNO_3]$ = 0.05 M. Concentrations expressed as millimoles per liter, $[Cd^{2+}]_O$ is original concentration of retentate, $[Cd^{2+}]_R$ concentration of retentate after equilibration, $[Cd^{2+}]_P$ concentration of permeate. Permeate and retentate results are the average of two SED runs, average %E or %R shown in bold type. Concentration of Cd^{2+} in stock solution was not determined. (b) Uncertainties expressed as average deviation from mean.

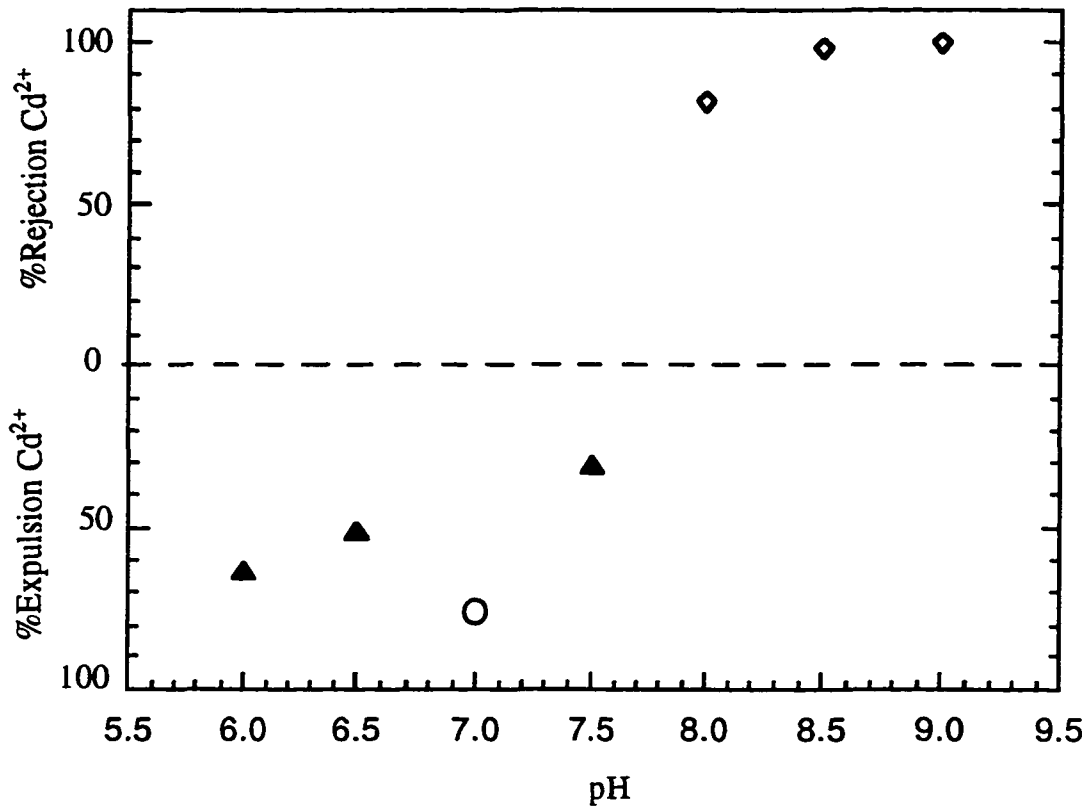

Figure III.41 Plot of SED results expressed as average %rejection (A) Cd^{2+} and %expulsion (H) Cd^{2+} as a function of pH in 0.05 M $CPNO_3$. %E at pH 7.0 is shown as an open circle.

Results of SED experiments in $C_{12}(EO)_6$ show that $\%R_{Cd}$ remains greater than 90% at pH 7.5 and above. It decreases rapidly at lower pH with $\%R_{Cd}$ only 18.6% at pH 7.0. $\%R_{Cd}$ in $CPNO_3$ solution is 99.7% at pH 9.0 but then decreases even more rapidly than it does in neutral surfactant with less than 90% rejection at pH 8.0. Cd^{2+} is expelled into the permeate at pH 7.5 and the $\%E_{Cd}$ generally increases with decreasing pH. The maximum average $\%E_{Cd}$ in this data set is 76% at pH 7.0. Average values for all data were plotted and are shown in Table III.19 and III.20 with the associated error. An interesting break in the trend of the data occurs in both surfactants at pH 7.0. These points are plotted in Figure III.40 and Figure III.41 as open circles. The direction appears to be consistent in the two cases with the $\%R_{Cd}$ low in neutral surfactant and the $\%E_{Cd}$ high in cationic surfactant.

Additional SED Studies of Kelex 100

A series of SED experiments was done to evaluate the effects of ions other then the target ion, Cd^{2+}, likely to be present in waste solutions treated with LM-MEUF. High levels of Na^{+}, Ca^{2+} and Cl^{-} are common in wastewaters. The presence of these ions means an increased electrolyte concentration. This may affect metal complexation and has been shown to effect physical properties of surfactants such as CMC. In addition, Ca^{2+} competes weakly for complexation of the ligand. Wastewaters that contain Cd^{2+} are also likely to contain Zn^{2+} since they always occur together naturally at ratios highly enriched in Zn^{2+}. Because of their similar complexation chemistry, Zn^{2+} could be expected to compete strongly for Kelex 100. Three SED studies are that examine these effects are described below. All were performed in $C_{12}(EO)_6$ surfactant solution. No studies were done in $CPNO_3$.

The first set of experiments investigated the effect of added electrolyte. Results of experiments in $C_{12}(EO)_6$ surfactant solution are shown in Table III.21 The concentration of Kelex 100 was held constant at 0.50 mM and the pH at 9.00 $\pm$ 0.05 with NaCl concentrations approximately 10-200 times the concentration of Cd^{2+} (0.06-0.14 mM). Rejections were 96% or greater for all experiments indicating that the ligand in neutral surfactant was affected very little by added electrolyte at these concentrations.

The effect of Zn^{2+} was investigated with results shown in Table III.22. The percent rejection of 0.06 mM Cd^{2+} is compared to percent rejection of 0.03-0.09 mM Zn^{2+} at pH 6.0, 7.0 and 9.0 for 0.5 mM Kelex 100 in 5 mM $C_{12}(EO)_6$. There

was at least a 2:1 excess of ligand over metal ion in all cases. Results of SED experiments with Zn^{2+} but no Cd^{2+} show that Zn^{2+} does complex strongly with Kelex 100. $\%R_{Zn}$ is greater than 99% at pH 9.0 and greater than 95% at pH 6.0. At pH 9.0, % rejection of both metal ions was greater than 99%. Rejection of Cd^{2+} was only 33.7% at pH 6.0.

Finally, the percent rejections of Cd^{2+} and Ca^{2+} were determined at pH 9.0 in 5 mM $C_{12}(EO)_6$ with 0.5 mM Kelex 100. Ratios of Ca^{2+} to Cd^{2+} were up to 100:1. Results are shown in Table III.23. The presence of Ca^{2+} at these concentrations appeared to have little effect on the $\%R_{Cd}$. In all cases the $\%R_{Cd}$ was 99.4% or greater and the $\%R_{Ca}$ was close to zero.

Table III.21 SED results for study of rejection of Cd^{2+} by 0.5 mM Kelex 100 in 5 mM $C_{12}(EO)_6$ as a function of [NaCl] at pH 9.0.[a,b,c]

$[Cd]_o$	[NaCl]	$[Cd]_R$	$[Cd]_P$	$\%R_{Cd}$
0.0654	0	0.0960	0.00028	99.7
0.0646	1	0.0647	0.0005	99.2
0.0584	10	0.0770	0.0004	99.5
0.143	0	0.160	0.0064	96.0
0.134	1	0.148	0.0020	98.6
0.119	10	0.135	0.0006	99.6

(a) All solutions contain 10 mM CHES buffer (b) Concentrations expressed as millimoles per liter, $[Cd^{2+}]_O$ is original concentration of retentate, $[Cd^{2+}]_R$ concentration of retentate after equilibration, $[Cd^{2+}]_P$ concentration of permeate (c) Permeate and retentate results are the average of two SED runs.

Table III.22 SED results for study of rejection of Cd^{2+} and Zn^{2+} by 0.5 mM Kelex 100 in 5 mM $C_{12}(EO)_6$ as a function of pH.[a, b, c]

pH	$[Cd]_o$	$[Zn]_o$	$[Cd]_R$	$[Cd]_P$	$[Zn]_R$	$[Zn]_P$	$\%R_{Cd}$	$\%R_{Zn}$
9.0	0.0654	0.0947	0.0947	0.0004	0.087	0.0005	99.6	99.4
9.0	0.0621	0.0940	0.0940	0.0019	0.0630	<0.005	98.0	>99.9
9.0	0	0.0498	0	0	0.0491	0.0001	---	99.8
8.0	0.0621	0.0568	0.0568	0.006	0.0610	<0.005	98.9	>99.9
7.0	0.0621	0.0632	0.0632	0.0151	0.0662	<0.005	76.1	>99.9
6.0	0.0621	0.0255	0.0255	0.0169	0.0574	0.0023	33.7	96.0
6.0	0	0.0596	0	0	0.0645	0.0029	---	95.5

(a) All solutions contain 10 mM appropriate buffer (b) Concentrations expressed as millimoles per liter, $[Cd^{2+}]_O$ and $[Zn^{2+}]_O$ is original concentration of metal ion in retentate, $[Cd^{2+}]_R$ and $[Zn^{2+}]_R$ concentrations of metal ion in retentate after equilibration, $[Cd^{2+}]_P$ and $[Zn^{2+}]_P$ are metal concentrations in permeate (c) Permeate and retentate results are the average of two SED runs.

Table III.23 SED results for study of rejection of Cd^{2+} and Ca^{2+} by 0.5 mM Kelex 100 in 5 mM $C_{12}(EO)_6$ at pH 9.0. [a, b, c]

$[Cd]_o$	$[Ca]_o$	$[Cd]_R$	$[Cd]_P$	$[Ca]_R$	$[Ca]_P$	$\%R_{Cd}$	$\%R_{Ca}$
0.0739	0.179	0.1068	0.0005	0.0900	0.0885	99.5	1.7
0.0818	0.2515	0.110	0.0003	0.1317	0.1499	99.7	(12.1)
0.0822	0.965	0.147	0.0005	0.472	0.433	99.7	8.2
0.0934	9.88	0.1610	0.0010	4.535	5.089	99.4	(10.9)

(a) All solutions contain 10 mM CHES buffer (b) Concentrations expressed as millimoles per liter, $[Cd^{2+}]_O$ and $[Ca^{2+}]_O$ is original concentration of metal ion in retentate, $[Cd^{2+}]_R$ and $[Ca^{2+}]_R$ concentrations of metal ion in retentate after equilibration, $[Cd^{2+}]_P$ and $[Ca^{2+}]_P$ are metal concentrations in permeate (c) Permeate and retentate results are the average of two SED runs.

Ultrafiltration Experiments

The results obtained from the SED studies were used to determine appropriate conditions of concentration and pH for UF experiments with Cd^{2+} and Kelex 100. $CPNO_3$ and $C_{12}(EO)_6$ were chosen as representative cationic and nonionic surfactants, respectively. Surfactant concentrations of 0.05 M for $CPNO_3$ and 5 mM for $C_{12}(EO)_6$ were employed for the UF studies. The concentration of Kelex 100 (0.50 mM) was approximately 10 times that of the Cd^{2+} (0.05 $\pm$ 0.01 mM) in order to assure an excess of ligand even with formation of 1:3 (Cd^{2+}:Kelex) complexes. Experiments were performed at pH 6.0 and 9.0. Based on SED results, complete complexation of the Cd^{2+} should occur and the rejection of Cd^{2+} should be greater than 99% at pH 9.0. Kelex-Cd^{2+} complexes should be extensively dissociated and the rejection quite low at pH 6.0. SED experiments showed that in $CPNO_3$ significant expulsion of Cd^{2+} into the permeate occured at this pH. This is desirable for stripping the metal from the complex to allow recycling of the ligand and surfactant. One set of experiments was performed with $C_{12}(EO)_6$ at pH 4.0 when rejections were higher than expected at pH 6.0. Two sets of blank experiments were performed at each pH: one with Cd^{2+} and surfactant and one with Cd^{2+} only. This was to determine the degree to which the Cd^{2+} was adsorbed onto the membrane and the effect that this adsorption might have on $\%R_{Cd}$.

Membranes were stored between runs in sodium azide solution to eliminate bacterial degradation of the cellulose and conditioned before each run with a flush treatment of 100 mL of D.D. water followed by 50 mL of Cd^{2+}

solution at the experimental pH and concentration. Experiments were done with 250-300 mL of original stock (feed) solution which was stirred with a magnetic stirrer while the feed solution was forced through the membrane. Permeate volume was measured with a 50 mL graduated cylinder and fractions taken at approximately 25 mL intervals until 150 mL were collected. Each fraction, as well as the final retenate solution was then analyzed for Cd^{2+} by flame AA.

The percent rejection for UF studies is calculated with the concentration of target ion in the permeate fraction at the halfway point of the ultrafiltration (125-150 mL). The concentration of Cd^{2+} in the retentate could not be measured directly at this point and was calculated by subtracting the millimoles Cd^{2+} in the permeate from the total analyzed Cd^{2+} in the 250-300 mL of original stock solution. Percent rejection was calculated in the same manner as it was for SED experiments, using Eqn I.1.

The concentration of Cd^{2+} in the permeate was plotted versus percent of the total volume of permeate to profile the concentration of Cd^{2+} in the permeate as the UF run proceeded. This was to determine whether adsorption or desorption from the membrane showed any sharp increase or decrease in the Cd^{2+} concentrations analyzed as the run progressed and whether the change affected the calculated percent rejection. Results for Cd^{2+} in Kelex 100 solutions in both $C_{12}(EO)_6$ and $CPNO_3$ surfactant solution are shown with blanks containing only Cd^{2+} and Cd^{2+} with surfactant on the same plot. Figures III.42 and III.43 show the results at the high pH (pH 9.0) used for separation. Figures III.44, 45 and 46 show results at pH 6.0 for $C_{12}(EO)_6$ and $CPNO_3$ and pH 4.0 for $C_{12}(EO)_6$.

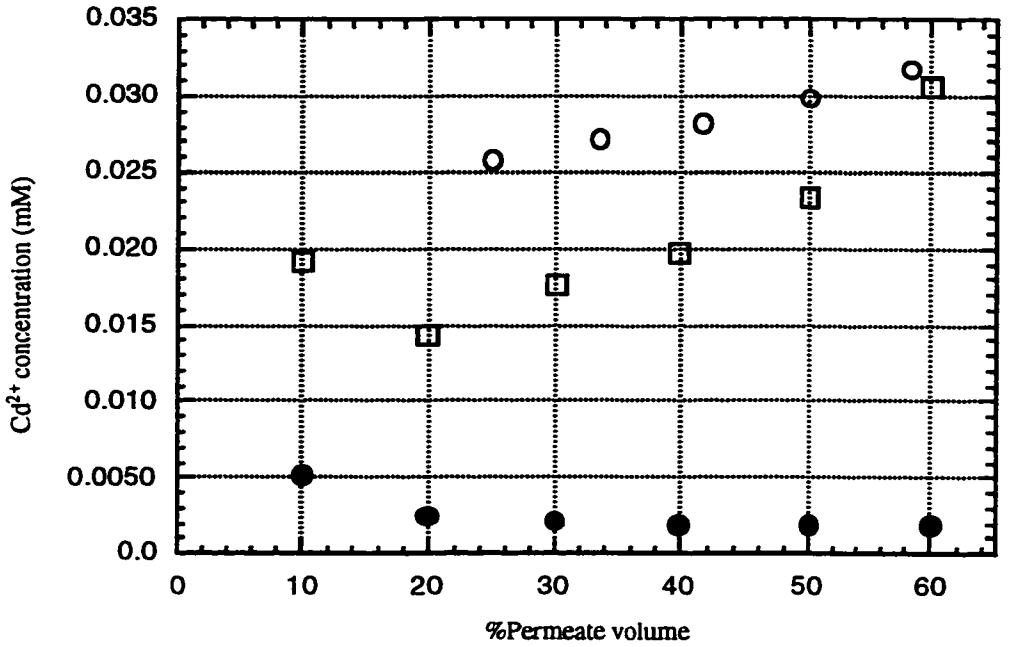

Figure III.42 Plot of UF results for Cd^{2+} at pH 9.0. (O) 0.045 mM Cd^{2+} without ligand or surfactant (❑) 0.045 mM Cd^{2+} in 5 mM $C_{12}(EO)_6$ solution without ligand (▲) 0.045 mM Cd^{2+} in 5 mM $C_{12}(EO)_6$ solution with 0.5 mM Kelex.

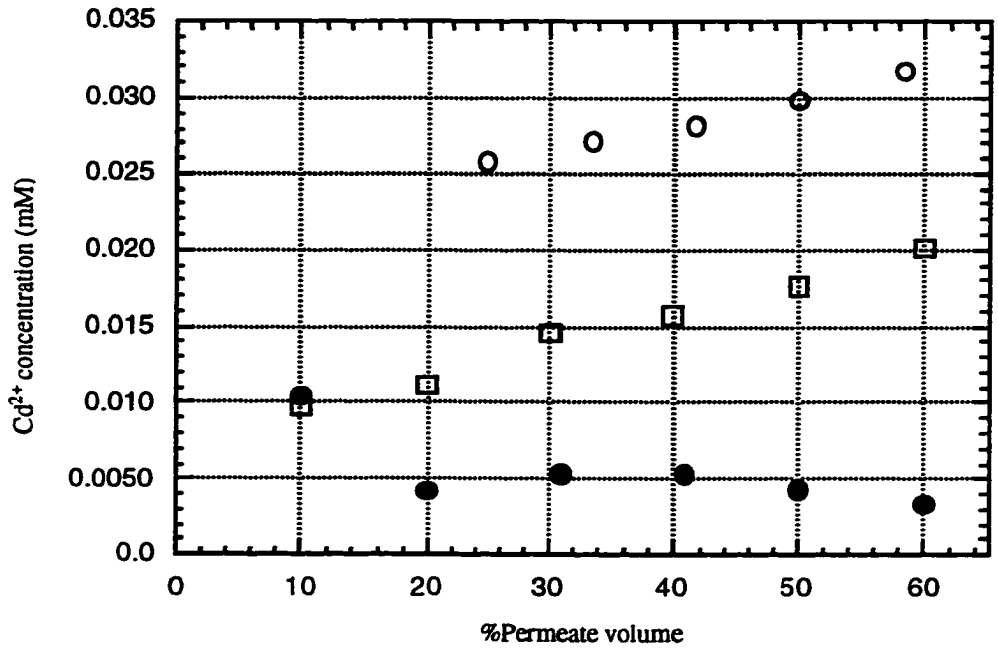

Figure III.43 Plot of UF results for Cd^{2+} at pH 9.0. (O) 0.045 mM Cd^{2+} without ligand or surfactant (❑); 0.045 mM Cd^{2+} in 0.05 M $CPNO_3$ solution without ligand (▲); 0.045 mM Cd^{2+} in 0.05 M $CPNO_3$ solution with 0.50 mM Kelex.

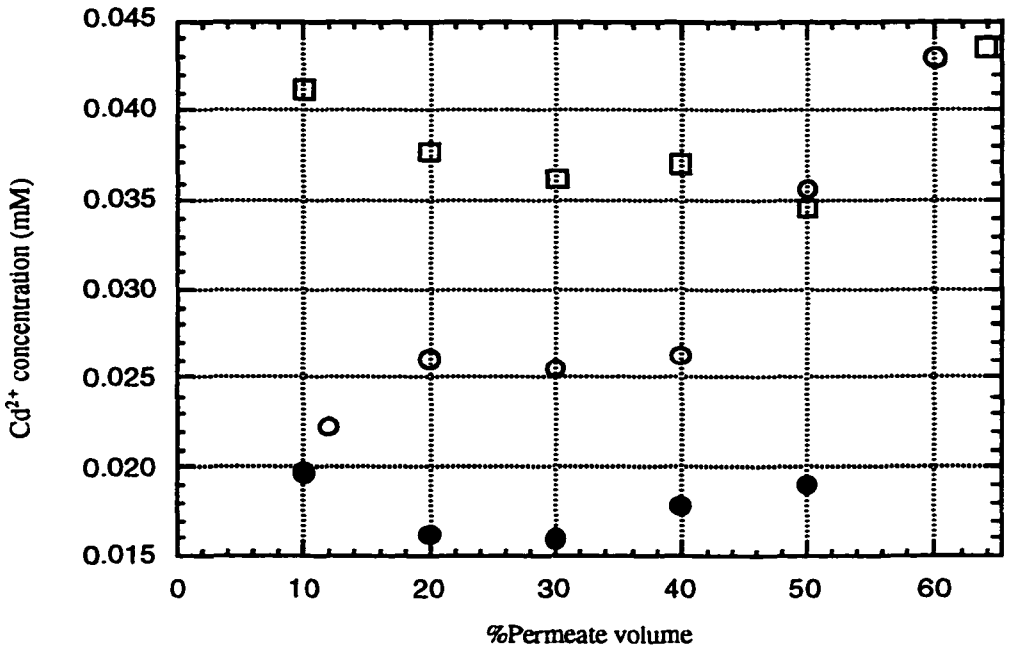

Figure III.44 Plot of UF results for Cd^{2+} at pH 6.0. (▲) 0.045 mM Cd^{2+} without ligand or surfactant at pH 6.0; (G) 0.045 mM Cd^{2+} in 5 mM $C_{12}(EO)_6$ solution without ligand at pH 6.0; (○) 0.045 mM Cd^{2+} in 5 mM $C_{12}(EO)_6$ solution with 0.5 mM Kelex at pH 6.0; (■) 0.045 mM Cd^{2+} in 5 mM $C_{12}(EO)_6$ solution with 0.5 mM Kelex at pH 4.0.

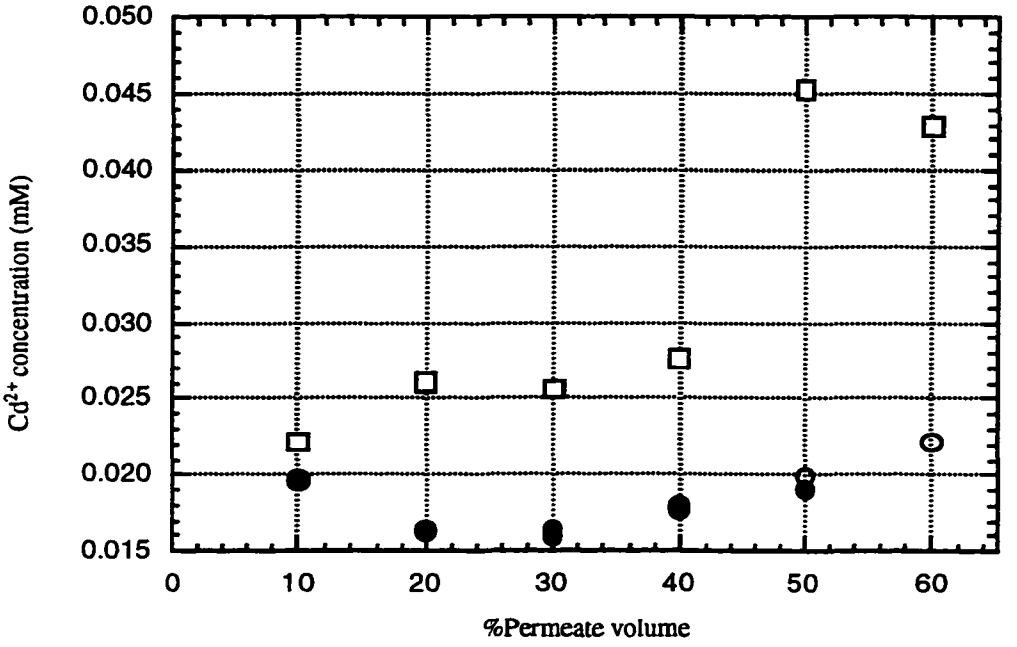

Figure III.45 Plot of UF results for Cd^{2+} at pH 6.0. (■) 0.045 mM Cd^{2+} without ligand or surfactant; (▲) 0.045 mM Cd^{2+} in 0.05 M $CPNO_3$ solution without ligand; (○) 0.045 mM Cd^{2+} in 0.05 M $CPNO_3$ solution with 0.5 mM Kelex.

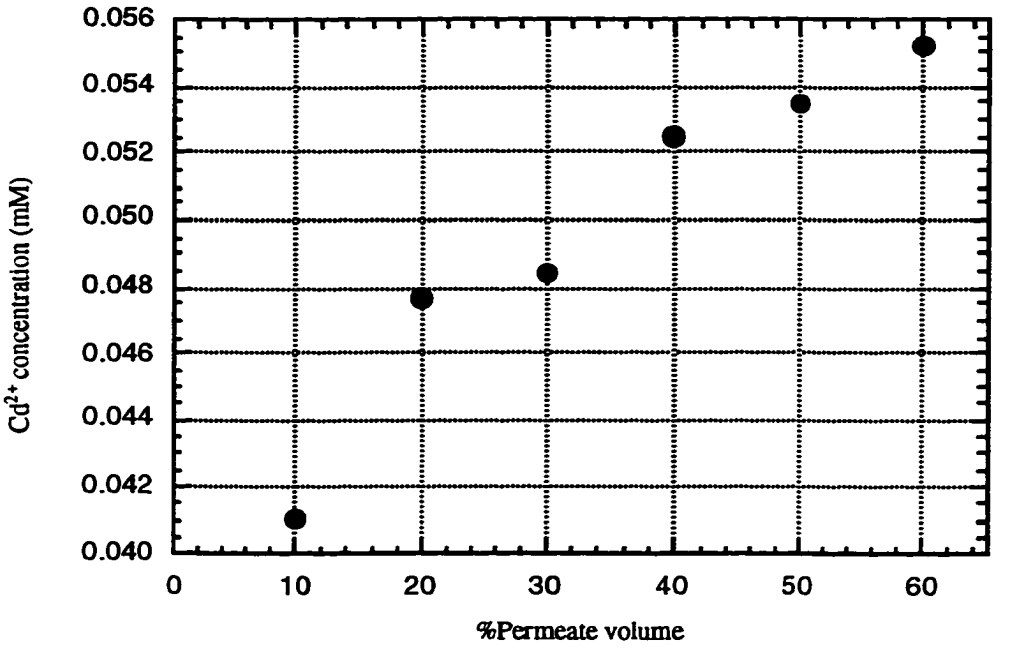

Figure III.46 Plot of UF results for 0.045 mM Cd^{2+} in 5 mM $C_{12}(EO)_6$ solution with 0.5 mM Kelex at pH 4.0.

Results of UF experiments without ligand are summarized in Table III.24. Some rejection of Cd^{2+} occurs at both pH 9.0 and 6.0 in all cases. Even without surfactant, 41% rejection of Cd^{2+} occurs at pH 9.0. There is less rejection with $C_{12}(EO)_6$ than there is with $CPNO_3$ and less at pH 6.0 than there is at pH 9.0.

Table III.24 Rejection of Cd^{2+} (%) for UF experiments without Kelex 100, $[Cd^{2+}]_O = 0.05 \pm 0.01$ mM.[a, b]

	Surfactant		
pH	0.05 M $CPNO_3$	5 mM $C_{12}(EO)_6$	None
9.0	74	54	41
6.0	73	32	14

(a) $[Cd^{2+}]_O = 0.05 \pm 0.01$ mM, [buffer] = 10 mM. (b) Results average of at least two runs.

Results of experiments with ligand are summarized in Table III.25 and compared to results of the corresponding SED experiments. Rejection of Cd^{2+} remains high in UF experiments at pH 6.0 though SED results indicate that there should be no rejection in $C_{12}(EO)_6$ or expulsion in $CPNO_3$.

Table III.25 Comparison of rejection of Cd^{2+} (%) for SED and UF separations of Cd^{2+} [a, b]

pH	Surfactant	SED $\%R_{Cd}$	UF $\%R_{Cd}$
9.0	5 mM $C_{12}(EO)_6$	99.8	98.1
9.0	0.05 M $CPNO_3$	99.7	96.4
6.0	5 mM $C_{12}(EO)_6$	2.4	69
6.0	0.05 M $CPNO_3$	(72.4)	70
4.0	5 mM $C_{12}(EO)_6$	---	6

(a) $[Cd^{2+}]_O = 0.05 \pm 0.01$ mM, [Kelex 100] = 0.50 mM, [buffer] = 10 mM; pH 4.0 prepared without buffer. (b) UF and SED results average of at least two runs

Analysis of Mercury in SED Solutions

In order to evaluate the effectiveness of SED separation, an analytical technique for mercury was needed that would be quick and sensitive. The chosen technique would need to have a detection limit of 1 μM or less for analysis of permeate solutions where there was 99% rejection of 0.1 mM Hg^{2+}, the concentration used in the experiments shown. The unique chemistry of mercury makes many solutions unstable due to the tendency of Hg^{2+} ions to be reduced to Hg^0 and then lost through vaporization. This process was discussed in detail in Chapter I. This is of particular concern with permeate solutions which typically contain low concentrations of Hg^{2+}. Therefore, a quick technique with minimal preanalysis preparation is advantageous. The presence of surfactant and ligand in retentate solutions, stock solutions and, to a lesser extent, permeate solutions creates potential for chemical interference. A number of different techniques were evaluated for analysis of mercury solutions. These are discussed, with the limitations of each as they pertain to SED solutions presented.

Spectrophotometric (colorimetric) techniques

A number of spectrophotometric techniques were tried due to the ready availability of reagents and instrumentation. Figure III.47 shows the structure of two reagents that are often applied to the analysis of mercury: 1-(2-pyridylazo)-2-naphthol or PAN and diphenythiocarbazone or dithizone. A direct method for determination of Hg^{2+} with PAN was described by Shibata (76) in which PAN is solubilized in methanol/water with the sample, the pH adjusted to 6.0-7.5 and the

absorbance measured at 550 nm versus a reagent blank. Spectra of 0.05 mM PAN in 80% methanol solution titrated with Hg^{2+} are shown in Figure III.48. Because it was necessary to be able to accurately determine the total concentration of Hg^{2+} in the presence of the thiourea ligand, the PAN-Hg^{2+} complex was titrated with thiourea and the spectra taken. Spectra are shown in Figure III.49. The Shibata method was used with the simulated permeate solutions containing 0.01 mM Hg^{2+} and 3.33 mM $C_{12}(EO)_6$ surfactant. A systematic decrease in absorbance with addition of thiourea is seen, indicating that the presence of thiourea in the solution will interfere with formation of the PAN/Hg^{2+} complex.

$$Hg^{2+}\text{-PAN} + 2Tu \rightleftharpoons Hg(Tu)_2 + PAN$$

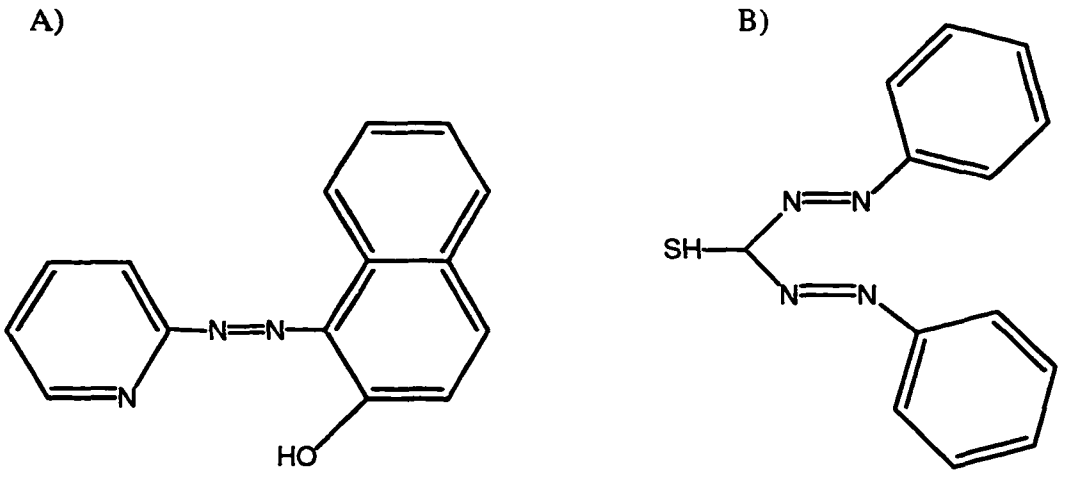

1-(2-Pyridylazo)-2-naphthol

Diphenylthiocarbazone

Figure III.47 Structures of (A) PAN and (B) Dithizone

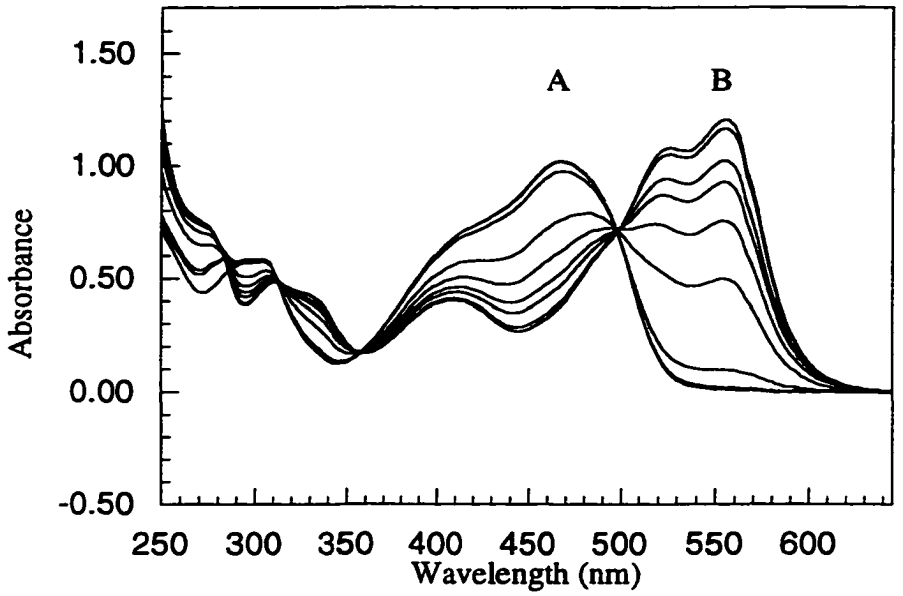

Figure III.48 UV-vis spectra of formation of mercury (II) PAN complex with 0.05 mM PAN and 9.2 mM Hg^{2+} in 80% methanol:water. (A) Absorbance maximum of the Hg-PAN complex (465 nm) (B) Absorbance maximum of uncomplexed PAN (568 nm).

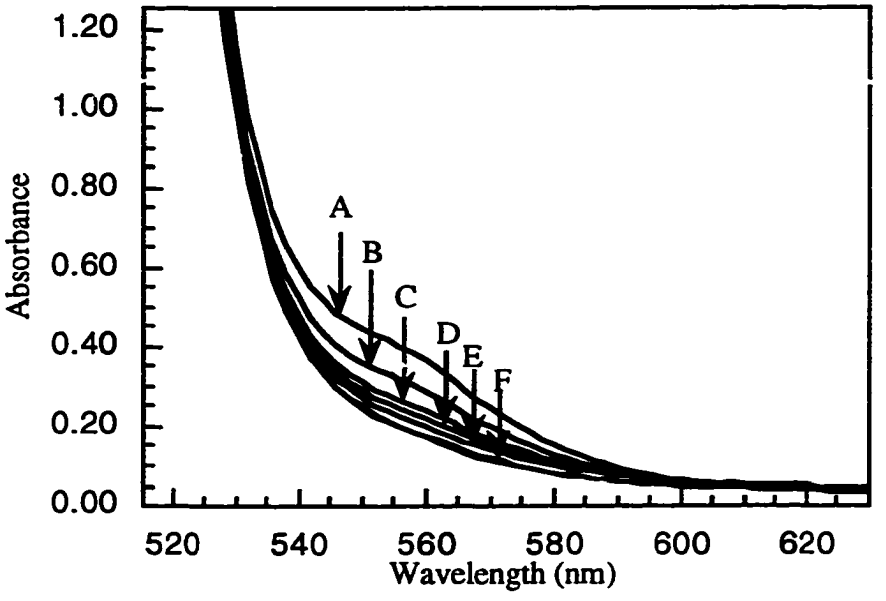

Figure III.49 UV-vis spectra of 0.02 mM PAN-Hg^{2+} complex in 0.05 M $C_{12}(EO)_6$ surfactant solution with (A) no thiourea (B-F) 15 μL aliquots of 1.06 X 10^{-2} M 1-hexyl-2-thiourea added.

Dithizone (Figure III.47B) is a sensitive and selective spectrophotometric reagent often used for determination of mercury. Due to its low solubility in water it is usually used as an extractant dissolved in chloroform or carbon tetrachloride. An extraction method was tried but was unsatisfactory due to the instability of the mercury/dithizone complex. Dithizone is readily oxidized and is unstable when exposed to light. Absorbance measurements were not reproducible. A number of techniques were tried to circumvent this problem. The most promising was formation of the copper dithizone complex to stabilize it against oxidation followed by dissolving it in surfactant solution then adding the sample containing mercury.

$$2H_2Dz + Cu^{2+} \rightleftharpoons Cu(HDz)_2 + 2H^+ \qquad \text{Log } \beta_2 = 19.18 \pm 0.07 \qquad \textbf{Eqn III.2}$$

$$2H_2Dz + Hg^{2+} \rightleftharpoons Hg(HDz)_2 + 2H^+ \qquad \text{Log } \beta_2 = 40.3 \pm 0.8 \qquad \textbf{Eqn III.3}$$

The conditional stability constant for formation of the mercury complex is much higher than that of the copper complex so copper is displaced and the mercury complex formed. The equilibrium expressions and cumulative formation constants are shown for the replacement of the copper dithizonate by mercuric ion in equations III.2 and III.3. (77) A dual wavelength correction for background absorbance of the copper dithizone complex, as well as impurities, was employed (78). Finally, hydroxylamine hydrochloride was added to analyzed solutions prior to taking spectra in order to prevent oxidation of the dithizone. Spectra for a typical calibration curve are shown in Figure III.50. The wavelengths selected for the dual

and the λ_{max} of the mercury/dithizone peak at 493 nm. Even with these attempts to minimize the instability of dithizone, a plot of absorbance change versus mmoles of mercury (Figure III.51) was still nonlinear at higher concentrations. None of these provided an acceptable technique for spectrophotometric quantitation of Hg^{2+} in SED solutions.

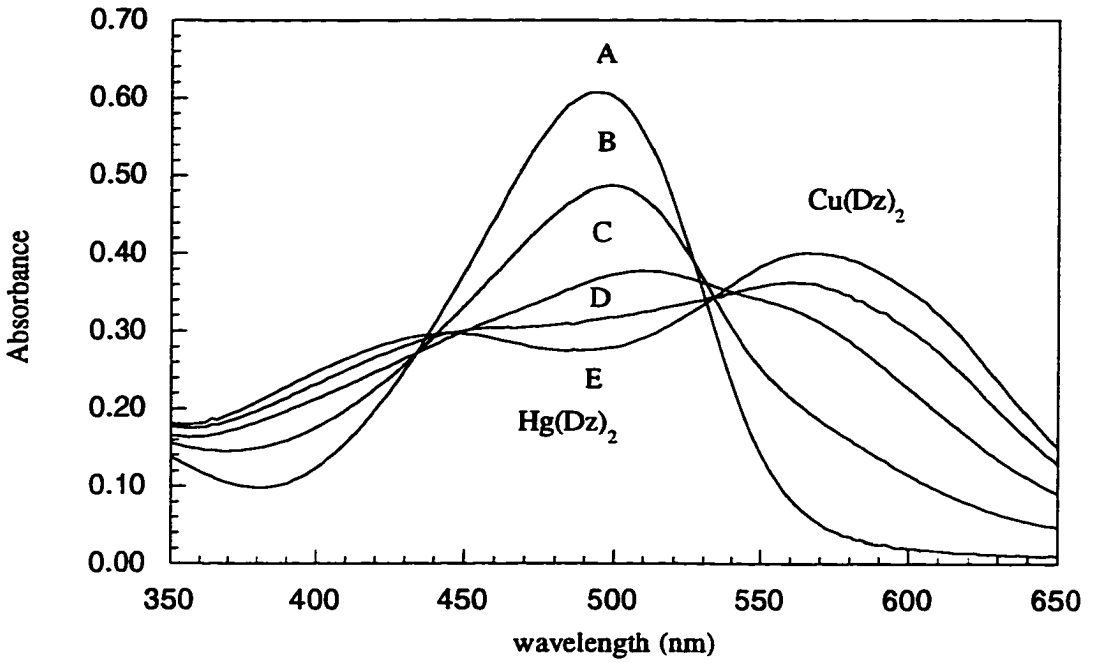

Figure III.50 UV-vis spectra of the exchange reaction of 0.20 mM copper (II) dithizonate with mercury (II) at pH 1.0. Mercury concentration in μM is (A) 5.0 (B) 2.5 (C) 1.0 (D) 0.5 (E) 0.

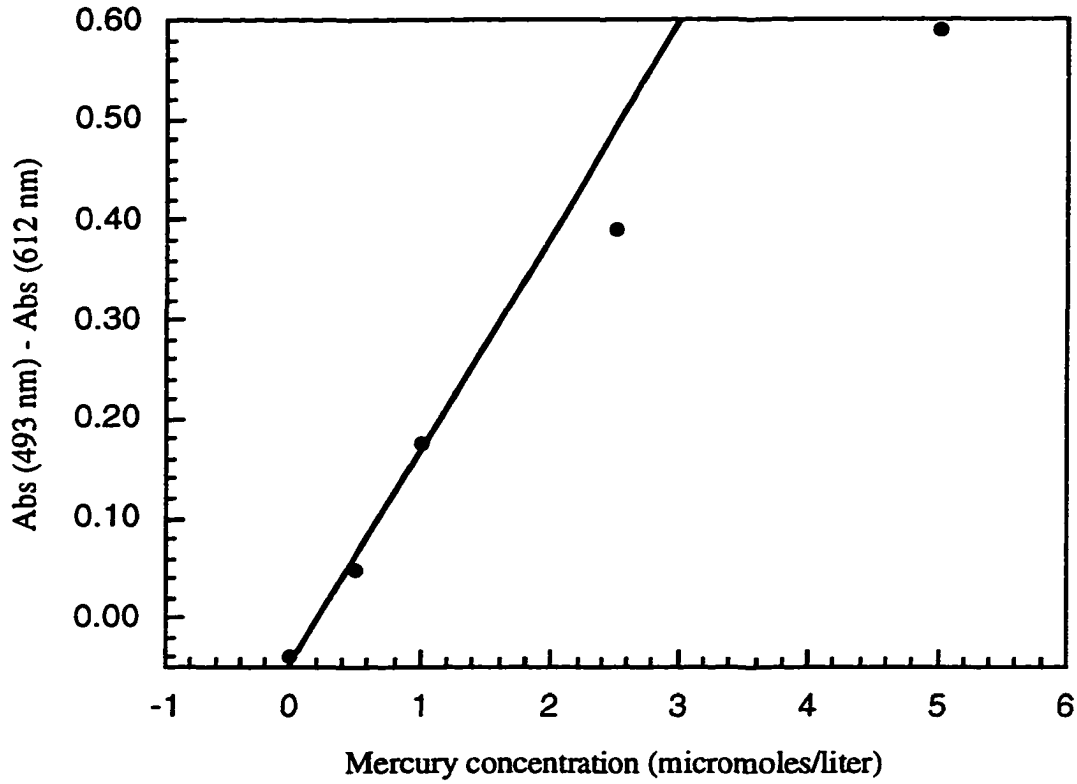

Figure III.51 Calibration line for dual wavelength determination of mercury at $\lambda_1 = 493$ nm and $\lambda_2 = 612$ nm by exchange with copper (II) dithizonate.

Mercury Determination by Cold Vapor Atomic Absorption

The method generally cited in the literature as being the preferred one for trace mercury determination is cold vapor atomic absorption (CVAA) and a CVAA apparatus was available from the Oklahoma Geological Survey (OGS). The technique is quite sensitive with the detection limit for this apparatus of approximately 0.1 μg/L (0.5 nM). This is quite adequate for application to SED

solutions because a detection limit of only 1 μM is required for determination of mercury in permeate solutions with 99% rejection.

CVAA is applicable solely to the determination of mercury because in it's elemental state mercury has a high vapor pressure. Stannous chloride is added to aqueous samples and the mercuric ions present are reduced to elemental mercury. The sample is aerated and the mercury vapor is swept into an absorbance cell in the beam path of the AA. The absorbance of the sample is proportional to concentration which is determined from a calibration curve. A sample calibration curve is shown in Figure III.48. Beer's law is obeyed up to about 2.5-3.0 μg

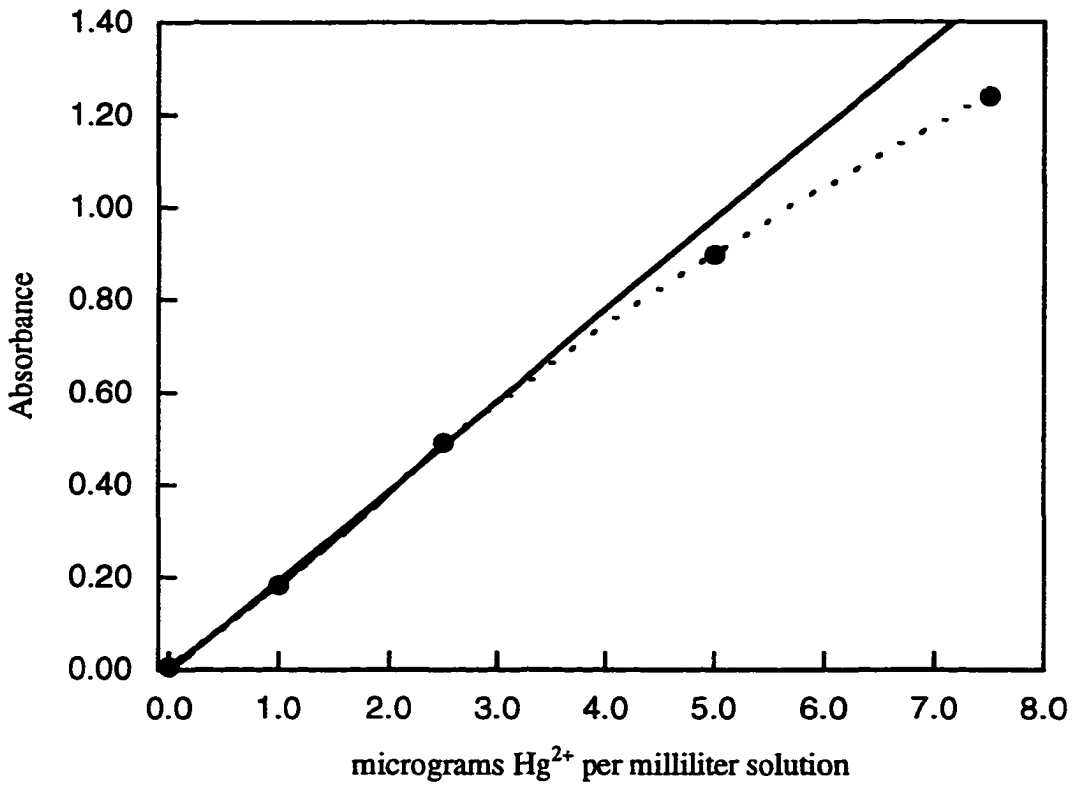

Figure III.52 CVAA calibration curve

Hg^{2+} of sample and the normal working range is 0.05-0.5 μg Hg. The sensitivity of the technique is derived from the fact that total mercury is determined . Results may be reported in concentration units by dividing by the sample volume and correcting for dilution. However, matrix interferences are a significant problem for SED solutions. Usually, concentration is determined from maximum peak height. If all the mercury is not vaporized, or if the rate of reduction and vaporization is

retarded, the peak height and analyzed concentration are decreased. Preliminary studies showed that ligand present in SED solutions caused peak broadening. In addition, foaming from surfactant carried over into the tubing and absorbance cell caused increased background absorbance. Therefore, a digestion step prior to analysis was necessary to oxidize the ligand and surfactant and reduce these interferences. With a hot digestion procedure there is some concern that mercury could be vaporized and lost prior to analysis. Therefore, a cold digestion technique was also evaluated to determine which would be more effective. Complete procedures for both methods are provided in Chapter II with the major difference between methods that the hot digestion involves heating the samples at 95°C for two hours and the cold procedure is done without heating and allowing samples to sit at room temperature for at least twelve hours. The analyzed standards were prepared containing 0.0010 mM Hg^{2+} (0.20 μg Hg^{2+}/L) with 0.003 mM thiourea in 1 mM SDS surfactant solution. These concentrations are typical of a 1:100 dilution of the stock or retentate solutions. Digestions were performed in triplicate with a reagent blank containing thiourea and surfactant and then analyzed. Standards were freshly prepared from a commercial AA Hg^{2+} standard and were not digested. Results, shown in Table III.26, showed that the absorbances were higher for samples using the hot digestion procedure than the cold digestion procedure, indicating that vaporization of mercury during digestion was not a problem and that the ligand was incompletely digested in the cold procedure. Foaming of the cold digestion samples also continued to be a problem. Based on these results, the hot digestion procedure was adopted for use with solutions from SED experiments.

Table III.26 Results for comparison of hot and cold digestion techniques prior to CVAA determination of mercury.[a,b]

Hot Digestion		Cold Digestion	
Absorbance[c]	Concentration	Absorbance[c]	Concentration
0.109	0.225	0.079	0.167
0.116	0.239	0.068	0.145
0.140	0.286	0.065	0.139

(a) All samples contained approximately 0.2 μg Hg^{2+} in 1 mM SDS with 0.003 mM thiourea. (b) Concentration expressed as μg Hg^{2+}/mL of sample (c) Absorbances corrected by subtracting absorbance of reagent blank.

Further experiments were done to verify that samples were sufficiently digested to prevent interference from surfactant and that no mercury vapor was lost during digestion. Results of mercury determination for samples which contained 0.2 μg Hg^{2+}/L with SDS show an average absorbance of 0.067 ± 0.005 and without SDS surfactant the average absorbance is 0.064 ± 0.002. A comparison of the results of digested and undigested samples which contained the same amount of mercury initially and did not contain thiourea also showed little difference in absorbance. The average corrected absorbance for hot digested samples was 0.050 ± 0.003 and for undigested samples the average corrected absorbance was 0.052 ± 0.003. Based on these results, the hot digestion procedure does appear to adequately destroy the surfactant and the ligand without any loss of mercury.

The last concern regarding digestion of samples was that the absorbances seemed to vary between runs for standards of the same mercury concentration. The absorbance measurements are affected by factors such as residual moisture or changes in the tubing and adsorbants in the CVAA apparatus, as well as variations

in the digestion reagents. A series of standards was digested and analyzed in order to determine whether they were reproducible. Multiple standards were prepared which contained mercury between 0-0.50 μg/L without surfactant or ligand. The results are shown in Figure III.53. The standard deviation for each point is indicated with error bars. The high and low ends of the calibration curve reflect 7-9 determinations for each standard. The results for standards containing 0.20 and 0.25 μg Hg^{2+} /L reflect two and three determinations, respectively.

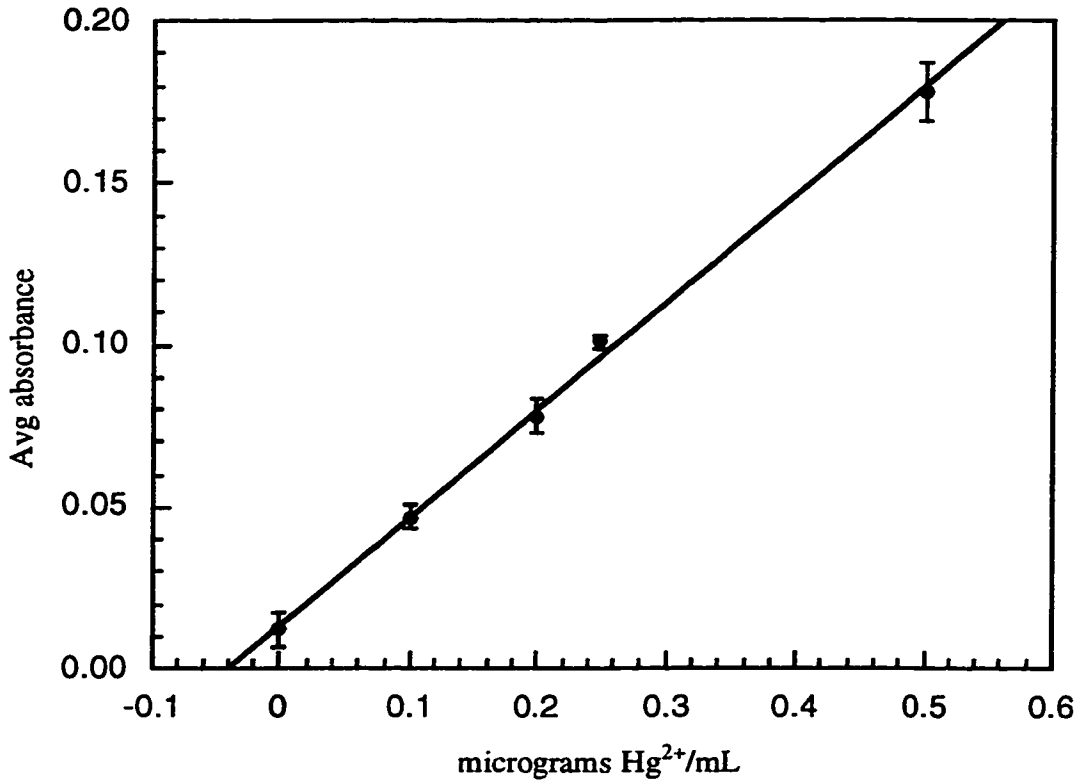

Figure III.53 Plot of average absorbance for CVAA calibration curves. Error bars indicate the standard deviation of each standard ($n \geq 7$ for blank, 0.1, 0.5 μg Hg^{2+} /L and n=3 for 0.2 μg Hg^{2+} /L and n=2 for 0.25 μg Hg^{2+}/L)

SED Separation of Mercury with Thiourea Ligands

Preliminary screening experiments were done with a number of commercial alkylated thiourea ligands to determine their solubility in both water and surfactant solution. The solubility of 1-decyl-2-thiourea (Dtu) was negligible in water and about 0.5 mM in $CPNO_3$ solution. In nonionic surfactant solubility was low and after the ligand was solubilized and mercury was added, a dark precipitate often formed so SED experiments were done in $CPNO_3$ solution. Based on solubility limitations and to allow an excess of ligand, experimental concentrations of ligand and Hg^{2+} were established at 0.3 mM and 0.1 mM, respectively. Since the acid-base properties of thiourea make it virtually unaffected by pH, the experimental pH was quite low, pH 2.0, in order to minimize hydrolysis side reactions of the mercury. In addition, a review of the literature indicated that adsorption of the Hg^{2+} to labware could be minimized at low pH.

Results of early SED experiments showed that with no ligand present up to 50% of the Hg^{2+} in the stock solution was not found in the analysis of the permeate and retentate solutions. Experiments with ligand showed similar poor mass balance results. Digestion and analysis of the SED membranes determined that mercury was being adsorbed onto the membranes. Membranes were then presoaked in a solution of Hg^{2+} at the experimental pH and concentration in an attempt to saturate the available binding sites and reduce adsorption. SED results with presoaked membranes did show less adsorption, though mass balance calculations for all experiments still averaged about 20% less than the concentration of the stock solution. The reverse effect of "bleeding" of Hg^{2+} from presoaked membranes

also noted. Analysis of retentate and permeate solutions from SED cells filled with D.D. water at pH 2.0 showed the presence of 2.0 μM Hg^{2+}.

A final attempt to quantitate the Hg^{2+} lost to the SED membranes was made by digesting the membranes and analyzing the total Hg^{2+} present. Membrane surface area is variable due to the elasticity of the hydrated membrane so exposed surface area could not be determined precisely. An average value for the adsorbed Hg^{2+} would allow a correction factor to be applied to the mass balance. However, analyzed values for Hg^{2+} were quite variable for identical systems and no reasonable correction factor could be determined.

Results of two sets of SED experiments with 0.1 mM Hg^{2+} and 0.3 mM Dtu in 0.03 M $CPNO_3$ showed 99.9% or greater rejection. Mass balance calculations for these runs showed that the total mercury was low, but the % rejection was reproducible. Blanks containing Hg^{2+} and surfactant were also analyzed. Runs with 0.1 M SDS and 0.1 mM Hg^{2+} showed 68% rejection which would be expected with an anionic surfactant. However, an experiment with 0.03 M $CPNO_3$ and 0.1 mM Hg^{2+} showed no rejection but also no expulsion. This may be explained by membrane adsorption since the total mercury for both blank experiments was low. Further experiments with Hg^{2+} were discontinued due to the continuing problems with membrane adsorption.

Chapter IV

Discussion

Spectrophotometric pH studies of Kelex 100 in surfactant solutions

The results of spectrophotometric studies of the acid-base behavior of Kelex 100 in surfactant solutions and Kelex 100 and 8-hydroxyquinoline in 80% (w/w) methanol:water are summarized in Table III.1. The effects of surfactant charge can be seen by comparing the protonation constants obtained for Kelex 100 in the three surfactant types. The nonionic surfactant $C_{12}(EO)_6$ can be considered the intermediate case where there are no electrostatic effects from micellar charge. Precise determination of the protonation constants was not possible with this spectrophotometric method but a plot of absorbance versus pH showed absorbance changes at the far ends of the pH range of the study. Log K_{H1} was estimated to be greater than 12.0 and log K_{H2} was less than 3.0. Log K_{H1} was shifted to 10.64 in cationic $CPNO_3$ solution and no spectral changes were seen between pH 7.0 and 2.0 so log K_{H2} was estimated to be less than 2.0. The opposite trend was seen in solution containing the anionic surfactant SDS where log K_{H2} was 5.68 and log K_{H1} was greater than 13.0.

As the ligand is solubilized into the surfactant micelle, the ionizable group is incorporated into the micelle between the head groups or into the palisade layer. Two different factors affect the protonation equilibria of the ligand at the micelle surface. The first is the decreased polarity, or dielectric

constant, of the micelle when compared to that of the bulk water solution. A study by Fernandez and Fromherz (42) of pK shifts in fluorescent pH indicators solubilized in neutral micelles found that the value of the dielectric constant at the neutral micelle surface was approximately 32, intermediate between that of bulk water (ε = 78.36) and the paraffinic micelle core (ε=2-3). The effects of decreased polarity is most easily seen in nonionic surfactants resulting in small shifts of the protonation equilibria. The intrinsic values in water for the protonation constants could not be determined for Kelex due to its low solubility. However, protonation constants have been determined in a variety of organic and aqueous mixed solvents for both Kelex 100 and 8-hydroxyquinoline (8HQ). These values are described here for comparison and summarized in Table IV.1. A number of the studies of the acid-base behavior of Kelex 100 available were done with the pre-1976 (old) formulation of Kelex 100. The active component in the old Kelex 100 was identified as

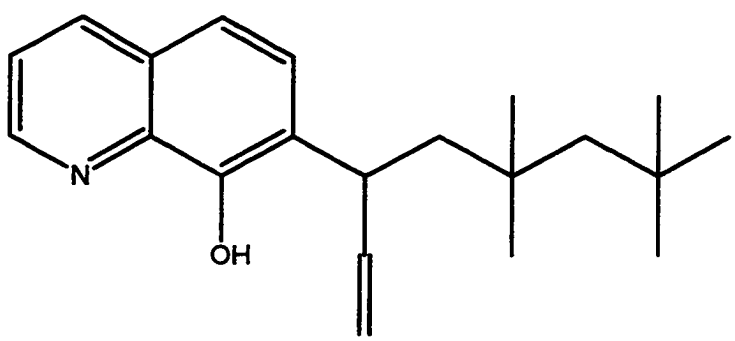

7-(Dodecenyl)-8-quinolinol

Figure IV.1 Structure of the active ingredient of the old formulation of Kelex 100.

7-(dodecenyl)-8-quinolinol (36, 37, 75, 79) as shown in Figure IV.1. After 1976, the synthesis was changed and the active ingredient of Kelex 100 (new) became 7-(4-ethyl-1-methyloctyl)-8-quinolinol, as shown in Figure IV.2. Though the structure of the alkyl side chain is different in the current synthesis, the values should be close to those of the old compound due to the similar number of carbons in the alkyl chain (C_{11} and C_{12}) and fact that the alkyl substituents are both at the same (7) positions on the ring. A study by Citores, et al. evaluated both the old and new formulations of Kelex 100 spectrophotometrically and, indeed, found them to be quite similar. The protonation constant values obtained in 40:60 ethanol:water were

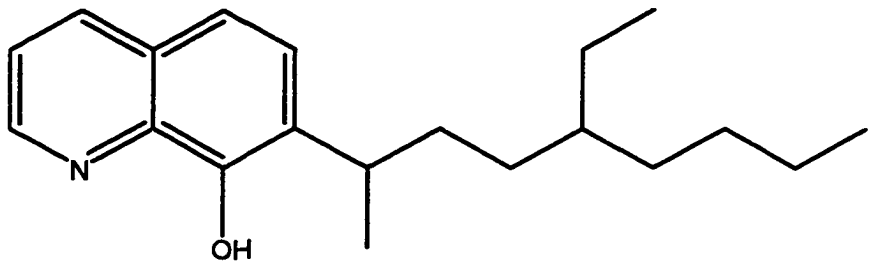

7-(4-Ethyl-1-methyloctyl)-8-quinolinol

Figure IV.2 Structure of the active ingredient of the new formulation of Kelex 100.

log K_{H1} = 12.17 ± 0.06 (old) and log K_{H1} = 12.40 ± 0.07 (new) with log K_{H2} = 3.77 ± 0.05 (old) and log K_{H2} = 3.98 ± 0.04 (new) (75).

Table IV.1 Protonation constants for old and new formulations of Kelex 100.

	Solvent	Log K_{H1}	Log K_{H2}
8HQ	water (a)	9.66 ± 0.03	4.99 ± 0.04
Kelex (old)	water (d)	11.2	4.4
Kelex (old)	50% dioxane:water (b)	12.30 ± 0.03	3.05 ± 0.03
Kelex (old)	40:60 ethanol:water (c)	12.17 ± 0.06	3.77 ± 0.05
Kelex (new)	40:60 ethanol:water (c)	12.40 ± 0.07	3.98 ± 0.04
Kelex (new)	Methanol (e)	14.4 ± 0.2	5.01 ± 0.2

(a) Ref. 43 (b) Ref. 74 (c) Ref 75 (d) Ref. 72 (e) <0.04% H_2O, Ref. 73

The effect of decreasing polarity can be seen by comparing the available K_H values for 8HQ and Kelex 100 in different solvents which are listed in Table IV.1. A comparison of the values for 8HQ and Kelex (old) in water show the effect of the alkyl substituent at the seven position on the ring. The value of log K_{H1} increases about 1.5 log units, from 9.66 to 11.2, and the value of log K_{H2} decreases about one half of a log unit, from 4.99 to 4.4. Protonation constants for Kelex in water were calculated by Cote and Bauer (72) from the results of partition experiments. The values in water for both 8HQ and Kelex are the lowest values shown for log K_{H1}. Values for log K_{H1} increase consistently as the polarity of the solvent decreases, from 11.2 in water to 14.4 in methanol. Changes in log K_{H2} are not symmetrical with those of log K_{H1}. Log K_{H2} values are highest in the most polar (4.4 in water) and the least polar (5.01 in methanol) solvents and then decrease in the solvent mixtures (3.05 to 3.98).

The value for log K_{H1} in $C_{12}(EO)_6$ solution is in the range obtained in water:solvent mixtures. In $C_{12}(EO)_6$ solution, the value for log K_{H1} can be estimated at about 12.5, while values for log K_{H1} in mixed solvents range from

12.71 to 12.40. Log K_{H2} is about 2.5 in $C_{12}(EO)_6$ solution, even lower than it is in mixed solvents which range from 3.05 to 3.98.

Protonation constants were also determined for both 8HQ and Kelex 100 in 80% (w/w) methanol:water solution in order to approximate the polarity of the micelle surface. Log K_{H1} for 8HQ and Kelex 100 were both greater than 12.0, consistent with values for Kelex 100 reported in other solvent-water mixtures. Though values are in the range of those determined in other mixed solvent systems, as well as in nonionic surfactant solution, the value for 8HQ is shifted significantly from that obtained in water (log $K_{H1} = 9.66 \pm 0.03$). The log K_{H2} value in 80% MeOH:water of Kelex is also consistent with the other values for mixed solvents. The 8HQ value is very close to the log K_{H2} value in both water and methanol though the value of 4.36 appears to be high compared to other mixed solvent systems.

The second factor which causes a shift in protonation equilibrium results from the electrostatic interaction between the excess charge of the head groups of ionic surfactants and the charged ligand species. Charged head groups are partially neutralized by the association of about 80% of the oppositely charged counterions in the Stern layer (20). The remaining 20% of the unneutralized charge of the headgroups creates the net charge on the micelle. The effect of this charge on the protonation constant is compared to the value of the intrinisic protonation constant in water or a zero charge environment, such as a neutral micelle. The first protonation of the Kelex 100 anion forms a neutral molecule and the second protonation step forms a monocationic species. Therefore, when Kelex 100 is incorporated as a guest molecule into a negatively charged micelle

the first protonation step is more energetically favorable than it is in neutral micelles due to the destabilizing effect of charge repulsion between the anion and the micelle. As a result, log K_{H1} is shifted to a larger value. Results in SDS show that log K_{H1} is greater than 13.0 with no spectophotometric changes visible up to this pH. The second protonation step is also more energetically favorable than it is in the neutral micelle due to the stabilization of the cation by the negative micelle; therefore, log K_{H2} is also shifted to a higher value. Log K_{H2} in SDS is 5.68 compared to less than 3.0 in $C_{12}(EO)_6$. The opposite trends are seen with the cationic surfactant. The first protonation is shifted down due to the stabilization of the anion by the positive micelle and the second protonation is shifted down due to the charge repulsion between the cationic species and the positive micelle. In $CPNO_3$, log K_{H1} is 10.70 compared to greater than 12.0 in $C_{12}(EO)_6$, and log K_{H2} is less than 2.0 compared to less than 3.0 in $C_{12}(EO)_6$.

Spectrophotometric metal complexation studies of Kelex 100 in surfactant solution

Results of metal complexation studies of Kelex 100 show that 1:2 (M^{2+}:Kelex) complexes are formed for all the metal ions tested except Cd^{+2} in $CPNO_3$ solution. Further studies with lead were discontinued due to precipitation problems as the metal to ligand concentration ratios approached 1:2. Attempts to work at lower pH showed that complexation was not quantitative. Mercury formed 1:2 complexes preferentially but as the added metal exceeded the 1:2 stoichiometry, a more gradual increase in absorbance indicated formation of a different complex, probably with 1:1 stoichiometry.

Cadmium formed 1:2 complexes exclusively with Kelex 100 (L) in solutions containing neutral surfactants (CO660, $C_{12}(EO)_6$, DDAO) at pH 8.5-9.0. In the cationic surfactant, $CPNO_3$, a plot of absorbance versus [M]:[L] at the isosbestic point (404 nm) showed formation of 1:3, CdL_3^-, complexes initially. Charge stabilization of the negative complex by the positive micelle would favor this stoichiometry. As the metal ion concentration increased, a plot of absorbance at another wavelength (440 nm) showed a decrease in absorbance indicating that 1:3 complexes disproportionated, probably forming neutral 1:2 complexes.

The predominance of 1:2 complexes agrees with results of previous studies of Kelex 100 complexation with Cu^{2+}, Ni^{2+} and Zn^{2+} in 80% (w/w) methanol:water (46). The chelating head group of Kelex 100 is 8-hydroxyquinoline (8HQ), a common reagent for analysis of metal ions.

Available data for 8HQ also shows that it commonly forms four coordinate complexes with divalent metal ions (82). Because 8HQ is a bidentate ligand this corresponds with 1:2 stoichiometry.

SED results with Cd^{2+}

SED membrane studies with Cd^{2+} and Hg^{2+} showed that adsorption of the target ion by the cellulose dialysis membrane created significant problems in interpreting results. Similar problems had been encountered in experiments with other metal ions, notably lead (50). Typically, membranes were soaked in a solution containing a low concentration of the target ion in order to saturate available metal binding sites, thus reducing the quantity of metal ions lost from the retentate or permeate solution to the membrane. The effectiveness of this technique was found to vary considerably with different experimental conditions. It was most effective for experiments where there were significant amounts of uncomplexed target ions, as with blanks (no ligand) and at low pH. For the Kelex 100-Cd^{2+} system, the case was reversed at high pH. Excess ligand complexed membrane-adsorbed Cd^{2+} and up to a 50% excess of Cd^{2+} was found in the combined retentate and permeate concentrations. Results of SED experiments with cationic surfactant solutions showed excess Cd^{2+} in the permeate due to ion expulsion. Since the quantity of Cd^{2+} adsorbed onto the membrane is difficult to determine, the quantitative effect of the extra metal ions on the calculated values of $\%R_{Cd}$ or $\%E_{Cd}$ is also difficult to evaluate.

A different method for dealing with membrane adsorption of metal ions is to introduce a correction factor based on the mass balance of the analyzed permeate, retentate and stock concentrations ($[Cd^{2+}]_P$, $[Cd^{2+}]_R$, $[Cd^{2+}]_O$, respectively). Without membrane adsorption the sum of the analyzed permeate and retentate concentrations should equal the stock concentration within experimental error, assuming equal volumes for the two compartments. A check of permeate and retentate volumes when unloading cells indicated that, by using careful filling technique, volumes were approximately equal, though a study by Simmons (83) found a 10-20% volume increase for the retentate with cationic surfactant. The sum of the permeate and retentate concentrations will be referred to as total Cd^{2+} ($[Cd^{2+}]_{Tot}$) as shown in Equation IV.1 and the difference between the $[Cd^{2+}]_O$ and $[Cd^{2+}]_{Tot}$ as the change in Cd^{2+} concentration, ($[Cd^{2+}]_\Delta$) as shown in Equation IV.2.

$$[Cd^{2+}]_P + [Cd^{2+}]_R = [Cd^{2+}]_{Tot} \qquad \textbf{Eqn IV.1}$$

$$[Cd^{2+}]_O - [Cd^{2+}]_{Tot} = [Cd^{2+}]_\Delta \qquad \textbf{Eqn IV.2}$$

The change in Cd^{2+} is assumed to be composed entirely of uncomplexed or free Cd^{2+} which was adsorbed on to the membrane. This is based on strong partitioning of the ligand into the micelle and previous studies which show that micelles do not come to equilibrium across the membrane within the 20-24 hour test period (27). In neutral surfactant solution, $[Cd^{2+}]_\Delta$ would be distributed

about equally between the retentate and the permeate if it were not adsorbed on the membrane (Eqn IV.3).

$$[Cd^{2+}]_{P,\Delta} = [Cd^{2+}]_{R,\Delta} \qquad \textbf{Eqn IV.3}$$

The corrected concentration of Cd^{2+} in the permeate and retentate solutions for SED experiments in neutral surfactant solution is:

$$[Cd^{2+}]_P \text{ (corrected)} = [Cd^{2+}]_P + 0.5[Cd^{2+}]_\Delta \qquad \textbf{Eqn IV.4}$$

and

$$[Cd^{2+}]_R \text{ (corrected)} = [Cd^{2+}]_R + 0.5[Cd^{2+}]_\Delta \qquad \textbf{Eqn IV.5}$$

The total corrected permeate concentration is equal to the analyzed concentration of Cd^{2+} in the permeate plus 50% of the free Cd^{2+} which was adsorbed by the membrane. The same applies to the retentate. In cationic surfactant about 75% of the free Cd^{2+} will be in the permeate and 25% in the retentate as a result of ion expulsion. Therefore, the corrected concentrations of Cd^{2+} in the permeate and retentate solutions for SED experiments in cationic surfactant are:

$$[Cd^{2+}]_P \text{ (corrected)} = [Cd^{2+}]_P + 0.75[Cd^{2+}]_\Delta \qquad \textbf{Eqn IV.6}$$

and

$$[Cd^{2+}]_R \text{ (corrected)} = [Cd^{2+}]_R + 0.25[Cd^{2+}]_\Delta \qquad \textbf{Eqn IV.7}$$

Corrections were applied to the data shown in Tables III.8 and III.10 from studies comparing the effectiveness of different membrane treatments. The

corrected data is compared to the uncorrected percent rejection of Cd^{2+} in Tables IV.2 and IV.3. These studies were performed in $C_{12}(EO)_6$ and $CPNO_3$ surfactant solutions at pH 7.0 with and without membrane treatments. This data was chosen for correction because the $[Cd^{2+}]_\Delta$ indicated a loss of 20% of the original stock concentration of Cd^{2+} for experiments without membrane treatments. Corrections were not made if total Cd^{2+} concentration was less than or equal to 10% of the stock concentration. This would be within reasonable experimental error. The corrected values of $[Cd^{2+}]_P$ and $[Cd^{2+}]_R$ were used to calculate corrected %R or %E using Equations II.1 and II.2. These values were then compared to the %R or %E for treated membranes.

Table IV.2 Corrected values of $\%R_{Cd}$ for 0.50 mM Kelex SED experiments in $C_{12}(EO)_6$ surfactant solution with different membrane treatment techniques at pH 7.0.[a]

Membrane treatment	$[Cd^{2+}]_O$	$[Cd^{2+}]_R$	$[Cd^{2+}]_P$	$[Cd^{2+}]_{Tot}$	$[Cd^{2+}]_\Delta$	$\%[Cd^{2+}]_\Delta$	$\%R_{Cd}$	$\%R_{Cd}$ (corrected)
D.D. water	0.0643	0.0127	0.0115	0.0242	-0.0401	-62.4	9.4	3.5
0.025 mM Cd^{2+}	0.0643	0.0377	0.0307	0.0684	+0.0041	+6.0	18.6	(b)
0.25 mM Cd^{2+}	0.0643	0.0283	0.0231	0.0514	-0.0129	-20.0	18.4	14.9
10 mM Ca^{2+}	0.0643	0.0153	0.0126	0.0279	-0.0364	-56.6	17.6	8.1

(a) Data from Table III-8. (b) No correction applied because $[Cd^{2+}]_{Tot} > [Cd^{2+}]_O$.

Table IV.3 Corrected values of $\%R_{Cd}$ for 0.50 mM Kelex SED experiments in $CPNO_3$ surfactant solution with different membrane treatment techniques at pH 7.0. [a]

Membrane treatment	$[Cd^{2+}]_O$	$[Cd^{2+}]_R$	$[Cd^{2+}]_P$	$[Cd^{2+}]_{Tot}$	$[Cd^{2+}]_\Delta$	$\%[Cd^{2+}]_\Delta$	$\%E_{cd}$	$\%E_{cd}$ (corrected)
D.D. water	0.0413	0.0058	0.0225	0.0283	-0.0130	-31.5	74.2	71.8
0.025 mM Cd^{2+}	0.0413	0.0159	0.0644	0.0803	+0.0390	+48.6	75.3	(b)
0.25 mM Cd^{2+}	0.0413	0.0111	0.0485	0.0596	+0.0183	+30.7	77.1	(b)
10 mM Ca^{2+}	0.0413	0.0068	0.0275	0.0343	-0.0070	-16.9	75.3	73.8

(a) Data from Table III-10. (b) No corrections applied because $[Cd^{2+}]_{Tot} > [Cd^{2+}]_O$.

Results in Table IV.3 for experiments in $CPNO_3$ solution show that there is little difference in the $\%E_{Cd}$ values either corrected or uncorrected. The highest $\%E_{Cd}$ value is 77.1% for experiments performed with membranes treated in 0.25 mM Cd^{2+} and the lowest value is 71.8% for membranes presoaked in D.D. water only and then corrected. Variations in %E or %R of $\pm$ 5% are within experimental error and not considered meaningful. However, results of experiments in $C_{12}(EO)_6$ solution show more variation. Experiments performed with membranes which were not treated with Cd^{2+} showed $\%R_{Cd}$ values of 9.4% and 17.6%. Correcting the calculations for the Cd^{2+} lost to the membrane gives results of 3.5% and 8.1% rejection, respectively. However, rejection values for experiments with Cd^{2+} treated membranes are both higher, about 18.5%. Comparing the effects of membrane treatment with the calculated correction of %R shows that membrane treatment tends to increase %R while the calculated correction will always decrease it. The trend for membrane treatment appears to be reversed where $\%R_{Cd}$ is high. Results for experiments with membrane treatments and 0.50 mM Kelex at pH 9.0 are shown in Tables III.15 and III.16. The calculated $\%R_{Cd}$ is slightly less for membranes treated with Cd^{2+} than for experiments without membrane treatments. The small quantity of Cd^{2+} which is released from the membrane into the permeate appears to be sufficient to decrease the rejection when compared to that of the experiments performed with untreated membranes. There were no calculated corrections necessary for this data set because total Cd^{2+} was either greater than or within 10% of the stock concentration.

The correction factor was applied to one additional data set. Figure III.39 shows a plot of Cd^{2+} rejection versus concentration of Cd^{2+} in the stock solution for a series of experiments with 0.50 mM Kelex in $C_{12}(EO)_6$ surfactant solution at pH 9.0. The Cd^{2+} concentration in the stock solution ranged from 0.0441 to 0.476 mM. The plotted data shows that the $\%R_{Cd}$ begins to drop when the concentration of Cd^{2+} in the stock solution begins to exceed 0.25 mM, or 1:2 [Cd^{2+}]:[Kelex 100]. The final point, however, is high and does not follow the downward trend of the data. This may be explained by a large amount of free Cd^{2+} being lost to the membrane. Calculating $\%[Cd^{2+}]_\Delta$ shows 51% of the stock Cd^{2+} was lost and that 28% of the stock Cd^{2+} was lost for the point at $[Cd^{2+}]_O$ = 0.224. Corrected values for the last two points were calculated and are shown in Figure IV.3 as open circles. The corrected values, particularly for the final data point at the highest $[Cd^{2+}]_o$, are in line with the general trend of the other values. Rejection begins to fall off at 0.17 mM Cd2+ which corresponds to a 1:3 ratio of [Cd^{2+}]:[Kelex 100].

Based on these limited data, the suggested correction factor appears to be an acceptable method for compensating for membrane adsorption of uncomplexed Cd^{2+}. It can be used in place of the membrane treatment technique and has the advantage of not introducing an unknown quantity of additional Cd^{2+} into the SED system. This can be most problematic under conditions at which the ligand is most effective due to high concentrations of Cd^{2+} in the retentate. Using corrected concentrations for $[Cd^{2+}]_R$ and $[Cd^{2+}]_P$ to calculate %R and %E will cause the values to be more conservative than they would be without the

correction. It will make the most difference in the data when the quantity of uncomplexed Cd^{2+} is large in relation to complexed Cd^{2+}. Since SED experiments are used to model UF systems, it should be pointed out that little effect from membrane adsorption is expected for UF experiments. Since the UF technique is dynamic, the quantity of Cd^{2+} which can be adsorbed by the membrane should reach a maximum at some point in the run beyond which it should not effect the values of %R or %E.

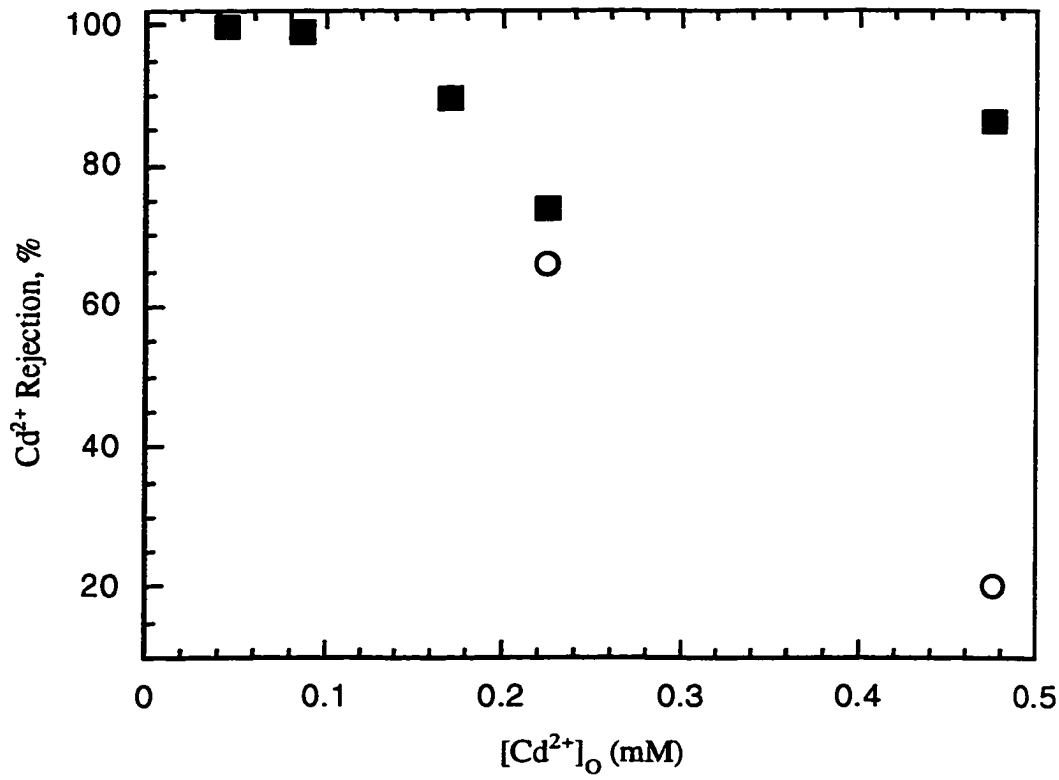

Figure IV.3 Plot of Cd^{2+} rejection (%) as a function of $[Cd^{2+}]_o$ in 5 mM $CPNO_3$ at pH 9.0 with $[Kelex]_o$ = 0.50 mM. Corrected values for the last two data points which are shown as open circles.

The effect of varying the concentration of Cd^{2+} while maintaining a constant concentration of Kelex 100 was investigated to determine the minimum amount of ligand, relative to the Cd^{2+} concentration, needed to achieve adequate separation in LM-MEUF. At pH 9.0 in $C_{12}(EO)_6$ surfactant solution, the Cd^{2+} rejection was 99.8% with a 2.5-fold excess of ligand. Rejection was greater than 90% with the ligand concentration equal to that of the metal ion. In $CPNO_3$ solution, rejection was 99.6% with a 10-fold excess of Kelex, only 90% with a 3-fold excess and decreased rapidly as the excess ligand was reduced further. This corresponds with the metal complexation data that showed CdL_3^- to be the preferred stoichiometry in $CPNO_3$.

Ligand cost is a consideration for industrial scale application of LM-MEUF technology; therefore, high rejections with a minimum of ligand are desirable. Since about 1.5 times more ligand is needed in $CPNO_3$ than in $C_{12}(EO)_6$ to achieve 90% rejection, higher loadings of Cd^{2+} can be achieved for a given quantity of ligand in $C_{12}(EO)_6$ before the ligand must be stripped of the Cd^{2+} to be reused. Therefore, the $C_{12}(EO)_6$ system would appear to be more economical with regard to ligand cost. However, uncomplexed metal ions are expelled into the permeate with $CPNO_3$ which enhances separation of target from nontarget metal ions. Expulsion of the Cd^{2+} is also an advantage during the stripping stage unless the pH required for stripping is too low. The presence of high concentrations of H^+ reduces the ion expulsion effect.

The advantages of expulsion are also seen in pH experiments. Kelex 100 complexes Cd^{2+} most effectively at high pH. In $C_{12}(EO)_6$ solution a pH of

8.5 is needed to achieve greater than 99% rejection and the pH must be lowered to 6.0 to achieve close to zero rejection. Adjusting the pH is the simplest way to strip the metal ion from the ligand and allow reuse of the ligand. A smaller pH range between complexation and release of the metal ion results in lower costs for the acid and base needed for pH adjustment. In $CPNO_3$ solution 99% rejection is achieved only at pH 9.0 but rejection drops off rapidly and Cd^{2+} is expelled into the permeate by pH 7.5. The nature and concentration of other ions in solution would be one factor in determining the relative advantages of utilizing expulsion with $CPNO_3$. The presence of another target ion which could be separated in a second stage would make expulsion attractive due to the ability to concentrate the second target species through expulsion.

SED studies were done to determine the effect of other ions likely to be present in the LM-MEUF waste stream. NaCl was added to the SED retentate at 200 times the concentration of the Cd^{2+} to determine the effect of added electrolyte (Table III.20). Experiments performed in $C_{12}(EO)_6$ with 1 mM and 10 mM NaCl showed little effect since %R remained greater than 95%. No experiments were done with Kelex 100 and added salt in $CPNO_3$, but added NaCl has been shown to decrease selectivity in cationic surfactant due to reduction of the ion expulsion effect. The higher concentration of ions in solution screens the charged micelle and reduces the repulsion of the cations in solution. An SED study of Ni^{2+} complexation with *N*-(*n*-hexadecyl)-di-2-picolylamine(HDPA) by Simmons showed that in cationic surfactant NaCl added at 200 times the concentration of the Ni^{2+} caused the percent rejection of Ni^{2+} to

increase from 81.8% to as much as 98.2% (83). The decreased ion expulsion effect allowed more Ni^{2+} to be available to the ligand. Scamehorn et al. studied the effect of salt on rejection of Cu^{2+} and Ca^{2+} with the ligand *N*-(4-(*n*-hexadecyl)-oxybenzyl)-iminodiacetic acid (C_{16}BIDA) in the cationic surfactant CPC (49). Results of UF experiments showed that rejection of Cu^{2+} remained high with a 400-fold excess of NaCl, although the decrease in Ca^{2+} expelled into the permeate reduced selectivity. In both cases %R remained high or improved though %E was reduced.

The utility of LM-MEUF for selective separation of metals has been demonstrated with several different ligands and surfactants (27, 29, 33, 35, 46,49). Kelex 100 had been used for selective removal of Cu^{2+} in the presence of Ca^{2+} in this laboratory (46). Experiments with added Ca^{2+} demonstrated no tendency for Kelex 100 to bind Group 2 metals. This same selectivity was shown for Cd^{2+} since no decrease in rejection of Cd^{2+} occurred with Ca^{2+} concentrations up to 100 times the Cd^{2+} concentration (Table III.23). Percent rejection of Cd^{2+} was greater than 99% in all cases.

Kelex 100 did show a definite tendency to bind strongly with Zn^{2+}. Results of experiments listed in Table III.22 show rejection of Cd^{2+} and Zn^{2+} as a function of pH. The concentrations of Kelex 100 and metal ions were such that excess ligand was present even if both metal ions formed complexes with 3:1 [Kelex]:[metal] stoichiometry. With no competition for the ligand, rejection of both Cd^{2+} and Zn^{2+} was greater than 98% at pH 9.0. Rejection of Cd^{2+} decreased to 33.7% at pH 6.0, while rejection of Zn^{2+} remained greater than

95%. This difference in rejection of Cd^{2+} and Zn^{2+} at pH 6.0 appears promising for stepwise stripping of the metals, thus allowing some selectivity in the separation. SED experiments with Cd^{2+}, but no Zn^{2+}, showed only 2.4% rejection at pH 6.0. The possibility of relatively high concentrations of Zn^{2+} in waste streams which contain Cd^{2+} suggests that further study is needed to determine the effects of increased competition by Zn^{2+} on rejection of Cd^{2+} by the ligand. In general, however, simultaneous removal of Cd^{2+} and Zn^{2+} could be beneficial since Zn^{2+} is also a pollutant regulated by the EPA.

SED studies of the removal of Cd^{2+} by Kelex 100 showed greater than 99% rejection at pH 9.0. Rejections were not decreased in neutral surfactant by either increased electrolyte concentration or the presence of competing ions provided that sufficient ligand was available. Studies of pH effects on rejection indicate that Kelex 100 binds and releases Cd^{2+} at moderate pH with stripping possible at pH 7.0 in $CPNO_3$ solution and pH 6.0 in $C_{12}(EO)_6$ solution. This is significantly less acidic than the pH needed for stripping other ligands studied thus far for LM-MEUF (49, 50). In addition, using a cationic surfactant can enhance separation through ion expulsion, causing other cations to be concentrated in the permeate while Cd^{2+} is held in the retentate. Metal complexation studies show that a tradeoff occurs, though, with cationic surfactant. Because the preferred stoichiometry of the Kelex-Cd^{2+} complex is 3:1 in cationic surfactant and only 2:1 in neutral surfactant, the relative loading of the ligand is less in the former; therefore, ligand costs will increase. This result is also seen in the Cd^{2+} concentration studies which showed that approximately

1.5 times more ligand may be needed in cationic surfactant than in neutral surfactant to achieve the same rejection.

Ultrafiltration Experiments

Cadmium concentration profiles are shown in Figures III.42-III.46. Several of the plots show a drop in the Cd^{2+} concentration from the first fraction at 10% of the total volume to the second fraction at 20% of the total volume. The higher value in the first fraction may be attributable to release of the adsorbed Cd^{2+} from the membrane. A comparison among experiments with (1) Cd^{2+} but no surfactant or ligand, (2) Cd^{2+}, surfactant but no ligand and, finally, (3) Cd^{2+} with both surfactant and ligand generally show expected trends. At pH 9.0, blanks with only Cd^{2+} have the highest concentration in the permeate and concentration increases as the run progresses. Blanks with Cd^{2+} and surfactant follow the same trend but with lower Cd^{2+} concentrations. Experiments with ligand have the lowest Cd^{2+} concentration at pH 9.0 and Cd^{2+} concentration in the permeate does not increase or increases only slightly as the run progresses. At pH 6.0, the Cd^{2+} and surfactant blank and the experiment with ligand have very similar profiles, especially with $CPNO_3$. This would be expected since the ligand does not complex effectively at this pH and so little binding of the metal by the ligand occurs.

Percent rejections were calculated for the blank UF experiments and the results are summarized in Table III.24. Rejection of Cd^{2+} is approximately 73-74% at both pH 6.0 and 9.0 in $CPNO_3$. UF results also show significant rejection with $C_{12}(EO)_6$ though values are lower than they are in $CPNO_3$. Results at pH 9.0 are 54% rejection of Cd^{2+} and, at pH 6.0, 32% rejection of

Cd^{2+}. Finally, with no surfactant present rejections of 41% occur at pH 9.0 and 14% at pH 6.0.

Ultrafiltration results with Kelex 100 show the highest rejection at pH 9.0 in $C_{12}(EO)_6$ solution, greater than 98%. Rejection is slightly less, 96%, in $CPNO_3$ solution at the same pH. At pH 6.0 there is still significant rejection in both $C_{12}(EO)_6$ and $CPNO_3$ solutions, about 70% in both cases, and at pH 4.0 in $C_{12}(EO)_6$ solution the rejection decreases to 6%.

SED results under the same conditions, shown in Table III.25, were in reasonable agreement with the UF results at pH 9.0. Rejections were slightly lower for the UF experiments than they were for the SED experiments. However, SED results at pH 6.0 indicated that in $C_{12}(EO)_6$ the rejection should be almost zero while in $CPNO_3$ there should be about 70% expulsion of Cd^{2+} into the permeate. The UF results were consistent and showed about 70% rejection for the experiments without ligand at both pH's and also with ligand at pH 6.0 where the ligand does not complex efficiently.

Rejection of species which are not complexed by the ligand has been noted in previous studies (49, 85). An ultrafiltration study of the ligand 4-hexadecyloxybenzyliminodiacetic acid (C_{16}BIDA) for removal of Cu^{2+} with LM-MEUF indicated that the rejection of Ca^{2+} was as high as 45% even though SED studies showed no rejection of Ca^{2+} (49). The tendency for species to be excluded by the membrane as the feed solution is forced through is known as concentration polarization (85). It results from a buildup of charged species at the membrane due to decreased diffusion. This effect is exaggerated with cationic surfactant. As the solution is forced through the membrane, high

molecular weight surfactant molecules build up at the membrane and charge repulsion of smaller cations is increased. A study of electrolytes in UF by Tondre and coworkers (84) showed that in solutions made with *N*-hexadecylpyridinium chloride (CPC), a cationic surfactant, the presence of nitrate was found to reduce the solution flux significantly. This suggests that in the present study, the presence of the nitrate counterion from $CPNO_3$ may also play a role in concentration polarization and the resulting increase in rejection of uncomplexed Cd^{2+}.

The impact of the increased rejection at lower pH is critical for the stripping stage of the LM-MEUF process. Additional studies are needed to determine the best combination of conditions for removing the metal and recycling the ligand and surfactant. Low rejection of the Cd^{2+} at pH 4.0 indicates that in nonionic surfactant this may be sufficient to achieve the desired result. However, to achieve adequate stripping in $CPNO_3$ solution, the effect of decreased pressure should also be examined. Concentration polarization increases with increased pressure and a study by Scamehorn et al. (49) of the effects of applied pressure showed that rejection of Cu^{2+} and Ca^{2+} approached the equilibrium SED values as the pressure was decreased from 60 psig to 20 psig. Since a decrease in the applied pressure increases the time needed for the separation this would need to be balanced with the need for separation efficiency.

Mercury separation with thiourea

An effective method was developed for analysis of Hg^{2+} in the presence of surfactant and decylthiourea (Dtu) ligand. The limited results of experiments with Dtu indicate that it is an effective ligand for complexing Hg^{2+} with LM-MEUF. Greater than 99% rejection was achieved for one set of SED experiments in $CPNO_3$ surfactant solution with a 3:1 ratio of ligand to Hg^{2+} where $[Hg^{2+}]_o = 0.10$ mM. In order to develop the use of Dtu with LM-MEUF further, a method for stripping the Hg^{2+} from the ligand would need to be developed. Since the Dtu complexation of Hg^{2+} is apparently insensitive to pH, acid stripping could not be applied for recycling the ligand. It is possible that a mild reducing agent, such as stannous chloride, could be used to release the Hg^{2+} and it could be collected as a vapor in the same manner that is used for cold vapor atomic absorption analysis. In addition, evaluation of any ligand for removal of Hg^{2+} would be more effective if membrane adsorption of Hg^{2+} could be minimized. The use of a different membrane type might reduce these problems.

References

1. Callahan, M. A.; Slimak, M. W.; Gabel, N. W.; May, I. P.; Fowler, C. F.; Freed, J. R.; Jennings, P.; Durfee, R. L.; Whitmore, F. C.; Maestri, B.; Mabey, W. R.; Holt, B. R.; Gould, C. *Water-Related Environmental Fate of 129 Priority Pollutants, Vol. I: Introduction and Technical Background, Metals and Inorganics, Pesticides and PCBs* EPA-440/4-79-029a, Dec 1979, U. S. Environmental Protection Agency, Washington D. C.
2. Tierney, D.R.; Blackwood, T.R.; Briggs, T.M. *Status Assessment of Toxic Chemicals: Mercury* EPA600/2-79-210i, Dec 1979 U. S. Environmental Protection Agency, Washington D. C.
3. *An Assessment of Mercury in the Environment:*; Panel on Mercury, National Research Council; National Academy of Sciences, Washington D.C. 1978.
4. Mance, Geoffrey *Pollution Threat of Heavy Metals in Aquatic Environments* ; Elsevier Applied Science: New York, 1987; pp
5. Bakir, F.; Damluji, S. F.; Amin-Zaki, L.; Murtadha, M.; Khalidi, A.; Al-Rawi, N. Y.; Tikriti, S.; Dhahir, H.I.; Clarkson, T.W.; Smith, J.C.; Doherty, R.A. *Science* **1973**, 181, 230-240.
6. Sargent, T.N.; Patrick, B.C.; Snider, E.H. *Field Manual Performance Evaluation and Troubleshooting at Metal-Finishing Wastewater Treatment Facilities* EPA-600/S2-84-152, Nov 1984, U. S. Environmental Protection Agency, Washington D.C.

7. Tierney, D.R.; Blackwood, T.R.; Wilson, R.D. *Status Assessment of Toxic Chemicals: Cadmium* EPA600/3-79-210f, Dec 1979, U. S. Environmental Protection Agency, Washington D. C.
8. Yasumura, S.; Vartsky, D.; Ellis, K.J.; Cohn, S.H. in *Cadmium in the Environment*; Nriagu, J.O., Ed.; John Wiley & Sons: New York, 1980; pp 12-34.
9. *Ambient Water Quality Criteria for Cadmium* EPA 440/5-80-025, Oct 1980, U. S. Environmental Protection Agency, Washington D. C.
10. Grum, E.E. *Cadmium Toxicity: Case Studies in Environmental Medicine*, 1990.
11. *Ambient Water Quality Criteria for Mercury* EPA440/5-80-058, Oct. 1980, U. S. Environmental Protection Agency, Washington D. C.
12. Burgess, W.A. *Recognition of Health Hazards in Industry: A Review of Materials and Processes*, John Wiley & Sons: New York, 1995; pp 342-346.
13. Watson, M.R. *Pollution Control in Metal Finishing*, Noyes Data Corporation: Park Ridge, NJ, 1973.
14. Laubusch, E.J. in *Modern Chlor-Alkali Technology, Vol. 2* Jackson, C., Ed.; Ellis Horwood Ltd.: Chichester, 1983; pp 367-375.
15. *Code of Federal Regulations*, 1998, 40 CFR Ch. 1 (7-1-95) EPA.
16. *Study on the Technical and Economic Aspects of Measures to Reduce Water Pollution Caused by Discharges from the Industrial Sectors Involved inthe Surface Treatment of Metal :* Commission of European Communities, Luxembourg, 1996.

17. *Evaluation of the HSA Reactor for Metal Recovery and Cyanide Oxidation in Metal Plating Operations* EPA/600/S2-86/094, Jan 1987, U. S. Environmental Protection Agency, Washington D. C.

18. McDonald, C.W. *Removal of Toxic Metals from Metal Finishing Wastewater by Solvent Extraction*, EPA600/2-78-011, Feb 1978, U. S. Environmental Protection Agency, Washington D. C.

19. *Recovery of Metals from Sludges and Wastewaters,* EPA/600/S2-91/041, Sept 1991, U. S. Environmental Protection Agency, Washington D. C

20. Rosen, M.J. *Surfactants and Interfacial Phenomena*, John Wiley & Sons: New York, 1989, pp 108-168.

21. Hiemenz, P.C. *Principles of Colloid and Surface Chemistry*, Marcel Dekker: New York, 1986, pp 427-454.

22. Rosen, M.J. *Surfactants and Interfacial Phenomena*, John Wiley & Sons: New York, 1989, pp 172-178.

23. Myers, D. *Surfactant Science and Technology*, VCH Publishers, Inc.: New York, 1992, pp 136-148.

24. Dunn, Jr., R.O.; Scamehorn, J.F.; Christian, S.D. *Sep. Sci. Tech.*, **1985**, *20*, 257-284.

25. Scamehorn, J.F.; Ellington, R.T.; Christian, S.D.; Penney, B.W.; Dunn, R.O.; Bhat, S.N. In *Removal of Multivalent Metal Cations from Water Using Micellar-Enhanced Ultrafiltration*, AICHE Recent Advances in Separation Techniques Part III, 1986, 82, pp 48-58.

26. Scamehorn, J.F.; Christian, S.D.; El-Sayad, D. A.; Uchiyama, H.; Younis, S.S. *Sep. Sci. Tech.*, **1994**, *29*, 809-830.

27. Klepac, J.; Simmons, D.L.; Taylor, R.W.; Scamehorn, J.F.; Christian, S.D. *Sep. Sci. Tech.*, **1991**, *26*, 165-173.

28. Pramauro, E.; Bianco, A.; Barni, E.; Viscardi, G.; Hinze, W.L. *Colloids Surf.*, **1992**, *63*, 291-300.

29. Fillipi, B.R.; Scamehorn, J.F.; Taylor, R.W.; Christian, S.D. *Sep. Sci. Tech.*, **1997**, *32*, 2401-2424.

30. Christian, S.D.; Smith, G.A.; Tucker, E.E. *Langmuir*, **1985**, *1*, 564-567.

31. Takeuchi, T. In *Environmental Mercury Contamination*, Hartung, R.; Dinman, B.D. Eds.; Ann Arbor Science Publishers, Inc.: Ann Arbor, MI., 1972, pp 247-289.

32. Mahmoud, F.Z.; Higazy, W.S.; Christian, S.D.; Tucker, E.E.; Taha, A.A. *J. Colloid Interface Sci.*, **1989**, *131*, 96-103.

33. Dharmawardana, U.R.; Christian, S.D.; Taylor, R.W.; Scamehorn, J.F. *Langmuir*, **1992**, *8*, 414-419.

34. Uchiyama, H.; Christian, S.D.; Tucker, E.E.; Scamehorn, J.F. *J. Phys. Chem.*, **1994**, *98*, 1714-1718.

35. Simmons, D.L.; Schovanec, A.L.; Scamehorn, J.F.; Christian, S.D.; Taylor, R.W. In *Environmental Remediation: removing organic and metal ion pollutants*; Vandegrift, G.F.; Reed, D.T.; Tasker, I.R. Eds.; ACS Symposium Series, 1992, 509, 180-193.

36. Demopoulos, G.P.; Distin, P.A. *Hydrometallurgy* , **1983**, *11*, 389-396.

37. Bokobza, L.; Cote, G. *Polyhedron*, **1985**, *4*, 1499-1505.

38. Barret, J.; Deghaidy, F.S. *Spectrochimica Acta*, **1975**, *31A*, 707-713.

39. Zuo, G.; Muhammed, M. *Sep. Sci. Tech.*, **1990**, 25, 1785-1802.

40. Underwood, A.L. *Anal. Chim. Acta*, **1977**, *93*, 267-273.

41. Underwood, A.L. *Anal. Chim. Acta*, **1982**, *140*, 89-97.

42. Fernandez, M.S.; Fromherz, P.; *J. Phys. Chem.*, **1977**, 81, 1755-1761.

43. Smith, R.M.; Martell, A.E. in *Critical Stability Constants*; Smith R.M.; Martell, A.E., Eds.; Volume 2; Plenum Press: New York, NY, 1975, p. 223.

44. Lindstedt, G. *Analyst*, **1970**, 95, 264-171.

45. "Mercury, dissolved"; United States Geological Survey Analytical method # I-1462-77, December 1976.

46. Schovanec, A.L. Ph.D. dissertation, University of Oklahoma, 1991.

47. Vogel, A. I. In *A Text-Book of Quantitative Inorganic Analysis including Elementary Instrumental Analysis*, Third Edition, John Wiley and Sons, New York, NY, 1961, pp 415-457.

48. Schwarzenbach, B. and Flaschka, H. *Complexometric Titrations*, Methuen and Co., Ltd.: London, 1969, pp 268-273.

49. Scamehorn, J.F.; Shadizadeh, S.D.; Schovanec, A.L.; Taylor, R.W.; Christian, S.D. in *Metal Ion Separation and Preconcentration: Progress and Opportunities*; Bond, A.H.; Dietz, M.L.; Rogers, R.D.; Eds. ACS Symposium Series 716; American Chemical Society: Washington D.C., 1998.

50. Roach, J. D. Ph.D. dissertation, The University of Oklahoma, 1996.

51. Urbanski, T.S.; Abbruzzese, C.; Fornari, P.; Massidda, R. *Hydrometallurgy*, **1990**, 25, 185-195.

52. Lakshmanan, V.I.; Lawson, G.J. *J. Inorg. Nucl. Chem.* **1973**, 35, 4285-4294.

53. Benguerel, E.; Cote, G., Lautie, A.; Demopoulos, G.; Bauer, D. *J. Chem. Tech. Biotechnol.* **1995**, 62, 380-384.

54. Haraguchi, K.; Freiser, H. *Inorg. Chem.* **1983**, 22, 1190-1197.

55. Zhou, T.; Pesic, B. *Trans. Instn. Min. Metall. (Sect. C: Mineral Process. Extr. Metall.),* **1989**, 98, 147-152.

56. Demopoulos, G.P.; Pouskouleli, G.; Ritcey, G.M. *Proc. Int. Solvent Extraction Conf. ISEC '86, Munich*, **1986**, 2:581.

57. Al-Bazi, S.J.; Freiser, H. *Proc. Int. Solvent Extraction Conf. ISEC '86, Munich*, **1986**, 2:393.

58. Smith, R.M.; Martell, A.E. in *Critical Stability Constants*; Smith R.M.; Martell, A.E., Eds.; Volume 4; Plenum Press: New York, NY, 1975, p. 104.

59. Smith, R.M.; Martell, A.E. in *Critical Stability Constants*; Smith R.M.; Martell, A.E., Eds.; Volume 4; Plenum Press: New York, NY, 1975, p.1.

60. Smith, R.M.; Martell, A.E. in *Critical Stability Constants*; Smith R.M.; Martell, A.E., Eds.; Volume 4; Plenum Press: New York, NY, 1975, p. 48.

61. Smith, R.M.; Martell, A.E. in *Critical Stability Constants*; Smith R.M.; Martell, A.E., Eds.; Volume 2; Plenum Press: New York, NY, 1975, p. 223.

62. Banerjee, S.N.; Vaz, C.E.S. *J. Indian Chem. Soc*, **1984**, 61, 498-501.

63. Bellomo, A.; De Marco, D.; De Robertis, A. *Polyhedron*, **1983**, 8, 735-740.

64. Goddard, D.R.; Lodam, B.K.; Ajayi, S.O.; Campbell, M.J. *J. Chem. Soc. (A)*, **1969**, 506-512.

65. Smith, R.M.; Martell, A.E. in *Critical Stability Constants*; Smith R.M.; Martell, A.E., Eds.; Volume 3; Plenum Press: New York, NY, 1975, p. 313.

66. Elworthy, P.H. Mysels, K.J. *J. Colloid Sci.*; **1966**, 21, 331-347.

67. Schick. J.J.; Gilbert, A.H. *J. Colloid Sci.*, **1965**, 20, 464.

68. Corkillo, J.M.; Goodman, J.F.; Ottewill, R.H. *Trans. Faraday Soc.*, **1961**, 57, 1627-1636.

69. Hartley, G.S. *J. Chem. Soc.*, **1938**, 1968-1975.

70. Rathman, J.F.; Christian, S.D. *Langmuir*, **1990**, 6, 391-395.

71. Sandell, E.B.; Onishi, H. *Photometric Determination of Traces of Metals: General Aspects, Part II.* John Wiley & Sons: New York, 1978, p. 631.

72. Cote, G.; Bauer, D. *Inorg. Nucl. Chem.* **1981**, 43, 1023-30.

73. Boumezioud, M.; Tondre, C.; Lagrange, P. *Polyhedron*, **1988**, 7, 513-21.

74. Bag, S.; Freiser, H. *Anal. Chim. Acta*, **1982**, 135, 319-325.

75. Citores, M.; Alonso, R.; Fernandez, L. *Sep. Sci. Tech.*, **1994**, 29, 1441-1459.

76. Shibata, S. in *Chelates in Analytical Chemistry*, Flaschka, H.A.; Barnard, Jr., A.J. Eds., Vol. 4, Marcel Dekker, Inc.: New York, NY, 1972, pp. 78-81.

77. Budesinsky, B.W.; Sagat, M. *Talanta*, **1973**, 20, 228-232.

78. Ueno, K.; Shiraishi, K.; Togo, R.; Yano, T.; Yoshida, I., Kobayashi, H. *Anal. Chim. Acta*; **1979**, 105, 289-295.

79. Ashbrook, A.W. *J. Chromatogr.*, **1975**, 105, 151-156.

80. Christian, S.D.; Tucker, E.E.; Scamehorn, J.F.; Lee, B.H.; Sasaki, K.J. *Langmuir*, **1989**, 5, 876-879.

81. Simmons, D.L., University of Oklahoma, unpublished results.

82. Ueno, K.; Imamura, T.; Cheng, K.L. *Handbook of Organic Analytical Reagents*, CRC Press: Boca Raton, FL; 1992, pp. 313-327.

83. Simmons, D.L . Ph.D. dissertation, The University of Oklahoma, 1994

84. Tounissou, P.; Hebrant, M.; Rodehuser, L.; Tondre, C. *J. Colloid Interface. Sci.*, **1996**, 183, 484-490.

85. Krehbiel, D.K.; Scamehorn, J.F.; Ritter, R.; Christian, S.D.; Tucker, E.E. *Sep.Sci. Technol.* **1992**, 27, 1775-1787.

86. Grieves, R.B.; Bhattacharrya, D., Schomp, W.G.; Bewley, J.L. *AIChE J.* **1973**, 19, 766.

IMAGE EVALUATION
TEST TARGET (QA-3)

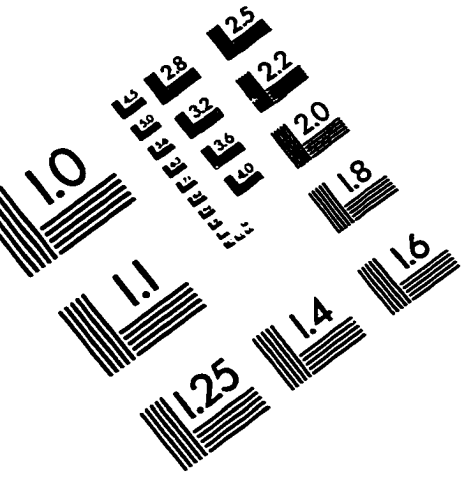

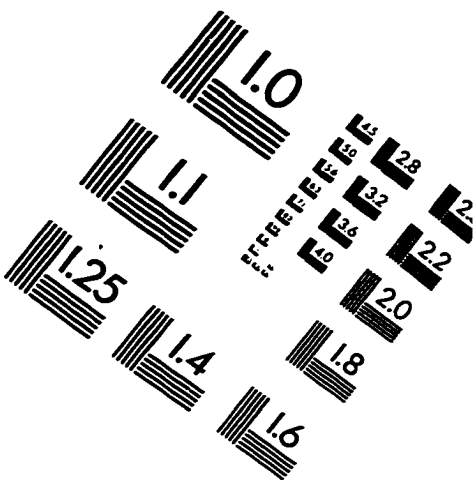

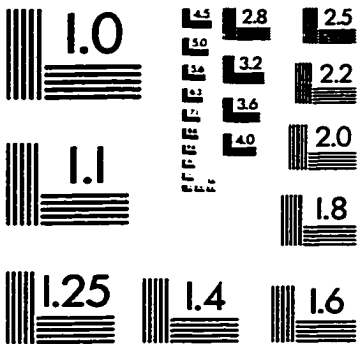

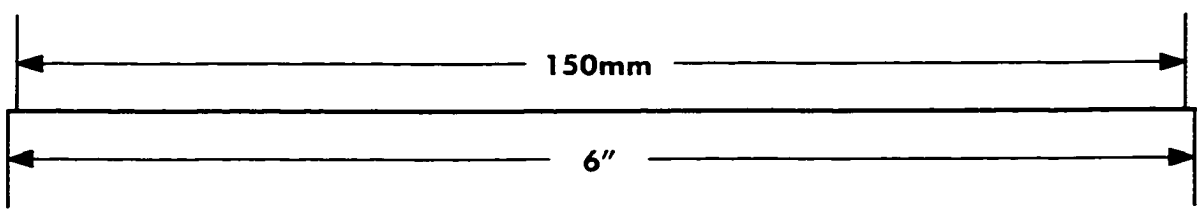

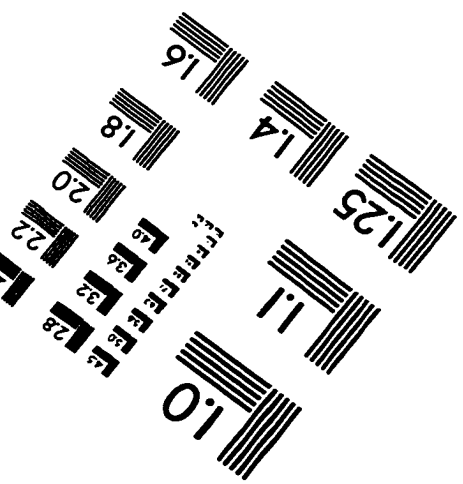

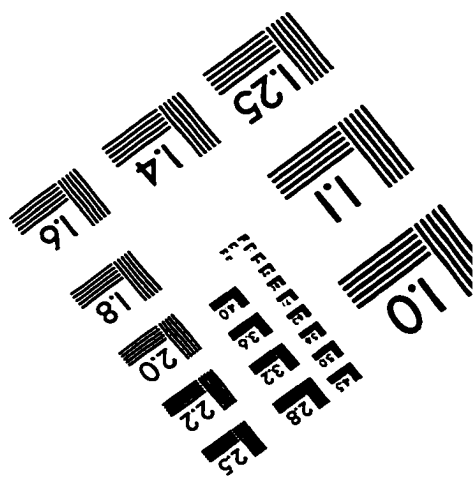

APPLIED IMAGE, Inc
1653 East Main Street
Rochester, NY 14609 USA
Phone: 716/482-0300
Fax: 716/288-5989